DISSERTATIONES SCHOLAE DOCTORALIS AD SANITATEM INVESTIGANDAM
UNIVERSITATIS HELSINKIENSIS

14/2019

ALISON KUONY

Lacrimal Gland Morphogenesis, Maturation and Function

INSTITUTE OF BIOTECHNOLOGY
HELSINKI INSTITUTE OF LIFE SCIENCE (HiLIFE) AND
DEVELOPMENTAL BIOLOGY PROGRAM
FACULTY OF BIOLOGICAL AND ENVIRONMENTAL SCIENCES
DOCTORAL PROGRAMME IN INTEGRATIVE LIFE SCIENCE
UNIVERSITY OF HELSINKI

Lacrimal Gland Morphogenesis, Maturation and Function

Alison Kuony

Institute of Biotechnology
Developmental Biology Program and Division of Genetics
Department of Biosciences
Faculty of Biological and Environmental Sciences
Integrative Life Sciences Doctoral School
University of Helsinki
2015-2019

ACADEMIC DISSERTATION

Academic dissertation of Alison Kuony, on lacrimal gland morphogenesis, maturation and function, to be presented for public examination with the permission of the Faculty of Biological and Environmental Sciences of the University of Helsinki in Sali 236 (Aud 1) at Infokeskus Korona (Viikinkaari 11), on the 15th of March 2019, at 12 o'clock.

Supervisor	Docent Frederic Michon University of Helsinki, Finland
Thesis committee members	Docent Satu Kuure University of Helsinki, Finland & Professor Jukka Jernvall University of Helsinki, Finland
Pre-examiners	Professor Kai Kaarniranta University of Eastern Finland, Finland & Associate Professor Heli Skottman University of Tampere, Finland
Opponent	Associate Professor Igor Adameyko Karolinska Institute, Sweden Center for Brain Research Medical University of Vienna, Austria
Custodian	Professor Juha Partanen University of Helsinki, Finland
Faculty representative	Associate Professor Susanna Fagerholm University of Helsinki, Finland

ISBN 978-951-51-4913-8 (paperback)
ISSN 2342-3161 (printed)
ISBN 978-951-51-4914-5 (PDF)
ISSN 2342-317X (PDF, http://ethesis.helsinki.fi)
The Faculty of Biological and Environmental Sciences uses the Urkund system (Plagiarism recognition) to examine all doctoral dissertations.

The cover of this thesis book was adapted from "Le Lanceur De Couteaux" (The Knife Thrower), part of Henri Matisse's Jazz collection of collages and pochoir prints from 1947. Henri Matisse (1869-1954) was a French artist known as a leading figure in modern art.

Layout: Tinde Päivärinta/PSWFolders Oy/Ltd
Press: Hansaprint Oy, Turenki 2019

"As a scientist I am indeed only an ant, insufficient and anonymous, but I am stronger than I look and part of something that is much bigger than I am."

– **Hope Jahren**, Lab Girl

TABLE OF CONTENTS

LIST OF ORIGINAL PUBLICATIONS

I. **Kuony, A.** and Michon, F. (2017), Epithelial Markers aSMA, Krt14, and Krt19 Unveil Elements of Murine Lacrimal Gland Morphogenesis and Maturation. Front. Physiol. 8:739.

II. Kalha, S., **Kuony, A.** and Michon, F. (2018), Corneal Epithelial Abrasion with Ocular Burr As a Model for Cornea Wound Healing. J. Vis. Exp. (137), e58071, doi:10.3791/58071.

III. **Kuony, A.**, Ikkala, K., Kalha, S., Magalhães, A.C., Pirttiniemi A. and Michon, F. (Submitted to Development), Ectodysplasin-A signaling as key integrator in the lacrimal gland/cornea feedback loop

In addition, unpublished data are presented in this dissertation.

Contributions:
I and III. The author contributed in planning and conducting the experiments, analysing the data and writing the manuscript.
II. The author contributed in conducting the experiments and writing the manuscript.

ABBREVIATIONS

αSMA	Alpha smooth muscle actin
βGal	β-galactosidase
ABCG2	Adenosine triphosphate binding cassette superfamily G member 2
Acta2	Alpha 2 Actin, Alpha smooth muscle actin
ALDH	Aldehyde dehydrogenase
Aqp	Aquaporin
BMP	Bone morphogenetic protein
Bmpr	Bone morphogenetic protein receptor
BSA	Bovine serum albumin
C57BL/6	Wild type mouse strain
Casp3	Caspase 3
cDNA	complementary deoxyribonucleic acid
CE	Corneal epithelium
CFP	Cyan fluorescent protein
Col	Collagen
DAPT	N-[N-(3,5-Difluorophenacetyl)-L-alanyl]-S-phenylglycine t-butyl ester
DED	Dry eye disease
Des	Desmin
Dkk	Dickkopf
Dlk1	Delta Like Non-Canonical Notch Ligand 1
DMSO	Dimethyl sulfoxide
E	Embryonic day
Ecad	E cadherin
ECM	Extra cellular matrix
Eda	Ectodysplasin, Eda-A1
Edar	Ectodysplasin A1 receptor
Edarrad	Edar-associated death domain
EDTA	Ethylenediaminetetraacetic acid
EGF	Epidermal growth factor
EMT	Epithelial to mesenchymal transition
EPCP	Epithelial cell progenitor
EtOH	Ethanol
FBS	Foetal bovine serum
FGF	Fibroblast growth factor
FGFR	Fibroblast growth factor receptor
Fn	Fibronectin
Fucci	Fluorescent ubiquitination-based cell cycle indicator
Fz	Frizzled
Gal	Galactosidase

GFP	Green fluorescent protein
GRN	Gene regulatory network
HED	Hypohidrotic ectodermal dysplasia
HGF	Hepatocyte growth factor
Hrs	Hours
HSPG	Heparan sulphate proteoglycans
ICD	Intra cellular domain
ICR	Wild type mouse strain
IgA	Immunoglobulin A
IL1	Interleukin 1
Jnk	c-Jun N-terminal kinase
Krt	Keratin
LG	Lacrimal gland
Lgr5	Leucine-rich repeat-containing, G-protein-coupled receptor 5
Lrp	Low-density lipoprotein receptor-related protein
Ltf	Lactotransferrin
Mapk	Mitogen-activated protein kinase
MEC	Myoepithelial cell
MET	Mesenchymal to epithelial transition
MG	Meibomian gland
Mmp	Matrix metalloproteinases
mRNA	Messenger Ribonucleic acid
mT/mG	Membrane-localized TdTomato/ membrane-localized EGFP
NCC	Neural crest cell
NECD	Notch extra cellular domain
NF-kB	Nuclear factor kappa-B
NICD	Notch intra cellular domain
NMRI	Wild type mouse strain
P	Postnatal day
PBS	Phosphate Buffered Saline
PCP	Planar cell polarity
PFA	Paraformaldehyde
Phospho-H3	Phosphorylated Histone 3
R26R	Rosa26 region
RFP	Red fluorescence protein
RNA	Ribonucleic acid
RT-PCR	Reverse transcription polymerase chain reaction
RT-qPCR	Reverse transcription quantitative polymerase chain reaction
SC	Stem cell
SjS	Sjögren's syndrome
SMA	Smooth muscle actin
SMG	Submandibular gland

Srl	Sarcalumenin
Tabby	Spontaneous Eda-null mouse strain
TEB	Terminal end bud
Tgfβ	Transforming growth factor beta
TNF	Tumour necrosis factor
Vdr	Vitamin D receptor
VIP	Vasoactive intestinal peptide
Wnt	Vertebrate homologue of the *Drosophila* Wingless gene
Wo	Weeks old
WT	Wild type
YFP	Yellow fluorescent protein
XLHED	X-Linked Hypohidrotic ectodermal dysplasia

Following the official guidelines for the nomenclature of genes, alleles, and mutations in mouse, the gene and transcript names are hereafter written in italics and the proteins are capitalized.
As an example: *Eda* gene and transcript; EDA protein and Eda representing the general signalling pathway.

SUMMARY

The lacrimal apparatus is responsible for producing the three-layered tear film which protects the eye surface. The tear film external or lipid layer is produced by the meibomian glands (MGs) located in the eyelid. The middle layer, or aqueous layer is the most abundant and is synthesized by the lacrimal gland (LG), localized in the orbit. The last layer is the internal or mucous layer, secreted by the goblet cells distributed within the conjunctival epithelium. Specifically, the aqueous component is the main source of growth factors destined to the avascular cornea. Those are necessary for corneal epithelium maturation and subsequent renewal.

A defective tear film leads to dry eye diseases (DEDs) affecting an increasing percentage of the population (more than 35% in the elderly). Although DEDs can lead to visual loss in extreme cases, no definitive treatment has been developed so far.

LG is a branched ectodermal organ, which starts to develop around embryonic day (E)13.5-E14 in mouse. Around E15, an epithelial bud invaginates into a mesenchymal capsule. Branching morphogenesis starts around E16 and continues in postnatal stages. In adult LG, the epithelium can be divided in three compartments: the acini, synthesizing the majority of LG fluid; the ducts, modifying its composition; and the myoepithelial cells (MECs), with contractile functions. LG maturation occurs in postnatal stages, and is concomitant with dynamic gene expression changes, necessary for cell terminal differentiation and *ipso facto* LG function.

In my thesis work, I first focused on the basis of LG morphogenesis, delineating early molecular and cellular events implicated in its formation. I characterized LG epithelium growth and patterning by investigating cell proliferation and gene expression profiles. I highlighted a major LG epithelial outgrowth around postnatal day (P)7, before the beginning of cornea stratification (around P10) and the eyelid opening occurring between P12-P14.

LG is known to play a role in corneal biology, notably during the wound healing process by secreting growth factors in the tear film. I studied the relationship between LG and cornea, first participating to the establishment of a reliable model to follow mouse corneal re-epithelialization after mechanical abrasion. This showed that the cornea heals within three days after the injury.

To go further, I used this abrasion model to study the communication between LG and cornea in a pathophysiological situation. I used X-linked Ectodermal Dysplasia (XLHED), resulting from an *Eda* loss-of-function mutation and leading to dry eye symptoms in human, to investigate LG-cornea interaction in a dry eye context. As the effect of $Eda^{-/-}$

mutation on LG biology were unclear, I first demonstrated the important role of Eda pathway in LG maturation and physiological functions. Next, I studied the impacts of LG maturation defects on cornea healing process and showed an altered gene regulation in *Eda*$^{-/-}$ LG in response to corneal injury. Moreover, I showed that Eda pathway gets inhibited in both LGs following corneal abrasion, further indicating a sophisticated cross-talk between bilateral LGs and the wounded cornea.

In addition of improving the general knowledge on LG biology, my work participated to shed a new light on the aetiology of XLHED-associated dry eye and on the resulting defective cornea wound healing.

RESUME (en français)

L'appareil lacrymal est responsable de la production du film oculaire protégeant la cornée. Le film oculaire est composé de trois couches. La couche externe ou couche lipidique est secrétée par les glandes meibomiennes, situées dans les paupières. La couche intermédiaire ou couche aqueuse est produite par la glande lacrymale, localisée dans l'orbite. Cette portion aqueuse représente la majeure partie du film oculaire. La cornée ne possédant pas de vaisseaux sanguins, la partie aqueuse est aussi l'unique source de facteurs de croissance nécessaires à la maturation et au maintien de l'intégrité de celle-ci. Pour finir, la couche interne ou partie muqueuse est secrétée par les cellules à goblet, localisées sur la conjonctive.

La glande lacrymale est un organe ectodermique branché dont le développement commence aux alentours du jour embryonnaire (E)13.5-E14 chez la souris. A E15, la glande lacrymale est séparée en un bourgeon épithélial s'invaginant dans un mésenchyme. Le branchement de l'épithélium commence vers E16 et continue après la naissance. Chez la souris adulte, la glande lacrymale possède trois compartiments : les acini, produisant la majeure partie du composant aqueux ; les canaux, modifiant cette sécrétion, et les cellules myoépithéliales, sécrétant la lame basale, nécessaire à l'intégrité structurelle de la glande, et ayant des propriétés contractiles importantes à l'excrétion du fluide produit.

La glande subit une étape de maturation pendant les stades postnataux. Cette maturation se traduit par des changements d'expression génique conduisant à la différentiation cellulaire terminale.

Dans mon projet de thèse, j'ai premièrement créé des outils indispensables pour l'étude du développement embryonnaire de la glande lacrymale. Je me suis intéressée à la caractérisation de sa formation précoce, ainsi qu'à sa maturation. De plus, j'ai étudié la glande lacrymale dans une situation pathologique, dans le cas de la dystrophie ectodermique liée à l'X. Ce syndrome est retrouvé chez l'homme, et est associé à des symptômes d'œil sec. J'ai mis en évidence le défaut de maturation des glandes lacrymales présentant une perte de fonction du gène Ectodysplasine (Eda), et j'ai fait le lien avec une réduction de leur fonction.

La production de protéines par la glande lacrymale à la suite d'une blessure de la cornée est nécessaire à la réparation de l'épithélium cornéen. Par la suite, j'ai participé à l'élaboration d'un protocole d'abrasion de la cornée et l'ai utilisé afin d'étudier le dialogue cornée-glande lacrymale. Dans l'ensemble, mes travaux de thèse ont permis de faire avancer les connaissances générales sur la glande lacrymale, ainsi que sur la communication établie entre la cornée et la glande lacrymale.

1. REVIEW OF THE LITERATURE

1.1. Lacrimal functional unit morphology and function

1.1.1. Overview

About 360 million years ago, the transitional period initiating the terrestrialisation of crossopterygian fish gave rise to the first amphibians. Among the adaptations required to survive in their new habitat, protection of the eye surface from the dry aerial environment became instrumental for clear sight. The adaptation of specialized glands to the production of the tear film was the key to maintain the eye surface moist (Murube 2009).

The tear film is composed of three layers, namely lipid or external layer; aqueous or middle layer and mucous or internal layer. These three different layers are mainly produced respectively by the meibomian glands (MGs), the lacrimal glands (LGs) and the goblet cells (**figure 1**). Lastly, harderian glands lubricate the nictitating membrane or third eyelid. The nictitating membrane is present in almost all mammals but in higher primate species and will not be described here. Overall, the lacrimal apparatus produces tears that are drained into the conjunctival sac via the puncta (**figure 2**) (Orge and Boente 2014).

The lacrimal film has both nutritional and protective (physical and anti-microbial) properties (Tiffany 2008) It is 3µm thick in human but thicker in the mouse, on average 7µm (King-Smith et al. 2000; Wang et al. 2003; Johnson and Murphy 2004).

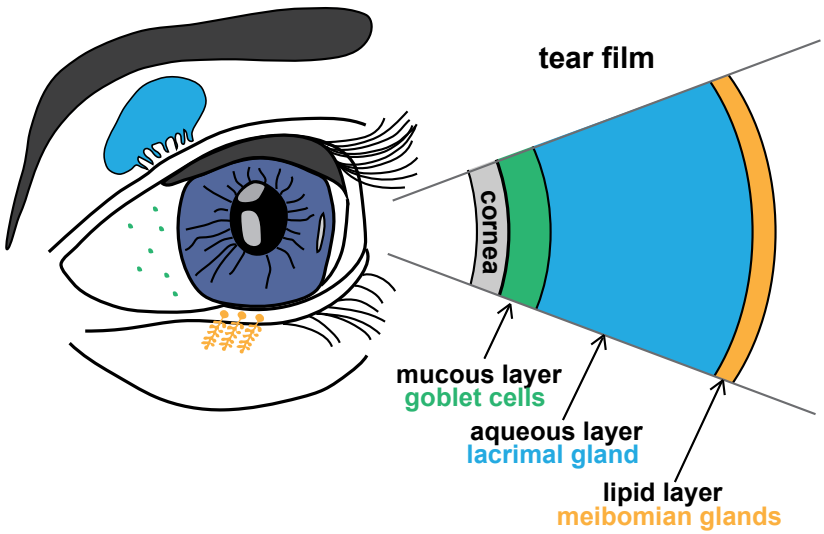

Figure 1: The tear film. The lacrimal apparatus is constituted of three compartments: the meibomian glands (orange) are localized in the eyelids and secrete the lipid layer of the tear film. The lacrimal gland (blue) is located in the orbit and produces the aqueous layer. The goblet cells (green) are distributed on the conjunctiva surface and form the mucous layer.

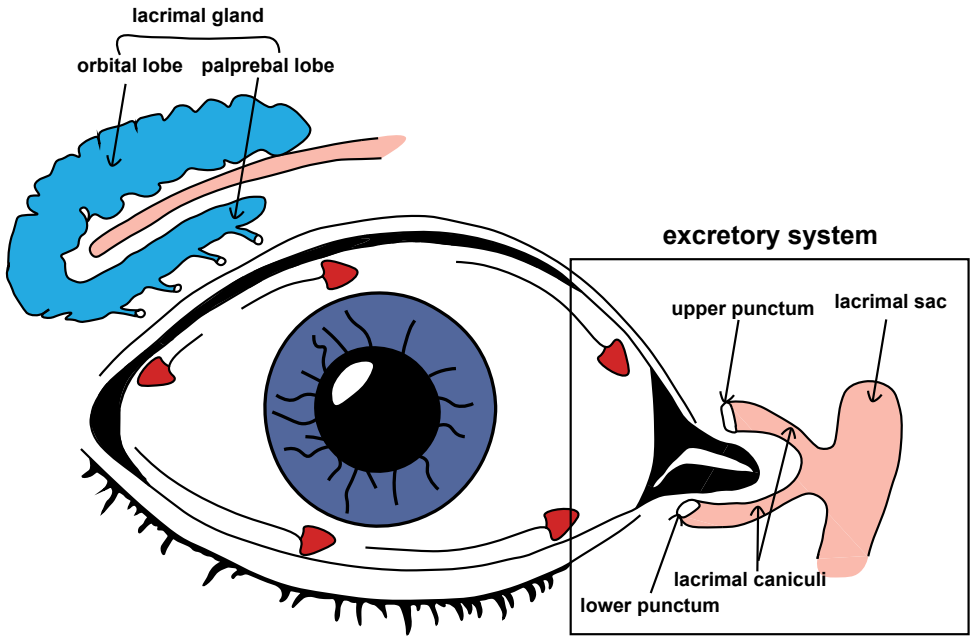

Figure 2: Tear distribution on the ocular surface. The lacrimal gland (LG) produces most of the tear fluid. In human, the LG is separated into two lobes – the palpebral and the orbital lobes, anatomically close from each other. The lacrimal fluid is distributed (red arrows) on the ocular surface due to eyelid movements and the presence of a tear meniscus. Subsequently, the tear fluid is collected and drained through the upper and lower puncta into the lacrimal sac via the lacrimal canaliculi. Modified from (Holly and Lemp 1977).

1.1.2. Meibomian glands

MGs are sebaceous glands distributed within the eyelids. In human, upper eyelids contain roughly 25 glands, and lower eyelids about 20 glands (**figure 1**). Each gland is composed of a long canal encircled by multiple lipid-producing acini (Obata et al. 1994; Obata 2002). MG histological and secretory functions are very similar in mouse and human (Butovich 2017).

MGs are responsible for the production of the lipid layer of the tear film, or meibum (Paulsen and Berry 2006), mainly composed of polar and nonpolar lipids (McCulley and Shine 2003; Butovich 2017). Phospholipids are the predominant polar lipids; while nonpolar lipids are represented by a mixture of cholesterol, cholesterol esters, and wax esters. Meibum is liquid at eyelid temperature, with a melting range between 19.5 and 32.9°C (Foulks and Bron 2003).

Directly in contact to the environment, the lipid layer protects the tear film from evaporation, enhances its stability and spreading, and creates a barrier to prevent from contaminations.

It is thought that a stable interaction between the lipid and aqueous layers requires the interaction between polar lipids from the lipid layer side, and lipophilic proteins (such as lipocalins) from the aqueous layer (Foulks and Bron 2003).

1.1.3. Main and accessory LGs

The main LG is an almond-shaped tubulo-acinar gland with secretory functions, divided in two lobes, and responsible for the production of the tear film aqueous layer. Interspecies differences exist between LGs of human, rabbit and rodent (including mouse and rat) (for review, (Schechter et al. 2010)). It seems that all species share the two-lobed LG feature. Nonetheless, the localization of the main lobe varies. In rodent and in some monkey species, a small lobe is found in the orbit and a bigger one is located away from the eye, close to the ear region (Veiga Neto et al. 1992) (**figure 3**). Human and rabbit species have both lobes in the orbit. The human orbital lobe is the biggest one, localized in the lacrimal fossa of the frontal bone (Lorber 2007; Orge and Boente 2014). The smaller palpebral lobe is located in the superolateral region of the eyelid, underneath the tendon of the levator palpebrae superioris muscle (**figure 2**) (Paulsen and Berry 2006).

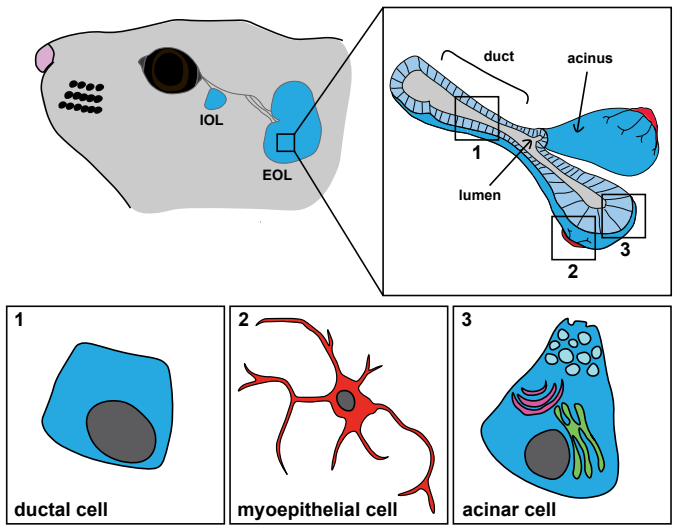

Figure 3: The murine lacrimal gland. The murine lacrimal gland (LG) is divided into two lobes away from each other. The intra-orbital lobe is close to the eye; the extra-orbital lobe (EOL) develop away from the eye, close to the ear region. LG epithelium is divided into three compartments. The ducts, participating to the LG fluid composition, are formed by cuboid cells (1). The myoepithelial cells (MECs, 2) secrete the basal membrane and have contractile functions. The acini are responsible for the production of the majority of LG fluid. They are composed of acinar cells, which contain a large number of secretory vesicles (3). During fluid excretion, the secretory vesicles fuse with the apical side of the acinar cell membrane and release their content into the lumen of the ducts.

Despite the location differences, the LG histological structure is conserved. Each lobe is divided into lobules, separated from each other by loose connective tissue, composed of extracellular matrix (secreted by fibroblasts), nerves, and blood vessels (Obata 2006). The tear product is delivered onto the eye surface via lacrimal ducts: one final duct in the mouse compared to numerous (6 to 12) in human (Lorber 2007).

Along with the main LG, in human, LG accessory glands (glands of Wolfring and Krause) are localized in the palpebral conjunctiva and in the conjunctival fornix, respectively (Chastain and Sindwani 2006; Lorber 2007; Kels et al. 2015). LG accessory glands are considered to have similar structures and functions to the main LG and participate for about 10% of the tear production (Orge and Boente 2014).

The mature LG is commonly formed of three distinct domains: acinar, myoepithelial and ductal compartments, each having a role in the production, modification and excretion of the LG fluid (**figure 3**).

Acini are composed of pyramid-shaped acinar cells with a central lumen (Obata 2006). They represent around 80% of the LG volume (Schechter et al. 2010) and secrete the majority of the proteins, electrolytes, water and other constituents composing the aqueous part of the tear film (Obata 2006). Basic histoarchitectural features (acinus ultrastructure and stromal compartment), appear to be the main differences between rodent and human LGs. The rodent LG depicts tightly compacted lobules and narrow lumen in the acini, while the human one has looser lobules, and larger lumen. Although rabbit LG has been reported to better match the human LG histoarchitecture, the functional aspects related to protein composition, production and secretion, seem to be conserved in human, rodent and rabbit LGs (Schechter et al. 2010). These species share a common heterogeneity in the acinar secretory vesicles, produced by both serous and mucous acinar cells in variable proportion. This observation defines the LG as a seromucous organ (Schechter et al. 2010).

Myoepithelial cells (MECs) are stellate and multi-processed cells with contractile functions, located around the acini. They maintain acinar integrity, secrete the basal membrane components and participate to acinar production excretion (Makarenkova and Dartt 2015).

Finally, ducts participate to LG fluid modification and secretion (Katona et al. 2014; Vizvari et al. 2016; Berczeli et al. 2018). Particularly, ductal cells are water permeable and exhibit ion channels acting on LG fluid osmolarity.

1.1.4. Goblet cells, conjunctival and corneal epithelium

Goblet cells are secretory cells distributed all over the conjunctival epithelium (**figure 1**). They are responsible for producing the majority of the tear film mucous or internal layer of the tear film (Takahashi et al. 2013). The mucous layer forms a soluble surfactant necessary to distribute the water on the whole eye surface (Holly and Lemp 1977) and represents a barrier against pathogens.

Amongst species, conjunctival goblet cells have similar functions but a variable distribution pattern. In human, goblet cells can be observed both as individuals as well as in clusters and the density is higher in the nasal region of the conjunctiva. Contrastingly,

mouse goblet cells are mainly found distributed as clusters all over the conjunctiva (Gipson 2016).

Although only the goblet cells are capable to supply a sufficient amount of soluble surfactant, various other cells are capable of producing mucins. These include conjunctival and corneal epithelial cells, and to a lesser degree the main and accessory LG acinar and duct cells (Paulsen et al. 2003).

Mucins, a general term for high molecular weight glycoproteins, form a hydrophilic layer on the eye surface. Two types of mucins can be found in the internal layer of the tear film: secreted and membrane-bound mucins. Goblet cells produce the majority of the secreted mucins, while conjunctival and corneal epithelial cells produce the membrane-bound ones.

Mucins dissolve partially in the aqueous layer, making it difficult to separate both layers (Takahashi et al. 2013). Finally, the glycocalyx, secreted by the surface corneal epithelial cells, forms a scaffold of long chain molecules binding and stabilizing the mucous layer at the corneal surface (Gipson 2004).

1.2. Spotlight on the eye

1.2.1. Overview

The human and mouse eyes are camera type eyes, which can be divided into the anterior and the posterior segments. The anterior eye segment comprises cornea, iris (separating the anterior and posterior chambers), ciliary body and lens (**figure 4**). The cornea represents the avascular transparent layer in contact with the external environment and covered by the

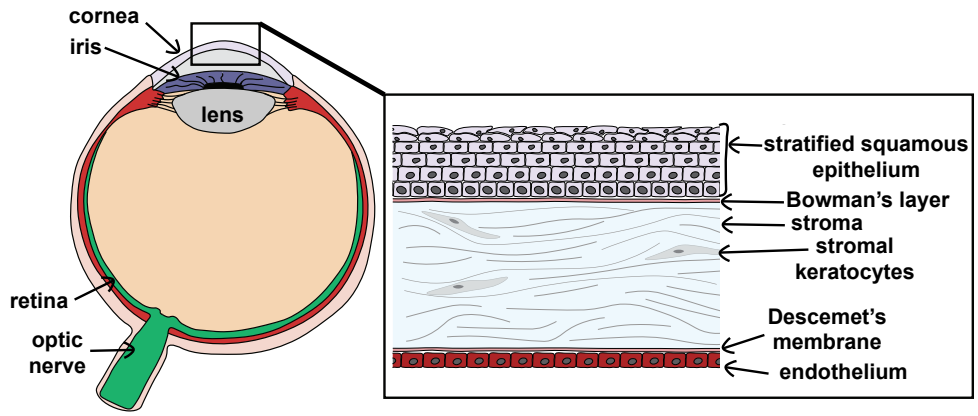

Figure 4: The human eye. The human eye is composed of the anterior and the posterior segments. The anterior eye segment notably includes the cornea, iris and lens. The cornea is formed by three compartments: the stratified squamous epithelium (5 to 6 cell layers), the stroma and the endothelium. The Bowman's membrane separates the stratified epithelium from the stroma and the Descemet's layer lays in between the stroma and the endothelium. The stroma is secreted by the stromal keratocytes. The retina and the optic nerves are part of the posterior eye segment.

tear film. Together with the lens, they form a single optical element, and are instrumental to light focusing onto the retina.

Finally, the posterior eye segment, which will not be described here, is composed of vitreous humor, choroid, retina and optic nerve.

1.2.2. Eye morphogenesis

In early development, one of the three embryonic layers, the ectoderm, differentiates into the surface ectoderm and the neurectoderm (subsequently giving rise to the neural crest and the neural tube) (**figure 5**). The first eye structures originally derive from the neurectoderm, producing both the neural crest and the neural tube. The neural tube will form the optic vesicle, invaginating to become the optic cup. The optic cup is responsible for the formation of the retina, ciliary body and iris. In parallel, the surface ectoderm interacts with the underlying structures and transforms into the different cranial placodes, depending on the molecular signals received. The cranial placodes gather the oral, olfactory, lens and corneal epithelium (CE) placodes. In absence of signal however, the surface ectoderm leads to the epidermal fate (for review, (Dhouailly et al. 2014)).

The different steps resulting in cornea development are conserved among species, but the timeline differs. For simplicity, only human and mouse timelines are described here. Current understanding is that the CE and lens placodes derive from surface ectoderm common eye precursors, and that CE presumptive territory becomes specified upstream the lens.

The optic vesicle sends positive signals to the above specified CE. This results in CE-derived committed lens placode, which invaginates to form the lens vesicle before detaching from the remaining CE. Subsequently, a wave of neural crest cells (NCC) migrates between the lens vesicle and the CE and forms the corneal endothelium along with the stromal fibroblasts, secreting the corneal stroma. NCC-derived endothelial cells produce necessary lens-suppressing signals directed to the overlaying specified CE, stabilizing CE fate over lens differentiation.

In mouse, CE and lens placodes arise around E8 (**figure 5**). The lens placode is specified by embryonic day (E) 10 and the presumptive CE can be observed at E11.5, laying above the lens vesicle. The NCC migration wave occurs between E12 and E14. By E15.5, the three corneal elements, i.e. CE, stroma and endothelium are already in place. At birth, the CE is composed of 1-2 cell layers (for review, (Swamynathan 2013)).

In human, the optic precursors arise around the fourth week of gestation. This corresponds approximately to stages 12-13 in the Carnegie classification by Ronan O'Rahilly (Gasser et al. 2014). By the end of the fourth week of gestation, the optic vesicle lies underneath the surface ectoderm. Subsequently, by the sixth-seventh week (stages 17-20), the lens is mostly formed, and CE commitment occurs. Cornea development takes place during the seventh and eight weeks of gestation (stages 18-23). CE, stroma and endothelium are formed by the end of the eighth week of gestation (stage 23) (Pearson 1980).

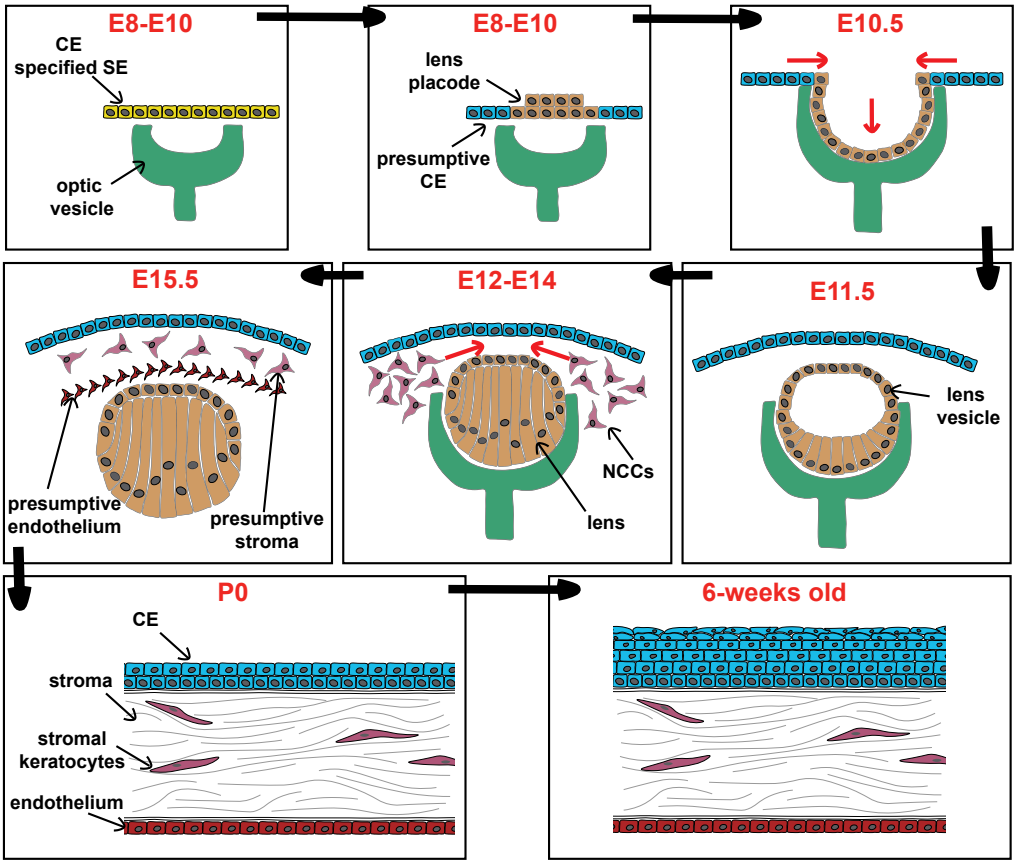

Figure 5: Eye development in mouse. Between E8 and E10, the optic vesicle sends positive signals to the above specified corneal epithelium (CE) to give rise to the lens placode. Subsequently at E10.5, the lens placode invaginates and forms the lens vesicle by E11. Between E12-E14, neural crest cells (NCCs) migrate between the lens vesicle and the CE to form the presumptive corneal endothelium and stroma by E15.5. At birth, the CE is composed of 1-2 cell layers, and stromal keratocytes secrete the stromal components. In postnatal stages, stratification results in the stratified CE by 6 wo. SE: surface ectoderm. Modified from (Swamynathan 2013).

1.2.3. Cornea postnatal maturation, renewal and regeneration

The mature cornea is formed by three compartments: a stratified epithelial outer layer, a stroma and an endothelial inner layer. In human and mouse, the stratified epithelium, the stroma and the endothelium are separated from each other by a basal membrane (the Bowman's membrane and Descemet's layer, respectively) (Kels et al. 2015) (**figure 4**). In mouse, the presence of a Bowman's membrane remains however controversial.

At birth in the mouse, CE is composed of 1-2 cell layers. In this specie, eyelid opening only occurs between postnatal day (P) 12-14, subsequently after the beginning of cornea stratification (P10) (Zieske 2004; Zhang et al. 2015). During this period, rapid cell proliferation results in a 5-6-layered CE by 3 weeks old (wo) and in a 6-8-layered squamous epithelium by 8-10 wo. Cornea maturation timeline observes tremendous differences between species. While in human, eyelids are already opened in the womb and the time of fully mature cornea has not been established (however occurring after birth), the cornea appears fully mature after the two first weeks of embryogenesis in chick embryo and around P12 in rabbit. Strikingly in mouse, the CE reaches full maturity only 6-7 months after birth (for review, (Dhouailly et al. 2014)). In the mouse, cornea maturation is assisted by LG growth factors secretion (Zieske 2004). It is however unclear if this would be the case in human, as cornea maturation time has not been rigorously established, and LG maturation occurs around 6 wo.

Corneal maturation can be followed by the expression of *Keratin19* (*Krt19*), high in embryonic CE but decreasing in postnatal stages (Kalha et al. 2018b). In addition, the differentiated central CE can be recognized by the expression of *Krt3/Krt12* (KRT3/KRT12 forming a pair) in numerous species but in the mouse, in which only *Krt12* is expressed in the mature CE (Chaloin-Dufau et al. 1993). The corneal SC niche or limbus localizes in periphery at the border between cornea and conjunctiva (Schermer et al. 1986). In contrast to the central CE, the adult limbus is overall marked by KRT19 (Kalha et al. 2018b), and the presence of KRT5/KRT14 pair in its basal layer. Moreover, *Krt15* was recently reported as a specific marker for mouse limbal cells (Nasser et al. 2018). In human, the limbus is formed by the palisades of Vogt, which are undulated regions forming crypts (for review, (Dhouailly et al. 2014)). In the mouse, however, no crypts can be detected. Nonetheless, recent findings demonstrated that upon limbal injury, central corneal-committed cells could dedifferentiate in order to repopulate the limbus area and form *Krt15*-expressing limbal SCs-like cells (Nasser et al. 2018). Besides, from birth to adulthood, mouse CE has been shown to be renewed by local pools of progenitors which are replaced by limbal SCs every 4 to 8 weeks (Kalha et al. 2018b). Together these findings highlight the important adaptive capacities of the cornea.

1.2.4. Cornea innervation

In all mammals, the major type of corneal nerve fibres are sensory afferent projections, mainly deriving from the ophthalmic division of the trigeminal nerve (for review, (Muller et al. 2003)). These nerves transduce any chemical, mechanical or thermal stimuli from the cornea to the central nervous system to ensure the maintenance of a healthy environment for the CE. These stimuli reflect for example the ocular dryness or possible external hazards (Yang et al. 2018). To a lesser measure, the cornea receives sympathetic innervation, coming from the superior cervical ganglion. In some mammals, corneal parasympathetic innervation arises from the ciliary ganglion, but there is up to date no evidences in human (Muller et al. 2003).

In the mouse, no innervation can be detected in the eye anterior segment at E11.5. The innervation of the cornea area begins by the stroma around E12.5-E13.5 in the mouse (for review, (Lwigale 2015)). The first nerves to appear are the afferent projections of the trigeminal nerve's ophthalmic branch and they arise from the four quadrants of the eye, i.e. dorsal-temporal, dorsal-nasal, ventral-temporal, and ventral-nasal quadrants. The secretion of axon guidance molecules (such as semaphorins) in the lens underlying the cornea have been reported to be necessary for proper patterning of the corneal nerves (Lwigale and Bronner-Fraser 2007).

The first signs of CE innervation are however only detected at E16.5 (McKenna and Lwigale 2011), when the stromal compartment is already fully innervated. At this stage, each projection or nerve bundle from the stromal compartment repeatedly ramifies into smaller branches as it projects perpendicularly to the corneal surface to reach the central CE. This ramification occurs concomitantly to CE stratification, in postnatal stages (**figure 6**).

Around P21, all nerve bundles form a sub-basal plexus within the stroma and subsequently invade the central cornea forming epithelial leashes. This results in a swirl pattern which is visible from birth to adulthood. This swirl pattern is also found in adult

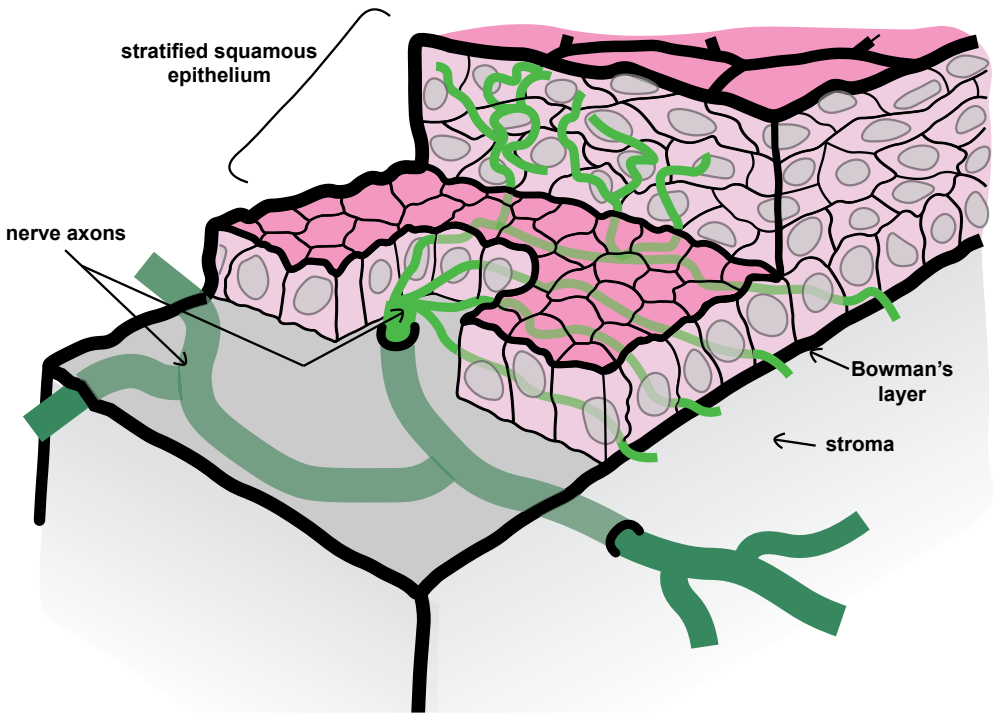

Figure 6: Innervation of the cornea. During corneal epithelium (CE) stratification, the nerve bundles localized in the stromal compartment travel perpendicularly through the Bowman's membrane and penetrate the CE. The nerves axons ramify into smaller branches to reach the corneal surface and colonize the different layers of the squamous stratified CE. Modified from (Rozsa and Beuerman 1982).

human (Patel and McGhee 2005; Marfurt et al. 2010). This is however not common to all species. The timeline of innervation varies from mouse to human, but the different steps remain similar in both species. In human, roughly 30 nerves can be detected in the stroma at 3 months after birth (McKenna and Lwigale 2011).

1.3. Spotlight on the lacrimal gland

1.3.1. LG morphology

1.3.1.1. LG embryonic development

Similarly to other ectodermal organs, including salivary, sweat and mammary glands, LG initially develops from a thickening of an epithelium in result to an interaction epithelium-mesenchyme (for review, (Yao and Zhang 2017)). The conjunctival epithelium, derived from the surface ectoderm, represents the LG origin (Makarenkova et al. 2000; Orge and Boente 2014).

In the mouse, LG formation begins around E13.5-E14 (Makarenkova et al. 2000). An epithelial bud invaginates in a mesenchymal capsule at the temporal edge of the eye around E15 and by E16, branching morphogenesis results in the formation of elongated branches with terminal end buds (TEBs) (Yao and Zhang 2017). Branching morphogenesis continues in postnatal stages (Makarenkova and Dartt 2015) (**figure 7**).

In human, LG early formation happens around the seventh week of gestation (Carnegie stages 19-20) (de la Cuadra-Blanco et al. 2003). LG ducts are formed later, at about 12 weeks of gestation. Human LG development can be divided into three stages: presumptive

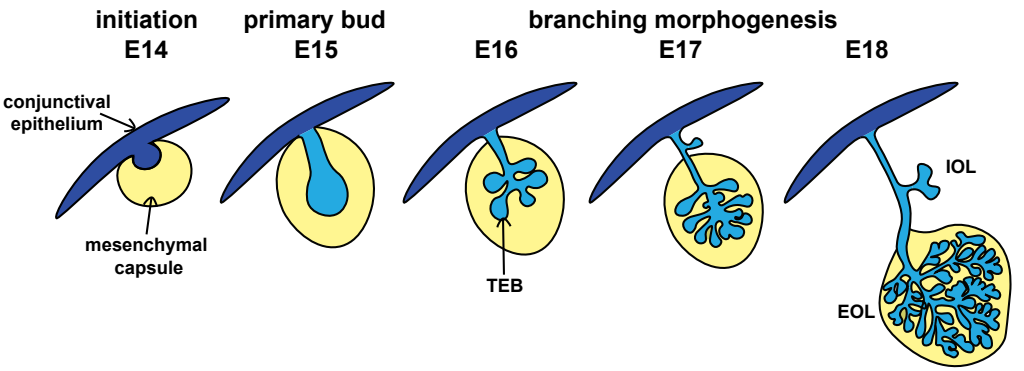

Figure 7: Mouse lacrimal gland embryonic development. Lacrimal gland (LG) development timeline differs according to the genetic background of the mouse, but the different steps are identical from one wild-type strain to the other. For clarity, the timeline depicted here is the one for the ICR mouse strain. LG extra-orbital lobe (EOL) formation initiates around E14 with the invagination of the conjunctival epithelium in a mesenchymal capsule. At E15, the primary bud (epithelial compartment, blue) elongates in the mesenchymal compartment (yellow). Branching morphogenesis starts around E16, forming terminal end buds (TEBs) and continues after birth. At E17, the intra-orbital lobe sprouts close to the eye, from the duct in elongation.

glandular (stages 19-20), epithelial bud (stages 21-23) and glandular maturity stages (9-16 weeks of gestation). Despite a fully formed LG at birth, the mature excretory functions are only acquired postnatally, during the first 6 weeks of life (Paulsen and Berry 2006; Orge and Boente 2014).

1.3.1.2. LG postnatal maturation

Postnatal observation of MEC and acinar compartments reveals a possible correlation between the maturation processes of both LG compartments (Wang et al. 1995). MECs morphological changes are correlated with the increased production of secretory vesicles in the acini. At birth and until P7, acinar cells do not exhibit secretory vesicles in their cytoplasm and MECs have an immature, round aspect. At P7, few secretory vesicles can be observed in the subnuclear region of the acinar cells. At this stage, acini are organized into small lobules and MECs, found around the acini, are flattened and develop short processes (Makarenkova and Dartt 2015). At P14, numerous secretory vesicles can be observed in the acinar cells cytoplasm. Later on, acini increase in size and MECs develop longer and wider processes, forming an arborization embracing the acini. The area occupied by MECs in comparison to acinar cells decreases with the age of the mouse, and by 4 wo, only 6% of the epithelial compartment is occupied by MECs. No significance morphological differences can be noticed in the LG epithelial compartment between 4 and 8 wo.

On the molecular level, Farmer and al. recently used single-cell RNA sequencing, RT-qPCR and immunohistochemistry staining to highlight the important differentiation process occurring in all LG compartments between embryonic and postnatal stages (Farmer et al. 2017). The study revealed the high diversity in LG cell populations, both in the epithelial and mesenchymal compartments. Notably, single-cell RNA sequencing shows that LG mesenchyme depicts four distinct cell subpopulations at P4, compared to only 2 at E16. Moreover, from P0 to 16 wo (adult LG), all LG compartments undergo a progressive maturation process. *Sox10, Aquaporin5* (*Aqp5*) and *BhlhA15* (also known as *Mist1*) dynamic expressions highlight acinar cell differentiation process. *Sox10*, known to be expressed in the LG bud (Chen et al. 2014), is downregulated after P7. In contrast, *Aqp5* and *BhlhA15* expressions increase from P1 to P14. Similarly, *Lactotransferrin* (also known as *Lactoferrin*, *Ltf)* expression progressively increases in postnatal stages and is highly upregulated in the adult LG, as expected from its high concentration in the tear film. Furthermore, *Krt19* and *Slc12a2* (also called *Nkcc1*), two ductal markers, are mainly downregulated in postnatal compared to embryonic LG. *Krt5* and *Krt14* expression, used to study MECs differentiation in this study, decrease as well in postnatal stages.

This recent study demonstrates the onset of LG compartments dynamics occurring between embryonic and postnatal stages. Taken together, LG epithelial compartment differentiation is very dynamic. Evidences suggest that the ductal compartment is predominant in embryonic LG while the postnatal and adult LGs are mainly formed by the acinar compartment.

1.3.1.3. LG stem cells and regeneration

Although stem cells (SCs) and progenitors have not been fully characterized in LG, it is assumed that such cell populations remain in adult as LG is known to have regenerative capacities. Interleukin 1 (IL1)-alpha injections in mouse LG extra-orbital lobe induce an inflammatory reaction resulting in a large acinar cell loss by apoptosis and autophagy (Zoukhri et al. 2007; Zoukhri et al. 2008). The resulting injury is followed by cell proliferation in all LG compartments and further restoration of aqueous tear physiological levels. Nonetheless, the time course of LG recovery varies from seven to thirteen days depending on the mouse genetic background.

SCs are involved in organ maintenance and repair. Therefore, several studies attempted to describe LG SCs. MECs are commonly thought to retain SC features. A study on rats revealed that MECs express adenosine triphosphate binding cassette superfamily G member 2 (*ABCG2*), along with *Musashi 1*, *Nestin*, *Pax6*, *Chx 10*, *DN p63* and *Sox2* (Shatos et al. 2012), all known as SC markers (Reynolds and Weiss 1992; Sakakibara et al. 1996; Osumi et al. 2008; Fischer and Reh 2000; Hernandez Galindo et al. 2003; Ding et al. 2010; Violini et al. 2012). Interestingly, a population of cells expressing *ABCG2*, as well as aldehyde dehydrogenase (*ALDH*, involved in stemness potential) has also been discovered in human LG (Tiwari et al. 2012).

Transcriptomic analysis on regenerating mouse LG revealed an increase in muscle related genes, including Sarcalumenin (*Srl*) and Desmin (*Des*). However, immunohistochemistry staining demonstrated that MECs do not belong to the same cell population showing upregulated muscle related genes (Hawley et al. 2017). In addition, this study demonstrated *Runx1* and *Runx3* upregulation (Voronov et al. 2013), both involved in SC fate control (Kim et al. 2014; Takacs et al. 2017).

It has been shown in other organs that wound closure, cell extrusion (in case of apoptosis for example) as well as cell migration, are well known mechanisms which require cell-cell mechano-transduction, cytoskeleton and extracellular matrix (ECM) remodelling as well as active cell movements (for review, (Ladoux and Mege 2017)). Therefore, the upregulation of muscle related gene expression in MEC-distinct cells could this way be linked to a repair mechanism parallel to stemness and cell proliferation.

LG self-regeneration also involves epithelial-to-mesenchymal transition (EMT). EMT leads to the generation of cells with mesenchymal SC-like properties, which migrate to the site of injury and initiate LG repair. Subsequently, mesenchymal-to-epithelial transition (MET) occurs to generate new acinar and ductal cells (You et al. 2012).

Additionally, the newly formed mesenchymal stem-like cells need to migrate to the site of injury, and ECM remodelling is known to play an important role in LG repair process. Particularly, numerous ECM modifying enzyme genes (matrix metalloproteinases (*Mmps*), *Adams* and *Adamts*), collagens (including *Col1a1*, *Col1a2*, *Col12a1*) and other ECM associated factors (including *Tgfb1* and *Fn1*) are differently regulated depending on LG regeneration stage (Hawley et al. 2017).

Up to date, LG SC populations remain to be fully characterized (for review, (Yao and Zhang 2017)). Numerous stem/progenitor cell related genes have been studied in LG field, aiming at the discovery of one or more LG pluripotent/multipotent cell population(s).

An epithelial progenitor cell population (EPCP) was recently discovered (Gromova et al. 2017). This cell population is negative for endothelial, hematopoietic and mesenchymal markers. EPCP cells are positive for c-kit protein, the receptor for a cytokine involved in the activation of SC proliferation, known as SC factor. In addition, they display an upregulation of *Oct4* and *Vdr* (vitamin D receptor) expression, previously reported to be involved in cell pluripotency (Blomberg Jensen et al. 2012; Yan et al. 2014). *Runx1*, reported as a regulator of SC survival (Scheitz and Tumbar 2013), was also upregulated. Majority of these epithelial progenitor cells are highly proliferative when placed into culture, express *Pax6* (reported to mark committed transit amplifying progenitors in the corneal epithelium (Kucerova et al. 2012; Ouyang et al. 2014)) and can differentiate into *Aqp5*$^{+}$ secretory cells. Finally, these cells are able to engraft into acinar and ductal compartments when transplanted into injured or chronically inflamed LGs and to ameliorate diseased LG physiology.

1.3.1.4. Pathways involved in LG biology

1.3.1.4.1. Fgf pathway

Fibroblast growth factor (Fgf) pathway depicts a ubiquitous role both in development and disease. Notably, in vertebrate species, Fgf signalling is involved in nearly all tissues, from the induction of several organ development in the embryo, to tissue repair in the adult (for review, (Ornitz and Itoh 2015)). For instance, Fgf signalling takes part in mammary gland and hair follicle formation (Elo et al. 2017; Nguyen et al. 2018).

Fgf pathway is conserved amongst species but the number of proteins in play in the signalling cascade varies from one specie to the other. In human and mouse, 22 Fgf ligands, four receptors and numerous regulator proteins are known so far (for review, (Ornitz and Itoh 2015)). The Fgf ligands are diffusible proteins and can be categorized according to their function as intracrine, autocrine, endocrine and paracrine. Minority of the ligands function either as intracellular ligand (intracrine Fgfs), directly acting in the nucleus, or via the circular system in a hormone-like fashion (endocrine Fgfs). Autocrine and paracrine Fgfs, also known as canonical Fgfs, represent the majority of Fgf ligands. This last category of Fgf ligands act either on the same ligand-expressing cell, or on a neighbouring cell.

Both paracrine and endocrine ligands bind to transmembrane tyrosin kinase Fgf-receptors (Fgfrs). Heparan sulphate proteoglycans (HSPGs) are regulator proteins and function as cofactors to regulate the specificity and affinity of Fgfs. Together, canonical Fgf and HSPGs form a ligand complex which bind to the receptor and triggers its homodimerization and activation by autophosphorylation. Fgfr activation triggers numerous intracellular cascades, including the activation of the Ras/Mitogen-activated protein (MAP) kinase pathway (Dorey and Amaya 2010).

Fgf signalling can be inhibited at different level by established negative feedback loops. Fgf inhibitors include Sprouty proteins, as well as XFLRT3 and Sef among others (for

review, (Thisse and Thisse 2005; Neben et al. 2017)). For instance, Sprouty-1 and -2 are implicated in mammary gland formation (Sigurdsson et al. 2013; Koledova et al. 2016).

In early LG morphogenesis, *Fgf7* (also known as *Kgf*) and *Fgf10* are expressed at the temporal edge of the eye, in the periocular mesenchyme at E13.5 (Makarenkova et al. 2000). FGF7 and FGF10 bind FGFR2. Around E14.5, *Fgf7* and *Fgf10* are expressed in LG mesenchymal compartment, and *Fgfr2* in the conjunctival epithelium, where an invagination takes place to form LG epithelial bud. Therefore, *Fgf10* was reported as an inducer of LG epithelium budding initiation. Lastly, FGF7 and FGF10 loaded beads can induce ectopic LG budding in *ex vivo* cultures.

1.3.1.4.2. Bmp pathway

Bone Morphogenetic Protein (Bmp) signalling was originally defined for its ability to induce ectopic formation of bone or cartilage (for review, (Wozney 1998)). All Bmp pathway members, except from the protease BMP-1 (Mac Sweeney et al. 2008), are part of the Tgf-β super family. Two pathways have been described: the canonical Bmp signalling is transduced through two types of serine-threonine kinase Bmp receptors (Bmpr I and II) and the non-canonical Bmp pathway signals via the MAPK cascade (for review, (Wang et al. 2014)). In addition, Bmp signalling can be inhibited at different levels via antagonist proteins which include Noggin, Follistatin and Gremlin among others (Yanagita 2005). In the canonical pathway, hetero- or homodimers of ligands bind dimers of receptors I, leading to the recruitment of constitutively active type II dimer receptors. Type II receptors phosphorylate type I receptors, resulting *in fine* in the phosphorylation of a Smad protein complex subsequently translocated to the nucleus. Smad proteins are Bmpr co-factors and act as transcription factor.

Non-canonical Bmp signalling drives the activation of the MAPK pathway via the activation of TAK-1, a MAP kinase kinase kinase. Bmp signalling outcomes are broad, as the ligands and receptors can associate as homo- or heterodimers, therefore modulating and increasing the possible responses. For example, Bmp signalling is involved in lung development (Weaver et al. 2000), feather as well as in hair follicle formation (Botchkarev and Sharov 2004; Michon et al. 2008).

Numerous Bmp ligands seem to be playing a role in LG biology. BMP4 was reported to act as an antagonist to FGF10, negatively regulating LG epithelium expansion. However, its action has not been completely unravelled so far (Dean et al. 2004). *Bmp7* is expressed in both mesenchymal and epithelial compartment during LG development, but mainly acts on mesenchymal compartment condensation and proliferation, thus playing an indirect role in LG epithelium branching morphogenesis (Dean et al. 2004). BMP7 signalling has also been involved in LG regeneration after an IL-1 induced injury (Zoukhri et al. 2008). *Bmp6* overexpression has been observed in LG of dry eye patients, resulting in a decrease of lacrimal fluid secretion (Yin et al. 2013). Last but not least, although the function as not been uncovered so far, *Bmp3* expression can be found in the LG acinar compartment of P12 to P18 mice (Thomadakis et al. 1999).

Together, these studies demonstrate the pleiotropic role of Bmp signalling on LG biology. These observations also suggest a possible implication in LG postnatal maturation process.

1.3.1.4.3. Notch pathway

Notch signalling is known to play numerous roles in regulating early organ formation, terminal differentiation and adult tissue homeostasis. Notch pathway is notably involved in cell-fate determination during lens, hair follicle and feather development (for review, (Andersson et al. 2011)).

Both Notch ligands and receptors are transmembrane proteins. Thus, Notch signalling requires cell-cell contact to be activated. This results in the initiation of canonical or non-canonical Notch pathways, of which canonical Notch signalling cascade is well characterized. In mammal species, four Notch receptors (Notch1-4) and five canonical ligands (Delta and Jagged proteins) have been described so far (for review, (Hori et al. 2013)). However, non-canonical pathways are diverse, involving many regulatory elements and downstream proteins which depict context-dependent functions (for review, (Heitzler 2010)). This results in increasingly complex responses.

Upon cell-cell contact, the ligand binding initiates the proteolytic cleavage of Notch receptor in two domains. Briefly, the complex formed by the ligand and Notch receptor extracellular domain (NECD) are endocytosed in the ligand-expressing cell and targeted for lysosomal degradation, ensuring a single activation of the receptor. The intracellular domain of Notch receptor (or NICD) is cleaved by the γ-secretase. Together with downstream proteins, the protein complex formed is translocated to the nucleus where it acts as a transcription factor (Hori et al. 2013). Numerous regulator proteins affect the outcomes of the signalling cascade, for instance by changing the affinity of the receptor for one or another ligand. Additionally, Notch signalling downregulation is mainly accounted for the degradation of NICD into the proteasome (for review,(Kopan and Ilagan 2009)).

Nonetheless, it is important to point out that both receptors and ligands are quite often expressed by one cell. It is therefore crucial for the cells to establish the signal direction. This is usually performed by quantitative receptor activation. A current model suggests the trans-activation of the receptors in the signal-receiving cell, versus the receptors cis-inhibition in the signal-sending cell. This would result for the cell in a mutually exclusive sending versus receiving signalling states, but it has not been tested *in vivo* (Andersson et al. 2011).

1.3.1.4.4. Wnt pathway

Wnt signalling plays an important role in ectodermal organs development and is highly conserved throughout evolution (Cho et al. 2010). The mechanisms of Wnt pathway regroup a large amount of proteins, including Wnt ligands, receptors, co-receptors and numerous downstream proteins involved in the transmission of Wnt signals. Wnt ligands, cell surface – Frizzled (Fz) receptors and low-density lipoprotein receptor-related

protein (Lrp) co-receptors act together as a ternary complex to activate one of the three intracellular pathways described so far (Bhanot et al. 1996). Lastly, negative feedback loops can downregulate Wnt pathway activity. This involves the action of Dkk and Axin proteins for example (for review,(van Amerongen and Nusse 2009)).

The canonical Wnt pathway, and two noncanonical pathways (Wnt/Ca^{2+} and Planar Cell Polarity (PCP) pathways) have been characterized (Liu and Millar 2010). However, it is important to point out that Wnt pathways are regulated at several levels and interact with other signalling pathways, resulting in multiple outcomes (van Amerongen and Nusse 2009).

The canonical Wnt pathway has been extensively studied in mouse ectodermal organs (Andl et al. 2002; Chu et al. 2004; Liu et al. 2008; Mikkola 2009). Notably, Wnt pathway is active in submandibular gland (major salivary gland, SMG) mesenchyme during morphogenesis (Haara et al. 2011). Interestingly, both the inhibition and activation of mesenchymal Wnt impairs branching morphogenesis (Patel et al. 2011; Haara et al. 2011), reflecting the need for fine-tuned Wnt activity in SMG development. Similarly, the precise regulation of Wnt pathway is crucial in other ectodermal organs development, including corneal epithelium differentiation (Pearton et al. 2004).

Wnt pathway is known to play a role in LG branching (Dean et al. 2005). Indeed, Wnt activation (in the epithelium only, or both in epithelium and mesenchyme) leads to LG branching inhibition. Reciprocally, the inhibition of Wnt pathway in both compartments leads to an increased number of branches.

Interestingly, Wnt and Eda pathways have opposite activation patterns in SMG morphogenesis. In this organ, Wnt pathway was previously reported to activate Eda pathway during branching morphogenesis (Haara et al. 2011).

1.3.1.4.5. Eda/Edar and Troy pathways

Ectodysplasin (*Eda*) belongs to the tumour necrosis factor (TNF) superfamily and is located, both in human and mouse, on the X-chromosome. In human, a complex alternative splicing can lead to numerous transcripts, but only *Eda-A1* and *Eda-A2* were so far reported as biologically significant (Bayes et al. 1998a; Mikkola et al. 1999). Human and mouse *Eda-A1* and *Eda-A2* are highly homologous. Although, in both species, only two amino acids differ from both Eda variants, the difference in both proteins accounts for their affinity to different receptors. EDA-A1 binds EDAR, encoded by *Edar* which was reported to be expressed during LG initiation (Pispa et al. 2003). EDA-A1 pathway is involved in numerous ectodermal organ development, including tooth and salivary gland morphogenesis (Pispa et al. 1999; Jaskoll et al. 2003). In the latter, Eda signalling is restricted to the epithelial compartment and is necessary for branching morphogenesis (Haara et al. 2011). EDA-A2, specific for EDA2R (also known as XEDAR), has not been reported to be involved in ectodermal organogenesis. Therefore, EDA-A1 is commonly referred as Eda ligand.

Eda signalling acts principally in a paracrine manner. Eda pathway elements are mainly composed of the Eda transmembrane ligand, its receptor Edar, and Edaradd, an

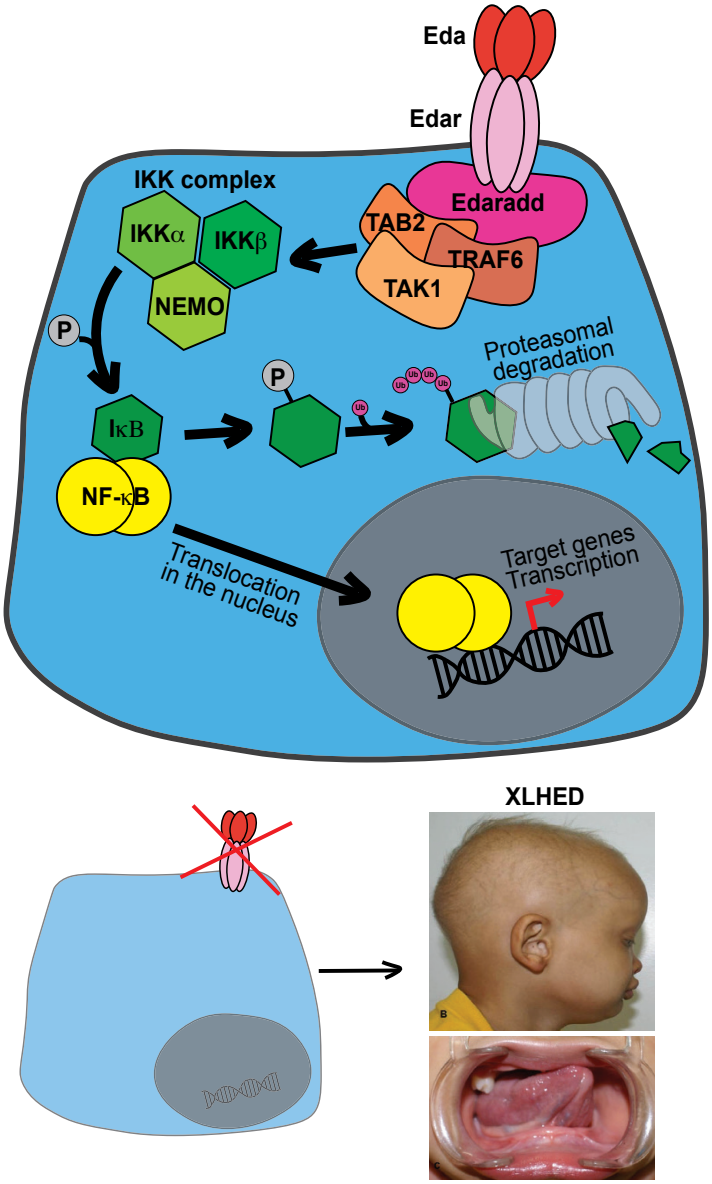

Figure 8: Eda pathway. Soluble EDA-A1 binds EDAR. Together, the ligand and receptor transmit the signal via an adapter molecule EDARADD. The EDA/EDAR/EDARADD complex activates the intracellular signalling cascade through TRAF6/TAB2 and TAK1 proteins, which further recruit IκB kinase complex (IKK). IKK complex phosphorylates IκB, which is directed to the proteasome after polyubiquitination. This last event leads to the degradation of IκB, releasing an active NF-κB. Consequently, NF-κB gets translocated to the nucleus where it acts as a transcription factor. In case of *Eda-A1* mutation, the signalling cascade is not initiated. This leads to X-linked hypohidrotic ectodermal dysplasia (XLHED) in human, which is characterized by several ectodermal deficiencies, including missing or abnormally formed teeth, and bone defects. Pictures from (de Aquino et al. 2012).

adaptor molecule, binding the receptor on its death domain in the intracellular portion. Upon activation, the extracellular domain of Eda ligand is cleaved and becomes soluble. The soluble Eda fragment binds Edar receptor on the signal-receiving cell. Eda/Edar/Edaradd complex activates an intracellular signalling cascade. The downstream pathway leads to the phosphorylation and ubiquitination of IκB, which is directed for proteasomal degradation. *In fine*, this results in the release of NF-κB and its translocation into the nucleus, where it acts as a transcription factor (**figure 8**). It was also reported that Edar signalling can weakly activate the c-Jun N-terminal kinase (Jnk) pathway, not described here (Kumar et al. 2001).

NF-κB signalling is active in numerous ectodermal organs, including those that are not severely affected by *Eda*, *Edar* or *Edaradd* loss-of-function mutations (Bhakar et al. 2002; Dickson et al. 2004). Therefore, another pathway was thought to be redundant to this one.

Edar receptor was previously established as the closest counterpart of Troy, another TNF receptor. In contrast to Edar, Troy does not contain a death domain, representing the binding site for Edaradd. For this reason, TROY is thought to be closer to EDA2R, and to activate the downstream cascade leading to NF-κB activation independently to Edaradd recruitment. Troy pathway was reported to act redundantly to Eda/Edar signalling in hair follicle formation (Pispa et al. 2008). However, Troy possible ligands remain to be elucidated.

1.3.1.4.6. Integrated regulatory network

Gene regulatory networks (GRNs) are constituted of numerous regulator substances leading to a precise control of gene expression, both spatially and temporally. GRNs regulation results in fine-tuned developmental processes (for review, (Levine and Tjian 2003)). Fgf10, Bmp7 and canonical Wnt signalling interact during LG morphogenesis. The integration of these signalling pathways is necessary for LG epithelial bud outgrowth and further controlled branching formation (Dean et al. 2005). Therefore, it is crucial to consider all the molecules included in the highly integrated regulatory networks, organ-specific and context-dependent during development.

1.3.2. LG physiology

1.3.2.1. Basal, reflex and psycho-emotional tear secretion

Three types of tears can be distinguished in human: basal, reflex and psycho-emotional tears. Main and accessory LGs are the main modulators of the different type of tear secretion (for review, (Tsubota 1998; Murube 2009)). Nonetheless, the different types of tears are variable in composition.

Basal tears represent the only type of tears already secreted during the foetal life (Murube 2009), before corneal and LG maturations are completed. Reflex tears production begins shortly after birth. Reflex tears participate to the return to homeostasis after corneal nociceptive stimuli which include corneal wounds, foreign bodies and inflammation. Therefore, reflex tears contain variable proteins helping to restore the basal tearing state (Tsubota 1998). Finally, psycho-emotional tears secretion starts the latest, some months

after birth. This type of tears is specific to human and is up to date thought to have rather a social purpose than a biological impact on the corneal environment (Murube 2009).

1.3.2.2. LG innervation

Adequate responses to environmental factors include pathogens elimination via tear film factor secretion. Although both parasympathetic and sympathetic nervous systems innervate the LG, parasympathetic signals are predominant and present in all species (for review,(Dartt 2009)). As a matter of fact, parasympathetic denervation leads to 70% tear production decrease, along with an accumulation of secretory vesicle in rabbit (Toshida et al. 2007). Up to date, the role of LG sympathetic innervation remains under discussion.

Efferent nerve activation leads the release of neurotransmitters directed to LG acinar compartment. Acetylcholine and Vasoactive intestinal peptide (VIP) are released by the parasympathetic nerves, norepinephrine by the sympathetic ones. These three neurotransmitters activate acinar secretion, resulting in the production and exocytosis of proteins, electrolytes and water in the acinar lumen. Neurotransmitters are integrated at the basolateral side of the acinar cells, protein exocytosis happens at the apical side,

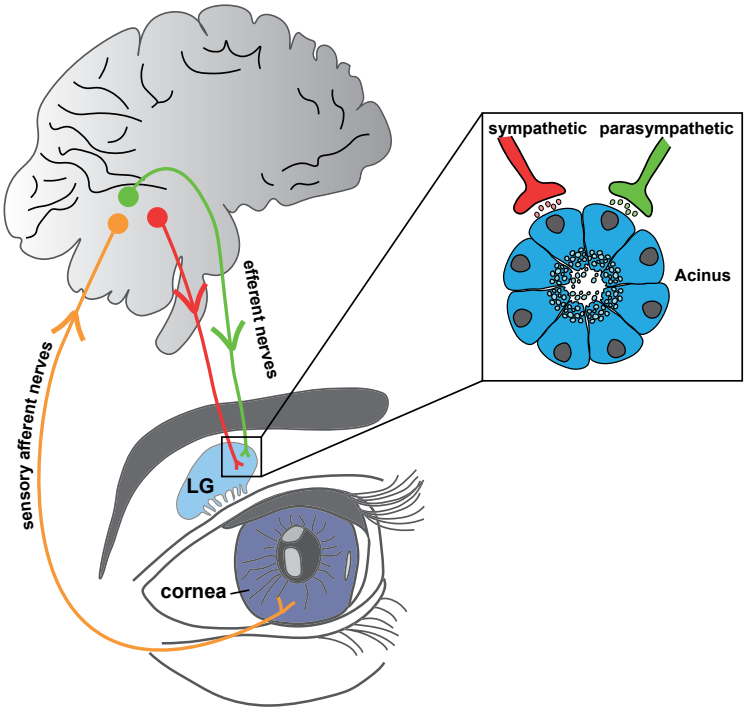

Figure 9: Innervation leading to tear secretion. Upon stimulus, afferent sensory nerves from the cornea and the conjunctiva get stimulated. They project in the central nervous system and activate parasympathetic and sympathetic responses. Efferent parasympathetic and sympathetic nerves stimulate the different lacrimal gland (LG) compartments to induce fluid secretion. This forms a nervous circuit connecting the LG and the ocular surface. Modified from (Zoukhri 2006; Dartt 2009).

towards the lumen (**figure 9**). In contrast, the parasympathetic system has been suggested to secrete enkephalin (Lehtosalo et al. 1989), and the sympathetic to secrete neuropeptide Y (Matsumoto et al. 1992), both thought to have negative effect on lacrimal fluid secretion. However, so far, very little is known about these opposite effects (for review, (Hodges and Dartt 2003)).

Neural stimulation is graded by combination of corneal sensory inputs and emotional inputs, which together determine the amount tears to be produced. A low nerve stimulation will result in the production of basal tear flow, necessary amount to cover the eye surface. A higher input will generate an increased lacrimal flow to wash away a foreign body for example.

1.3.2.3. LG hormonal stimulation

Numerous studies reported gender differences in LG morphology and function (for review, (Warren 1994)). Moreover, dry eye diseases (DEDs), resulting from a deficiency in the lacrimal functional unit, have a higher prevalence in females. Moreover, DED incidence in female increases after menopause. These evidences triggered the study of sex hormone influence on LG functions. It is now acknowledged that hormones, including the sex hormones androgens, progesterone and oestrogens, play a role in the modulation of LG secretive functions. Higher levels of androgens have been associated with higher LG fluid secretion and heavier weight in males. In contrast, changes in oestrogen levels in female have been indirectly associated with lower LG function through androgen availability reduction (Johnson and Murphy 2004).

1.3.2.4. LG ageing

Ageing is associated with a decrease in reflex tear volume. These tears are mainly secreted by the LG, which encounters age-related structural and functional changes (for review, (Rocha et al. 2008)). In mouse, the first signs of ageing represent a decline in both innervation density and parasympathetic nerve activity occurring around 8 months of age. The decrease in acini innervation seems to be followed by immune cell infiltration and structural changes, including general fibrosis and interlobular ductal dilatation (Rios et al. 2005). In addition, LG acinar mass has been reported to decline from 12 months of age in mice (Rios et al. 2005). Except from the innervation density decrease, similar structural changes were also reported in human (Obata et al. 1995). Nonetheless, corneal sensitivity decrease was highlighted in human. Together, these structural changes were suggested to affect the secretory response (both tear quality and quantity) observed in elderly mice (from 24 months of age onwards) and human (Rocha et al. 2008). Moreover, in rodents, the type of acini tends to switch with age from serous to mucous (Draper et al. 1999). Up to date, this last characteristic has not been reported in human.

The effects of ageing on LG function depict inconsistencies amongst the different studies. On a molecular level, only the total protein secretion is consistently reduced during aging in rodent (Rocha et al. 2008).

1.4. Lacrimal functional unit deficiency and therapeutic strategies

1.4.1. Tear film and lacrimal gland function

Tears carry a large amount of proteins, of which the main representatives are portrayed by four proteins. LTF and lysozyme, two proteases, have antibacterial and antiviral functions; lipocalin and secretory type A immunoglobulins (Eiraku et al. 1998) are involved in the activation of the immune system response on the eye surface. LG acinar cells primarily release LTF, lysozyme and lipocalin via fusion of secretory vesicles in the lumen. IgAs are however produced by interstitial plasma cells. These four factors represent up to 80% of the finely regulated tear film proteome (Walcott 1998; Hodges and Dartt 2003).

Moreover, LG is secreting all growth factors necessary for corneal maturation and homeostasis maintenance, as the cornea is an avascular organ. Growth factors are involved in cell survival, proliferation, differentiation and migration and the outcomes are often dose-dependent (for review, (Klenkler et al. 2007)). Growth factor secretion is variable upon numerous factors which affect both the quality and the quantity of LG fluid composition. For this reason, it is difficult to determine the precise concentration of each specific growth factor in the tear film. LG-secreted growth factors include transforming growth factor-beta (TGFb), hepatocyte growth factor (HGF) and epidermal growth factor (EGF), among others. TGFb and HGF play pleiotropic roles in corneal epithelium homeostasis (Klenkler et al. 2007). EGF notably acts as a paracrine factor by increasing CE proliferation as well as an autocrine factor by enhancing LG protein secretion (Xiao et al. 2012).

1.4.2. Cornea wound healing

Corneal abrasion is one of the most common clinically found eye injuries which, in human, heals spontaneously. Cornea repair follows several steps that are well conserved. After feline corneal insult, an early CE cell migration occurs as early as 8 hrs post abrasion. Late migration continues until the wound closure, around 2 days post injury, and is followed by CE stratification from day 3 to day 6 post injury. At day 7 post wound, the CE is back to its original state (Petznick et al. 2013). LG secretion supports the CE repair process. Upon cornea wounding, LG specific production is increased in response to the injury (for review,(Klenkler et al. 2007)). This leads to the upregulation of growth factors in LG fluid. These factors initiate the corneal healing process. Although the molecular events occurring during CE regeneration are not yet fully unravelled, it is established that LG growth factors production is differently regulated in response to cornea wounding (Tervo et al. 1997; Wilson et al. 1999). For instance, it is known that EGF concentration is highly increased immediately after the wound but returns to a more basal concentration rapidly after corneal healing initiation (Sheardown and Cheng 1996).

1.4.3. Dry eye diseases

1.4.3.1. Overview

Irregularities in the pre-ocular tear film quality results in the deterioration of the CE and dry eye. Dry eye diseases (DEDs) are also known as keratoconjunctivitis sicca (KCS) or keratitis sicca. Although the percentage varies tremendously, in the nineties, the prevalence of DEDs could be estimated between 11-22% of the general population (for review, (Abelson et al. 2009) (Brewitt and Sistani 2001)). Since environmental factors influence DEDs prevalence (Alves et al. 2014), it is to be expected that this number will increase further due to climate changes and pollution affecting the quality of the air (for review, (Kinney 2008)). Moreover, the ageing of the population raises DEDs incidence: more than 35% of the elderly suffer from DED (Gayton 2009) and up to date, no curative treatment is available.

DEDs can be categorized into either evaporative or aqueous deficient DEDs, resulting from multifactorial causes (for review, (Bron 1997) and (Craig et al. 2017)) (**figure 10**). Aqueous deficient-DEDs originate from LG deficiencies and are usually categorized as Sjögren's syndrome (SjS) and non-SjS types (for review, (O'Brien and Collum 2004)). In case of aqueous deficient-DED, LG aqueous component secretion mainly is reduced which leads to a shortage in tear film (Messmer 2015). These types of DEDs can result from numerous phenomena impacting LG function, including, in a non-exclusive manner, reduced neural or hormonal stimulation, ductal occlusion or acinar cells loss.

MG deficiencies and eyelid affections lead to evaporative-DEDs. In this case, the tear film has a decreased evaporation time, resulting from lipid composition variation (both in quality and quantity) as well as in the reduced thickness of the tear film lipid layer (for review, (Zhang et al. 2017)). Moreover, in case of evaporative dry eye, LGs try to compensate by increasing their production. This commonly results in waterier eyes.

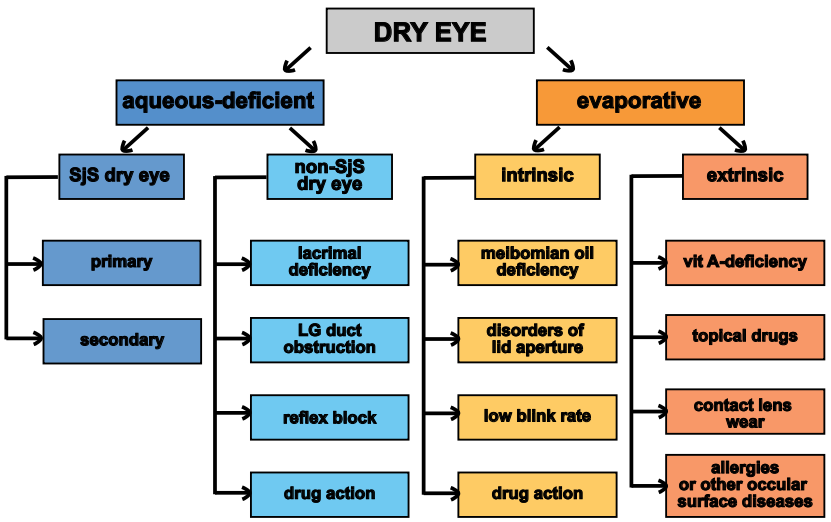

Figure 10: The different types of dry eye diseases. Modified from (Craig et al. 2017)

Nevertheless, these categories simplify the reality, as both types of dry eye often coexist (Johnson and Murphy 2004; Craig et al. 2017).

1.4.3.2. X-linked Hypohidrotic Ectodermal Dysplasia

As detailed above, Eda pathway plays a role in the formation of several ectodermal organs. In mammals, *Eda* loss-of-function leads to X-linked hypohidrotic ectodermal dysplasia (XLHED, OMIM 305100) (Srivastava et al. 1997; Bayes et al. 1998b; Headon et al. 2001; Kowalczyk et al. 2011), characterized by severe symptoms. These include dry eye, xerostomia and body temperature misregulation, respectively linked to lacrimal, salivary and sweat gland hypoplasia (Dietz et al. 2013; Jones et al. 2013). In addition, XLHED patients depict severely affected MGs (Tyagi et al. 2011), contributing to the dry eye phenotype.

The tabby mouse model depicts a spontaneous *Eda* loss-of-function mutation (*Eda*$^{-/-}$, tabby). *Eda*$^{-/-}$ mutants share similar symptoms with XLHED human patients and are therefore commonly used as XLHED models (Srivastava et al. 1997; Cui et al. 2005). Up to date, *Eda*$^{-/-}$ mutants dry eye phenotype was solely attributed to their atrophied or completely missing MGs, characterizing it as an evaporative dry eye model (Wang et al. 2016). Although *Eda*$^{-/-}$ mutants depict atrophied LGs in mouse embryos (Grüneberg 1971), Eda pathway implication in LG biology has been disregarded so far.

1.4.3.3. Other types of dry eye

As mentioned above, DEDs often combine evaporative and aqueous deficiency, and the following examples only highlight the multifactorial characteristics of these affections.

A transgenic mouse model with mitochondria-induced oxidative damage in the LG has been developed to study aged-related aqueous-deficient DED (Uchino et al. 2012). Although ageing is one of the most common condition leading to dry eye, numerous other causes can also lead to symptomatic dry eye (both aqueous-deficient and evaporative) (Javadi and Feizi 2011).

These include genetic disorders (above mentioned XLHED), autoimmune diseases (SjS, see below), medication intake (Acan and Kurtgoz 2017) or contact lenses wear (Lubis and Gultom 2018) and specific physiological status such as pregnancy (Ding et al. 2011), eye surgery (Levitt et al. 2015) or diabetes (Imam et al. 2013).

Notably, SjS is an autoimmune affection leading to lacrimal and salivary glands chronic inflammation. SjS results in DED and xerostomia. Particularly, LGs from SjS patients present an immune cells infiltration and high acinar cell death by apoptosis (Tabbara and Sharara 1999). Numerous mouse models depict SjS-like diseases, including NOD and MRL/lpr mice (for review, (Jabs and Prendergast 1994; Lee et al. 2009)).

LG neural and hormonal stimulations play a crucial role in LG secretion. For instance, pituitary adenylate cyclase-activating polypeptide (PACAP)-null transgenic mice display dry eye symptoms and PACAP is known to act both as hormone and neurotransmitter (similar to VIP, specific of the parasympathetic nervous system) (Nakamachi et al. 2016). Physical trauma, such as bone fractures, can lead to the disruption of parasympathetic

innervation and LG deficiency. This represent the most common cause of DED in horses (Ollivier 2004). A more drastic aqueous deficient dry eye model consists in the complete excision of the extra-orbital LG lobe in mouse (Shinomiya et al. 2018).

Finally, environmental factors such as air humidity is also a risk factor for dry eye. A controlled-environment chamber has been developed to study the effect of dry air on eye surface allowing imposed variations to the environmental factors (Barabino et al. 2005).

1.4.4. Therapeutic strategies

Various therapeutic strategies are employed to target dry eye aetiology, derived symptoms and to mostly bring palliative relief (for review, (Zhang et al. 2017)). Amongst them, artificial tears or tear substitutes; bioengineered LGs and SC injections, as well as artificial plugs can be used to address LG deficiency.

1.4.4.1. Tear substitutes

A lot of research efforts are directed towards the establishment of various lacrimostimulants, stimulating tear production, and lacrimomimetics, replacing all or parts of the tear film, to treat dry eye conditions (for review, (Grahn and Storey 2004)). However, artificial tears are up to date the most common treatment used to alleviate dry eye symptoms. Other type of tear substitutes are also investigated. Notably, autologous serum has a composition close to the tear one, and the beneficial effect of autologous serum drops has been reported to improve eye health in human studies (for review, (Kojima et al. 2008)). However, acquisition and conservation of the serum is a major issue (Lee and Chen 2008), and the efficacy of the autologous serum-based treatments are variable from one clinical trial to the other (Pan et al. 2013). Similarly, the use of Albumin to supplement artificial tears reflect an improvement of the symptoms in patients suffering from SjS-derived aqueous deficiency (Shimmura et al. 2003).

Whether these tear substitutes are only mimicking the basal salinity of the endogenous tears, or whether it is supplemented with other components, the technique is nowadays only destined to ease the discomfort, leaving the source of the problem unresolved.

1.4.4.2. LG bioengineering

The transplantation of entire organs as a therapeutic strategy to replace a deficient organ is a method in use for numerous organs nowadays. However, organ availability and the possibility of allogenic immunological rejection bring important issues. Therefore, organ bioengineering was developed to overcome these and create functional organs to replace dysfunctional ones. These new regenerative methods take advantage from organ-specific SC and use an *in vitro* three-dimensional setup to reconstruct entire organs (for review, (Hirayama et al. 2013b)).

Similarly to tooth and hair follicle, bioengineered LG was developed from a previously reported organ germ method (Hirayama et al. 2017). Following, endogenous LG removal, the transplantation of a bioengineered LG showed similar physiological function in engrafted mice compared to controls (Hirayama et al. 2013a; Hirayama et al. 2015).

This included tear volume, major protein secretion (including lactoferrin) and neural stimulation.

Consequently, some studies reported the successful development of human LG spheres, or "lacrispheres" as a promising therapeutic strategy to be further investigated (for review, (Tiwari et al. 2014) and (Tiwari et al. 2012)).

1.4.4.3. Other approaches

In some clinical cases, autologous submandibular gland transfer was reported to be an option (Yao and Zhang 2017). Although the outcomes seem very positive and DED symptoms are reduced, this operation is not a possibility for patients suffering from autoimmune diseases or any physiological condition leading to xerostomia (Yu et al. 2004) (Macleod et al. 1990).

Mesenchymal SCs have demonstrated interesting tissue repair functions in the case of LG function deficiency derived from specific autoimmune diseases (such as SjS) (for review, (Lu et al. 2017)). Mesenchymal SCs can be isolated and cultured from LG (You et al. 2011). The injection of mesenchymal SCs thus represents one promising therapeutic approach to treat the source leading to DEDs, rather than the symptoms.

Finally, lacrimal puncta or canalicular plugs have been used to reduce the loss of tears by occluding the lacrimal drainage system (for review, (Tost and Geerling 2008) and (Ervin et al. 2017)). Artificial plugs represent a possible treatment in case of severe dry eye, helping to preserve the natural tears by temporary or permanent blockage. In the most extreme situations, surgical closure of the puncta can be an option.

2. AIMS OF THE STUDY

LGs represent a crucial element in the production of the eye-protecting tear film. Numerous affections can impair LG function, especially the tear quality and quantity. Lower tear film quality results in reduced eye vision. To develop therapeutic strategies aiming at restoring proper eyesight in human, a general knowledge improvement on the mechanisms governing LG biology is required. I used several mouse models to generate new information participating in the understanding of the physiology of the eye anterior segment.

My research work focused on the understanding of LG development, maturation and function.

The main aims of my thesis were:

1. To elucidate the principal cellular events occurring during LG early formation,

2. To investigate the molecular mechanisms promoting cell differentiation and their implication in early LG development,

3. To unravel the role of Eda signalling in LG morphogenesis, maturation and function,

4. To study the crosstalk occurring between LG and cornea during cornea wound healing, both in healthy and dry eye conditions.

3. MATERIALS AND METHODS

3.1. Mouse lines

The mouse lines used were previously described. Table 1 recapitulates the different mouse strains involved in each study, along with the original publication describing the corresponding transgenic line and its genotyping.

Wild-type ICR mice were used in study I and II, C57BL/6 mice in study III.

In the study I, αSMA-cre (LeBleu et al. 2013) and Krt14-cre43 (Andl et al. 2004) were crossed with R26R-Confetti (Snippert et al. 2010), R26R-TdTomato (Madisen et al. 2010) and R26R-mT/mG (Muzumdar et al. 2007) reporter lines to follow the cell progeny of α*SMA*+ and *Krt14*+ cells respectively. In the study III, all mice were kept in C57BL/6 genetic background to avoid LG development timeline difference. In this study, Krt14-*Eda* (Mustonen et al. 2003) and Krt14-*Edar* (Pispa et al. 2004) were crossed with NF-κB-gal (Bhakar et al. 2002) reporter line to follow Eda pathway activity in gain-of-function conditions.

The mice were used at different embryonic, postnatal and adult stages. Plug date was considered as embryonic day (E)0, and birth date as postnatal day (P)0.

Table 1. Mouse lines used in the doctoral thesis project

Mouse strain	Used in	Reference
αSMA-cre	I	LeBleu et al., 2013
C57BL/6	III	
Eda$^{-/-}$ (tabby)	III	Falconer, 1952; Srivastava et al., 1997
Fucci	I	Sakaue-Sawano et al., 2008
ICR	I; II	
Krt14-cre43	I	Andl et al., 2004
Krt14-*Eda*	III	Mustonen et al., 2003
Krt14-*Edar*	III	Pispa et al., 2004
NF-κB-gal	III	Bhakar et al., 2002
R26R-Confetti	I	Snippert et al., 2010
R26R-TdTomato	I	Madisen et al., 2010
R26R-mT/mG	I	Muzumdar et al., 2007

All aspects of the mouse experiments performed in this thesis followed the approval by the Finnish National Board of Animal Experimentation (ESAVI/1284/04.10.07/2016).

3.2. Methods

All methods used are described in detail in the original publications (Kuony and Michon 2017; Kalha et al. 2018a) and in the manuscript of the study III. The following techniques were used during the accomplishment of the doctoral dissertation project:

3.2.1. Gene expression profiling

- RNA extraction, cDNA synthesis, RT-PCR and RT-qPCR analyses (*studies I and III*)

RNeasy microkit and QuantiTect Reverse Transcription Kit (Qiagen) were used respectively to extract total RNA from snap-frozen tissues samples and generate the corresponding cDNAs.

Following cDNA synthesis, RT-PCR or multiplex RT-qPCRs were performed to analyse specific gene expression profiles. The advantages offered with multiplex RT-qPCR include the possibility to analyse 4 genes simultaneously (3 genes of interest + one house keeping gene).

- Microarray analysis (*study I*) and RNA sequencing (*study III*)

Microarray analysis and RNA sequencing were performed by the Functional Genomics Unit (FuGU, University of Helsinki), for genetic expression profiling.

The transcriptome of embryonic (E18) and adult (34 wo) LGs (epithelial and mesenchymal compartments) were compared by microarray in the study I. E18 was chosen due to the relative stability of the branching state between individuals at this stage. The microarray results are available on the Genome Expression Omnibus (Michon et al.) platform under the GEO accession number GSE103743. For the microarray analysis, we used a cut-off value of $P < 0.05$, and studied the differently expressed transcripts presenting a fold change whether below -2, or above 2.

Gene expression differences between 13 wo-*Eda*$^{-/-}$ and -control LGs (epithelial and mesenchymal compartments) were analysed by RNA sequencing in the study III. The RNA sequencing results will be available on the Genome Expression Omnibus (Michon et al.) platform upon acceptance of the manuscript. For the RNA sequencing analysis, we used a cut-off value of $P < 0.05$, and studied the differently expressed transcripts presenting a fold change whether below 0.7 or above 1.3.

- RNAscope technology for *in situ* hybridization (*study III*)

Single molecules of target mRNA were detected on paraffin sections using RNAscope® 2.5 HD Duplex chromogenic kit (Advanced Cell Diagnostics) according to previously reported protocols (Wang et al. 2012).

3.2.2. Tissue processing (studies I-III)

Tissues were fixed at 4°C with 4% PFA in PBS, except from NF-κB-gal samples (*study III*) which were fixed with 2% PFA complemented with 0.2% glutaraldehyde in PBS. For whole-

mount staining (*studies I and III*), dissected LG samples were dehydrated and kept in 70% EtOH at 4°C until further use. For histology, immunofluorescence on slide, RNAscope and X-gal staining, samples were embedded in paraffin and cut at 5 μm thickness.

Embryonic stages E17 and E18 were decalcified using EDTA for up to 2 weeks at 4°C prior embedding.

3.2.3. Histology and Immunohistochemistry

- Histology *(studies I-III)*

Haematoxylin-Eosin and nuclear fast red staining were used to counterstain cell nuclei (Haematoxylin and nuclear fast red) and cytoplasm (Eosin) in tissue sections, following well established routine protocols.

- Immunofluorescence staining on sections *(studies I and II)*

An antigen retrieval machine (Aptum Biologics Ltd) was used to unmask epitopes. Primary and secondary antibodies used, and their concentration are described in another section.

- Whole-mount Immunofluorescence staining *(studies I and II)*

The antibodies used, and their concentration are described in the section 3.3.

3.2.4. Eda pathway activity assessment *(study III)*

NF-κB promoter-driven β-galactosidase (gal) expression was detected with an X-gal staining solution. After pre-fixation and washing, the samples were incubated overnight at room temperature of +37C in an X-gal staining solution. Following washing and post-fixation, the samples were further processed for paraffin embedding, sectioning and counterstaining.

3.2.5. Ex vivo cultures *(study I)*

Embryonic LGs were cultured in an *ex vivo* setup for up to 4 days, at the interface liquid-air, following a protocol previously described (Munne et al. 2013). Dissected LGs (epithelial and mesenchymal compartments) were cultured on nucleopore filter membrane (Whatman), on a metal grid in tissue culture petri dishes containing culture medium. *Ex vivo* cultures were maintained in a control atmosphere (5% CO2, +37°C).

- Notch pathway inhibition

Notch pathway was inhibited by adding 10 μM DAPT (γ-secretase inhibitor) to the culture medium. Medium was changed every day, away from light. Although DAPT is known to have an effect on off-targets (Zhao et al. 2008; Yoo et al. 2012), it is commonly used to inhibit Notch pathway by impairing NICD cleavage (Jiang et al. 2011; Dvoriantchikova et al. 2017; Jing et al. 2017).

3.2.6. *In vivo experiments*

- Cornea wounding (*studies II and III*)

Central corneal epithelial surface was injured using an ocular burr (Alger company), following the published protocol (*study II*) (Kalha et al. 2018a). The wound borders and further closure were followed with 0.1% fluorescein staining.

- Blinking rate measurement and tear collection (*study III*)

Blinking rate and tear volume measurement were used to assess the level of ocular dryness in adult mice. Tear collection was performed using 0.5 µl glass micro-capillaries (Drummond Scientific).

3.2.7. *Imaging, data analysis and statistics (studies I-III)*

- Imaging

Ex vivo cultures images were acquired with a Zeiss Lumar stereomicroscope. Fixed samples containing fluorescence staining were imaged using Leica TCS SP5 and SP8 confocal microscopes. Haematoxylin-Eosin, Haematoxylin counterstained RNAscope and nuclear fast red counterstained X-gal staining were imaged using a Leica DM6000 microscope. Whole-mount X-gal staining samples were imaged using an Olympus SZX9 binocular microscope.

- Data analysis

Images were analysed using Imaris 8.4.1 (Bitplane) software and processed with Photoshop CC (Adobe Systems). All panels were made on Illustrator CC (Adobe Systems).

- Statistics

Standard deviation and student *t*-tests (unpaired, two-tailed) were used to determine the statistical significance of the results.

3.3. Antibodies *(studies I and III)*

Table 2 describes the primary antibodies used in this thesis. The secondary antibodies used included anti-mouse AlexaFluor 568 and anti-rabbit AlexaFluor 488 (1/500, Life Technologies). All samples were counterstained with Hoechst 33342 (1/2000, Life Technologies) prior mounting in Vectashield (Vector Laboratories).

Table 2. Primary antibodies used in the doctoral thesis project

Antibody	Host	Reference	Concentration in WM	Concentration in IHC
Anti-αSMA	mouse	Abcam, ab7817	1/100	1/100
Anti-αSMA	rabbit	Abcam, ab5694	1/100	1/100
Anti-Casp3	rabbit	Cell Signalling, 9661S	1/400	-
Anti-ECAD	mouse	BD Biosciences, 610182	1/500	1/750
Anti-ECAD	rat	ThermoFisher, 13-1900	-	1/750
Anti-Krt14	rabbit	Thermo Fisher Scientific, RB-9020-P	1/100	1/100
Anti-Krt14	mouse	Abcam, ab780	1/100	1/100
Anti-Krt19	rabbit	Abcam, ab52625	1/100	1/100
Anti-Notch2	rabbit	Abcam, ab8926	1/100	1/100
Anti-Notch2	rabbit	ImmunoWay, YC0069	1/100	-
Anti-phospho-H3	rabbit	Abcam, ab5176	1/100	-

4. RESULTS AND DISCUSSION

4.1. Epithelial cell populations diversity in embryonic and postnatal LG *(study I)*

4.1.1. Overview

Little was known about the genetically encoded program involved in the specific cell differentiation leading to LG patterning. I performed a microarray analysis to compare the transcriptomic signature of developing (E18) and fully mature (34wo) LGs. As expected, the microarray results highlighted that genes commonly found in mature LG (Farmer et al. 2017) were enriched in the adult sample. In contrast, the analysis revealed numerous genes enriched in embryonic LG, uncovering specific epithelial markers not reported previously during LG embryonic development. This showed LG postnatal maturation and brought new leads to characterize LG epithelium territory formation.

4.1.2. Acinar compartment and MECs

Keratin 14

Hirayama *et al.* reported an increased expression of *Krt14* and *Krt5* in 7 wo LGs (Barabino et al. 2005). In addition, *Krt14* and *Krt5* expression have recently been proposed to mark a unipotent SC population in adult LG epithelium (Farmer et al. 2017)a. LG encounters a gradual maturation from 8 wo to 16 wo (Farmer et al. 2017). Reciprocally, I found that *Krt14* expression is higher in 34 wo adult LG compared to embryonic LG. Using RT-qPCR, I showed a constant increase of *Krt14* expression levels from E15 to 34 wo (see study I, figure S1A).

I used immunohistochemistry staining to determine KRT14 location in developing and mature LG. I found that KRT14 is localized in LG epithelium, from the early LG germ onwards. Specifically, KRT14 gets restricted to the basal cell layer with the beginning of branching morphogenesis in the embryo (see study I, figure 2). In adult LG, KRT14 is found in MECs and in the basal layer of the ducts. Although KRT14 is broadly found in embryonic stages, acinar cells are KRT14 negative in adult LG (see study I, figure S3A).

Alpha smooth muscle actin (*Acta2*, encoding for αSMA)

αSMA is a well-established marker for MECs (Makarenkova and Dartt 2015). I demonstrated that *Acta2* is expressed at all stages in the LG, its expression continuously increasing from E15 to 34 wo (see study I, figure S1A). While *Acta2* was previously reported in LG (Makarenkova and Dartt 2015), *Acta2* embryonic expression pattern had not been established before. I showed that αSMA is scattered in LG epithelial germ and gets gradually restricted to the basal cell layer in the TEBs (see study I, figure 3A and B). Although *Acta2*+ cells are less abundant than *Krt14*+ cells in embryonic LG, whole-mount and section immunohistochemistry staining demonstrated that αSMA partially colocalizes

with KRT14 during LG development (see study I, figure 3C). In adult LG, αSMA remains in MECs (Makarenkova and Dartt 2015). In addition, αSMA also marks the basal layer of suspected blood vessels, as *Acta2* is known to be expressed in vascular smooth muscle cells (Granata et al. 2015) (see study I, figure S3A).

My results showed that *Krt14* and *Acta2* define three specific cell populations, i.e. *Krt14*+ and *Acta2*+ single positive, and *Krt14*+;*Acta2*+ double positive cell populations.

Aquaporins

Aquaporins (AQPs) can be separated into three categories: conventional and unorthodox AQPs, and aquaglyceroporins (Schey et al. 2014). Interestingly, my transcriptomic analysis only depicted a significant expression of conventional and unorthodox AQPs in the LG. Particularly, while *Aqp1* transcripts were enriched in embryonic LG (18 fold), *Aqp5* and *Aqp8* were more expressed in the adult (13 and 132 fold respectively). Although AQP5 is known to be localized in the acini (Schey et al. 2014), AQP1 and AQP8 localizations are unclear in the LG. It was previously suggested that AQP1 is at least found in LG microvascular endothelia, but no precise expression pattern has been established so far (Hamann et al. 1998). *Aqp5* expression can be used as a marker of mature secretory system in the acini (Ishida et al. 1997). However, I showed by RT-PCR that while *Aqp1* was only expressed until P21, *Aqp5* was expressed at any embryonic and postnatal stages. Finally, I found that *Aqp8* expression was restricted to postnatal stages (see study I, figure S3B). Therefore, I suggest that studying these three AQPs together might give a better overview of the progressive secretory program acquisition in LG. Indeed, as the eyelid opening happens between P12 and P14 in the mouse, it is possible that the AQPs profile changes to adapt to the cornea needs.

4.1.3. Ductal compartment

Keratin 19* and *17

KRT19 staining was previously used to mark salivary gland ducts (Nedvetsky et al. 2014). My microarray results depicted a *Krt19* enrichment in embryonic LG (18 fold). Using RT-qPCR, I confirmed that *Krt19* expression was higher in E18 rather than in 34 wo LG. Moreover, studying *Krt19* expression during embryonic LG formation revealed a constant increase from E15 to E18 (see study I, figure S1B).

To go further, I studied KRT19 location by immunohistochemistry staining and established it as a marker for LG ductal compartment. KRT19 depicted a dynamic pattern, first located in the presumptive ductal territory at the LG epithelial germ stage, before getting restricted to the luminal side of the ducts in later stages (see study I, figure 8, 9 and S6).

I used an *ex vivo* culture method (Munne et al. 2013) to investigate LG epithelial germ extension (**figure 11**; see study I, figure 8). The study revealed that KRT19+ cells form a spring-like shape structure in the elongated bud which dissipated after the first branching event. Interestingly, an observation of Krt17-GFP embryonic LGs revealed a

similar expression pattern in the ductal territory (unpublished data). Krt17-GFP transgenic animals could be used with live imaging to study the mechanical forces at play during LG duct early morphogenesis, and the benefit of the spring-like shape territory.

As a summary, the first part of my work was dedicated to the characterization of gene expression patterns in order to set up a tool box to study LG biology. The studied genes included *Acta2*, *Krt19* and *Krt14*.

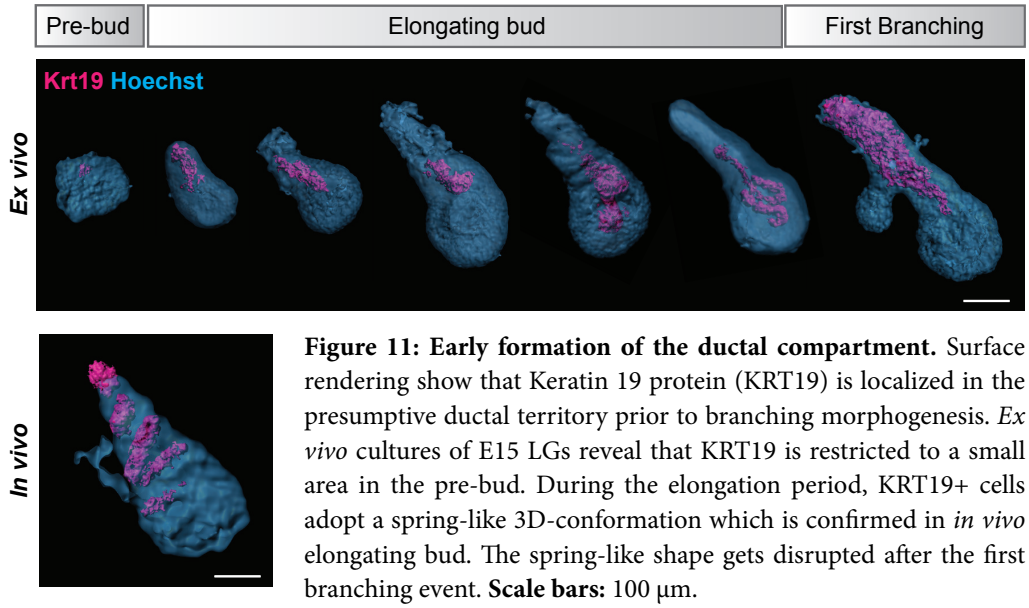

Figure 11: Early formation of the ductal compartment. Surface rendering show that Keratin 19 protein (KRT19) is localized in the presumptive ductal territory prior to branching morphogenesis. *Ex vivo* cultures of E15 LGs reveal that KRT19 is restricted to a small area in the pre-bud. During the elongation period, KRT19+ cells adopt a spring-like 3D-conformation which is confirmed in *in vivo* elongating bud. The spring-like shape gets disrupted after the first branching event. **Scale bars:** 100 µm.

Notably, we pinpointed *Krt14* as a marker for the epithelial basal cell layer, establishing it as an interesting candidate to follow LG epithelium expansion. Using *Krt14* promoter-driven recombinase in association with the R26R-Tdtomato reporter line (table 1), I observed the embryonic and postnatal LG morphological changes. I noticed a constant increase in LG size from P0 to P50, with a major outgrowth occurring between P7 and P13 (**figure 12**).

This last observation directed me to investigate the growth of LG epithelial compartment.

4.2. Growth/expansion of the embryonic epithelium *(study I)*

4.2.1. Tubulogenesis and branching

Ductal formation, or tubulogenesis, is associated with lumen formation. This mechanism can occur through cell death (Wells and Patel 2010). I used cleaved-Caspase 3 (Casp3) staining and showed that LG lumen formation involved luminal cell apoptosis. In contrast to a previous report (Wang et al. 1995), I found that the lumen began to form early on during LG embryonic development. Specifically, the first apoptotic cells were detected at E16. At E17, numerous microlumens were observed in the ducts, and by E18, they fused to

form the lumen in the larger ducts. At this later stage, the remaining apoptotic cells were scarce (see study I, figure 7).

I used KRT19 immunostaining as a tool to follow branching morphogenesis. 3D-surface rendering allowed me to determine the number of branching events along with the number of TEBs at each embryonic stage during LG ductal tree expansion. Notably, I found that from E16 to E18, both the number of branching events and the number of TEBs increased (see study I, figure 10). While the increase of both branches and TEBs was coherent with general growth of the organ, it raised questions regarding the mechanisms involved in ductal tree expansion. Therefore, I studied LG cell proliferation dynamics.

4.2.2. Proliferation

To understand LG growth, I analysed the cell cycle status in LG development. I used phospho-histone 3 (phospho-H3) immunostaining and the Fucci transgenic mouse line (Sakaue-Sawano et al. 2008) to assess cell proliferation during LG embryonic development. The Fucci mouse line depicts proliferative cells (S/G2/M) with green fluorescence and non-proliferative cells (G0/G1) with red fluorescence. As the mesenchymal compartment was mainly non-proliferative, I used phalloidin staining to visualize the different LG compartments and specifically quantify epithelial proliferation.

At E15, the whole epithelial bud was globally proliferating. Therefore, I focused on branching morphogenesis, from E16 to E18. My results revealed that cell proliferation rapidly undergoes a restriction to the acinar domain (mostly in suprabasal cell layers) after the first branching event. Indeed, I noticed that LG ductal compartment gradually appeared non-proliferative. For this reason, I focused on quantifying cell proliferation in the TEB domain. Despite few cells remaining in an active cell cycle throughout LG embryonic morphogenesis, a large part of the cells exited the cycle by E18. The quantification of these results revealed that while more than half of the cells were proliferating at E16, this number dropped to roughly 40% at E17, and 30% at E18 (see study I, figure 5).

Although suprabasal cell proliferation fuelled LG early morphogenesis, the percentage of cells in an active cell cycle overall progressively decreased. Nevertheless, I reported a constant LG epithelium growth in embryonic stages (**figure 12**), and an important outgrowth of LG epithelium in postnatal stages (**figure 12**). Therefore, I investigated alternative mechanisms which could contribute to ductal tree expansion and LG general growth.

4.2.3. Cell intercalation and MET

To go further, I used genetic fate mapping to decipher the cellular events engaged in branching morphogenesis and epithelial territory patterning. By using a constitutive *Krt14* promoter-driven recombinase (Krt14-cre43) in association with R26R-Confetti, -mT/mG and -TdTomato reporter lines (see table 1), I followed *Krt14*+ cells clonal expansion.

The Confetti construct is a Cre recombinase fluorescent reporter containing two dimers segments, each one encoding for two colours. Upon recombination, the Confetti

construct can randomly generate four possible colours. The use of a constitutive Cre recombinase results in a continuous inversion of the dimer left after the first recombination event, cleaving away one of the two dimers. Therefore, as long as the recombinase is active, the cell can continuously switch back and forth from GFP to YFP, or from RFP to CFP (see study I, figure S4). R26R-Confetti *ex vivo* cultures revealed a mix of the four possible fluorescent dyes imaged, i.e. GFP, CFP, RFP, and YFP (**figure 12**). As I used a

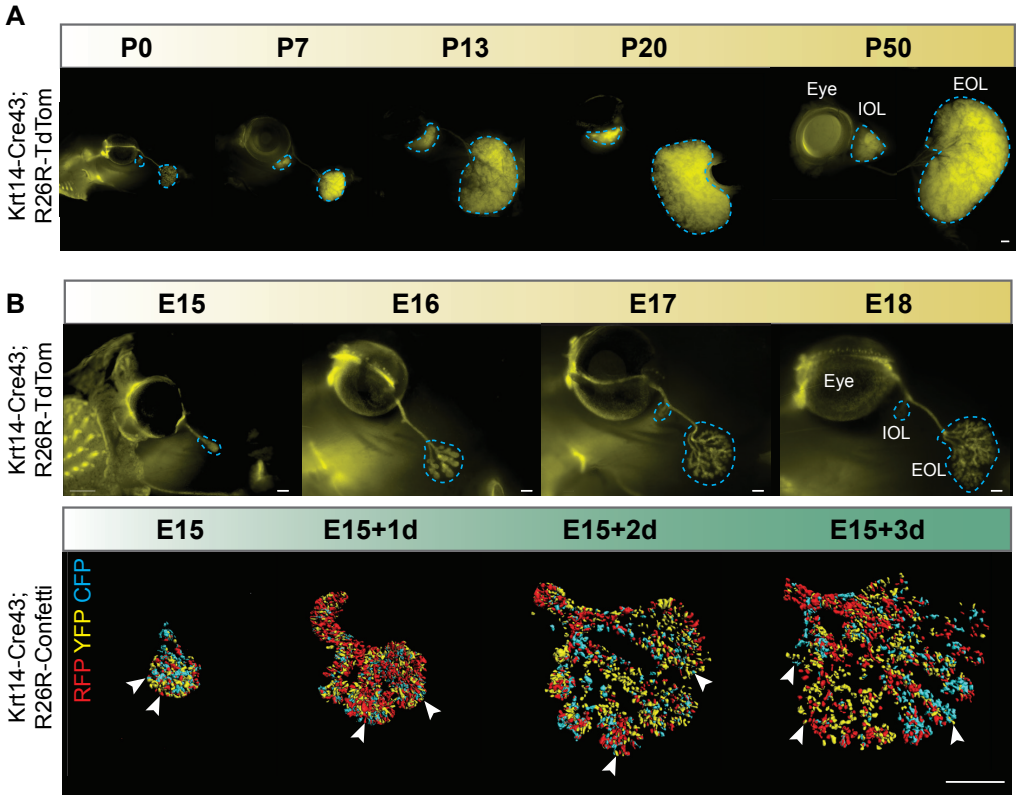

Figure 12: Embryonic and postnatal LG epithelium expansion. (**A**) External views of *in vivo* K14-Cre43;R26R-Tdtomato postnatal animals show LG epithelial compartment morphological changes from P0 to P50. The LG undergoes an important epithelial expansion between P7 and P13, period of eyelid opening in mouse, and continues its growth until P50. (**B**) External views of *in vivo* Krt14-Cre43;R26R-Tdtomato embryos depict LG epithelial compartment morphological changes from E15 to E18. The LG bud is not branched at E15 but from E16 onwards, branches develop. At E17 the intra-orbital lobe (IOL) starts to form (upper panel). The use of Krt14-Cre43;R26R-Confetti in *ex vivo* cultures (from E15 to E15+3 days of culture) shows the involvement of epithelial cell rearrangement during LG branching morphogenesis. The representation of three possible colours with surface rendering demonstrate the intercalation of *Keratin 14* (*Krt14)* positive clones from different origins. Indeed, in all stages, single *Krt14*+ cells of one colour can be observed intercalated in a domain of another colour (white arrowheads, lower panel). **Scale bars:** (**A**) 200 µm; (**B**) 500 µm. EOL: extra-orbital lobe. Dotted lines delimitate epithelial regions.

constitutively active recombinase, I separated the recombined cells into two domains, corresponding to the GFP-YFP (arbitrary represented in orange) and the RFP-CFP (in violet) cell populations. I did not detect the formation of vast territories during branching morphogenesis, as I could have expected from a proliferating and expanding epithelium. Rather, after three days of culture, I showed that the TEB basal layer is formed from series of small orange and violet domains (see study I, figure 6A). Thus, my study suggested a continuous cell intercalation process, offering a faster elongation mechanism as previously reported in branching epithelia (for review, (Wang et al. 2017)). Moreover, single *Krt14*+ clones could also be visualized at this point.

Strikingly, I detected non-recombined cells when using the constitutive Cre in association with any of the three above mentioned reporter lines. In the R26R-Confetti and -TdTomato lines, this resulted in unlabelled cells. We ruled out the possibility of a low recombination efficiency by immunolocalizing KRT14 in Krt14-cre43;R26R-mT/mG samples (see study I, figure 6B and S5). In this combination, the recombined cells express *GFP* and other cells *Tomato* at the membrane. We found KRT14 negative cells which did not undergo the recombination process in the epithelial compartment (red cells). As Krt14-cre43 recombinase is active early on in the development (Andl et al. 2004), I hypothesized that these cells could arise from *Krt14* negative origin.

Cell intercalation has been associated to MET in kidney morphogenesis (Campbell et al. 2010; Carroll and Das 2013). This process involves mesenchymal cells adopting an epithelial phenotype and invading a nearby epithelium. The transition requires a change in several gene expression, such as the induction of *Ecad* expression (Vanderburg and Hay 1996). From E16 to E18, I distinguished few positives mesenchymal cells in close contact to the epithelial basal cell layer. Moreover, these cells seemed to intercalate within the epithelial compartment during branching morphogenesis. ECAD staining at E16 showed few ECAD+ mesenchymal cells in similar locations (see study I, figure 6C). MET was previously suggested in the LG context (Dean et al. 2004), but my results gave the first evidence of MET involvement during LG morphogenesis.

4.3. Signalling pathways in LG biology *(study I and III)*

4.3.1. Notch pathway (study I)

4.3.1.1. Expression of Notch pathway elements in LG

Notch pathway was previously involved in salivary gland acini formation (Garcia-Gallastegui et al. 2014) and cell differentiation in other branching organs (Tsao et al. 2008). My transcriptomic analysis revealed an enrichment of different Notch pathway elements in embryonic LG compared to adult LG (see study I, figure S7A and B). Among them, the receptors *Notch1* and *Notch3* were more expressed in embryonic LG (4.9 and 4.17 fold respectively) and *Notch2* was significantly expressed both in embryonic and adult LGs. The target gene *Hey1,* numerous *Adam* (Notch receptor associated proteins) and *Dlk1* were also enriched in embryonic LG (45.29 fold for *Hey1,* 79.86 fold for *Dlk1*). Notably, *Dlk1*, a Notch

ligand implicated in the non-canonical pathway, was recently reported as involved in LG embryonic development (Dvoriantchikova et al. 2017).

I analysed the expression of numerous Notch pathway elements by RT-PCR and observed a dynamic expression of Notch pathway related genes. Additionally, RT-qPCR for *Notch2* and *Hey1* confirmed the expression of both genes during LG morphogenesis, from E15 to E18. *Notch2* expression was low during the early phases of LG formation, but increased by E18, reaching its highest expression levels in adult LG. *Hey1* expression, reflecting Notch pathway activation, was overall steadily expressed. However, I could observe a peak of *Hey1* expression at E16, along with the start of branching morphogenesis (see study I, figure S7C). These results, in association with the previous report on *Notch1* (Dvoriantchikova et al. 2017), pointed towards the involvement of different Notch receptors to activate Notch pathway during LG formation.

I studied the localization of NOTCH2 and JAGGED1 (one of NOTCH2 ligand) by immunohistochemistry and found that both proteins were localized in the epithelium from E15 to E18 (see study I, figure 11). Moreover, I targeted NOTCH2 intracellular domain (ICD), cleaved and translocated to the nucleus upon NOTCH2 activation. Cleaved NOTCH2 was mainly found during branching morphogenesis, both in the TEBs (basal and suprabasal layers) and in the ductal territory. Although NOTCH2 activation seemed to have a specific time window, its expression levels seemed to be uncorrelated to its level of activation, as the RT-qPCR analysis revealed a higher *Notch2* expression at E18 and at the adult stage. It would be interesting to study Notch2 cleavage in the adult stage.

Particularly, the enrichment in Notch target gene *Hey1*, along with the immunolocalization of NOTCH2 ICD specifically pointed towards an active Notch pathway in the epithelial compartment of embryonic LG. Therefore, I investigated Notch pathway role in LG early formation.

4.3.1.2. TEB territory establishment and maintenance

To decipher the role of Notch pathway in LG morphogenesis, I inhibited Notch pathway activity in *ex vivo* cultures, using a γ-secretase inhibitor (DAPT) treatment. Notch pathway inhibition was confirmed by RT-qPCR analysis for *Hey1* expression, downregulated upon DAPT addition in the *ex vivo* cultures. Immunohistochemistry staining for NOTCH2 ICD also revealed a drastic reduction upon DAPT treatment (see study I, figure S7D and E). I found that Notch pathway inhibition induced the formation of holes within the TEBs, already after 24 hrs of treatment (when compared to DMSO treated control glands). The hollowed TEB phenotype was maintained as long as Notch pathway inhibitor was present and was rescued as early as one day after DAPT removal (**figure 13**). I performed immunohistochemistry against cleaved Caspase3 and showed that TEB suprabasal cell loss occurred via apoptosis, as previously described in salivary gland *ex vivo* cultures treated with DAPT (Garcia-Gallastegui et al. 2014) (see study I, figure S8). Strikingly, LG *ex vivo* cultures were capable of rapid regeneration upon DAPT treatment removal. This phenotype was associated with extra-branching, as recently described (Dvoriantchikova et al. 2017), which was maintained after DAPT removal (see study I, figure 12).

I investigated further this phenomenon and showed an increase in *Acta2* expression after 4 days of culture, both by RT-qPCR and αSMA immunohistochemistry (see study I, figure 13B and S9). This was correlated with a reduced ductal tree expansion and a diminution of KRT19+ cells (see study I, figure 13A). Notch inhibition induced a switch in territory identity as previously described in lung development (Tsao et al. 2008), extending the TEB territory to the branches. These results pointed towards a role for Notch pathway in TEB patterning.

To summarize, I identified a novel role for Notch pathway in LG for the TEB maintenance and territory establishment. Notch pathway inhibition induced suprabasal cells reversible loss and maintained extra-branching, suggesting a switch of cell identity from ductal to acinar fate.

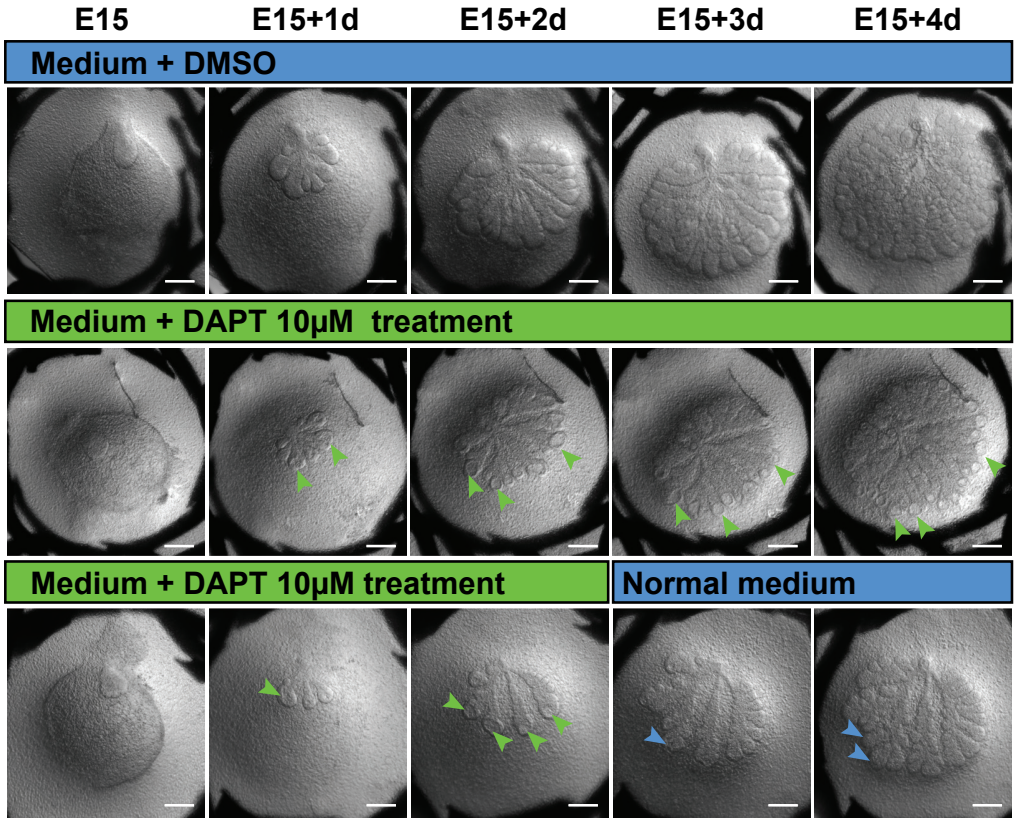

Figure 13: Effect of Notch signalling inhibition in LG *ex vivo* cultures. The inhibition of Notch pathway with DAPT treatment (10 µM) induces the loss of TEB suprabasal cell layers and extra-branching in LG *ex vivo* cultures. Upper panel demonstrates the normal LG development in DMSO-treated *ex vivo* cultures. Hollowed TEBs (green arrowheads) appear rapidly after 1 day of treatment (middle and lower panel) and are maintained throughout Notch inhibition. When the inhibition is removed, hollowed TEBs are quickly regenerated, while extra-branching remains. **Scale bars:** 200 µm.

4.3.2. *Eda pathway (study III)*

Eda loss-of-function mutation results in MGs deficiency. Therefore, Eda pathway was previously implicated in DEDs. However, its role on LG biology was so far disregarded. I performed an RNA sequencing analysis to compare control and *Eda* loss-of-function (*Eda*$^{-/-}$) LG transcriptomes in adult mice and found that 3% of *Eda*$^{-/-}$ LG transcriptomic signature was different from the control one. These results already demonstrated that Eda pathway has some impact on LG biology. Therefore, I decided to investigate the role of Eda pathway in LG development, maturation and function.

In this part of the project, I took advantage of four mutant mouse strains: *Eda*$^{-/-}$ loss-of-function (*tabby*) mouse, Krt14-*Eda* and Krt14-*Edar* mice, exhibiting a forced expression of *Eda* and *Edar* in *Krt14*+ cells respectively, and NF-κB-gal transgenic model, reporting for Eda pathway activity (see table 1).

4.3.2.1. Role of Eda signalling in LG development

I used the RNAscope technology (Wang et al. 2012) to determine *Eda* and *Edar* localization during LG early formation from E16 to E18. I demonstrated that *Eda* and *Edar* have opposite, although partially overlapping, expression patterns during LG formation. *Eda* was mostly expressed in LG mesenchyme, while *Edar* was mainly restricted to the epithelial compartment (see study III, figure 1A). In addition, I used the NF-κB-gal reporter to study Eda pathway activity. In agreement with *Edar* expression pattern, I showed that Eda pathway was only active in LG epithelium. Although Eda pathway was broadly active both in basal and suprabasal cell layers, the activity seemed stronger in the basal cell layer. By E18, cells exhibiting an active Eda pathway were scattered in the epithelial compartment, progressively restricted to the acinar compartment (see study III, figure 1B).

I took advantage of our previously reported methods to study the ductal tree expansion, TEB formation and proliferation status during LG embryonic development (*study I*). Although *Eda* loss of function had a variable impact on LG global morphology, I reported that *Eda*$^{-/-}$ mutant TEB number and ductal tree volume were similar to control during branching morphogenesis. Nonetheless, quantifying TEB cell proliferation revealed an increased number of phospho-H3+ cells in *Eda*$^{-/-}$ compared to controls at the end of embryonic morphogenesis (1.25 fold at E18). Therefore, although the number of TEB was consistent in control and mutants, there was no obvious correlation between this parameter and the TEB proliferation status (see study III, figure 3).

Finally, I characterized the phenotype of Krt14-*Eda* and Krt14-*Edar* mutants, in which Eda pathway is forced in *Krt14*+ cells. As a reminder, *Krt14* expression becomes restricted to the basal cell layer during LG embryonic development (*study I*). I could this way assess the consequences of Eda pathway misregulation in LG epithelium. Using the NF-κB-gal reporter, I studied Eda activation pattern in these mutants. The forced expression of Eda ligand led to a broader activation of Eda pathway in LG epithelium, but not to any major morphological impact (see study III, figure 2). Krt14-*Eda* mutants displayed a ductal tree volume similar to control. Nevertheless, Krt14-*Eda* LGs showed an increased proliferation

in the TEBs at both E17 and E18 (1.46 fold and 1.2 fold respectively), but a reduced TEB number at E18 (0.68 fold) (see study III, figure 3).

Conversely, Krt14-*Edar* mutants exhibited a reduced Eda activity and a delayed starting point in branching morphogenesis. However, this delay had no major impact on the proliferation status, ductal tree expansion, nor on the number of TEBs as Krt14-*Edar* LGs were similar to the control morphology by E18 (see study III, figure 2 and 3).

Eda activity was differently patterned in Krt14-*Eda* and Krt14-*Edar* mutants, possibly due to *Eda* and *Edar* forced expression in a restricted cell population. However, it is interesting to highlight that the global LG morphology remained similar to the control one by the end of embryonic development. I concluded that there was a possible implication, however limited, of Eda pathway activity on LG early morphogenesis.

4.3.2.2. Role of Eda signalling in LG maturation

NF-κB-gal staining revealed an active Eda pathway in postnatal LG (P21), as well as in the adult (34 wo) (see study III, figure 1B).

I studied LG maturation in the three mutants by evaluating the expression level of previously reported cell terminal differentiation markers. I used *Acta2* for the MECs; *Ltf*, *BhlhA15* and *Aqp5* for the acinar compartment and *Krt19* and *Slc12A2* for the ducts (Farmer et al. 2017) (see study III, figure 4).

Eda loss-of-function mutation led to an alteration of cell terminal differentiation, revealing an impaired maturation process. From P0 to P21, acinar specific genes exhibited an almost constant upregulation in $Eda^{-/-}$ mutant compared to control LGs (*Ltf*: 3 fold; *BhlhA15*: 1.5 fold and *Aqp5*: 2 fold at P21). In contrast, although ductal markers did not display strong expression changes from P0 to P13, both *Krt19* and *Slc12A2* were upregulated at P21 (4 fold and 1.45 fold respectively). Lastly, while *Acta2* was enriched in the mutant at P0, $Eda^{-/-}$ LG exhibited a reduced *Acta2* expression at P13 (0.75 fold).

I studied the maturation process in the two gain-of-function mutants (Krt14-*Eda* and Krt14-*Edar*). Duct and MEC specific genes were expressed in a similar pattern in both mutants. From P0 to P13, duct specific genes were downregulated or close to control values. However, at P21, both *Krt19* and *Slc12A2* were generally upregulated in both mutants compared to control (*Krt19*: 5.5 fold and *Slc12A2*: 1.25 fold for Krt14-*Eda*; *Slc12A2*: 1.55 fold for Krt14-*Edar*). Moreover, in both mutants and at all stages, *Acta2* was less expressed or close to the control level of expression. Finally, acinar specific genes exhibited a less sustainable expression pattern. In both mutants, *Aqp5* was downregulated from P0 to P13, but enriched at P21 (1.57 fold for Krt14-*Eda* and 1.22 fold for Krt14-*Edar*). *BhlhA15* expression was similar to control or upregulated between P0 and P21 (1.9 fold for Krt14-*Eda* at P21). Conversely, only *Ltf* expression depicted a differential expression between Krt14-*Eda* and Krt14-*Edar* mutants. In Krt14-*Eda*, *Ltf* was only enriched compared to control at P21 (1.8 fold), while in Krt14-*Edar*, this gene was downregulated at P0 (0.38 fold), but similar to control after this stage.

In summary, both forced activation and inhibition of Eda pathway led to an increased expression of differentiated acinar and ductal specific genes by P21. At this stage, however, the MEC compartment was not affected by Eda pathway modulation. The gene expression modulations were more striking in *Eda*$^{-/-}$ than in the gain-of-function mutants, Krt14-*Edar* mutant being the least different from the wild type LG.

As mentioned above, we demonstrated that *Krt14*+ cells were mainly distributed in the basal cell layer from the start of branching morphogenesis (*study I*). Krt14-*Eda* and Krt14-*Edar* therefore respectively overexpressed *Eda* and *Edar* predominantly in the basal cell layer. One hypothesis was that the overexpression of *Eda* ligand in *Krt14*+ cells led to the saturation of all accessible receptors in those cells. As endogenous *Eda* ligand was mainly found in the mesenchymal compartment, the overexpression of *Edar* receptor in the *Krt14*+ cells could lead to a similar outcome by intercepting all Eda ligand available in the surrounding mesenchyme. In both situations, the abnormal activation of Eda pathway in *Krt14*+ cells could lead, based on the Gierer and Meinhardt model (Gierer and Meinhardt 1972; Babloyantz and Hiernaux 1975), to short-range activation of the pathway, and long-range lateral inhibition. *In fine*, this would result in the overall diminution of the pathway activity mainly in the suprabasal cell layers in Krt14-*Eda* and Krt14-*Edar* mutants. *Eda*$^{-/-}$ mutants present the lowest level of Eda signalling possible, both in basal and suprabasal cell layers.

A second hypothesis could involve a third party, such as the Troy pathway, previously shown to act in a redundant way to Eda signalling in hair development (Pispa et al. 2008), or EDA2R, for which the biological implications remain to be clarified.

This could bring possible explanations for the similar outcomes arising from the three different mutations. It was previously suggested that a deregulation of normal Eda pathway activity could lead to instabilities in developmental processes (Kangas et al. 2004). Indeed, it was reported that both Krt14-*Edar* and *Eda*$^{-/-}$ mutations lead to similar molar phenotypes in the mouse, associated with polymorphism (Pispa et al. 2004; Tucker et al. 2004). Gain- and loss-of-function of Eda pathway have opposite outcomes in salivary gland development: *Eda*$^{-/-}$ salivary glands depict fewer branches while Krt14-*Eda* salivary glands have significantly increased branches number (Haara et al. 2011). In the case of LG it seems that any modification of Eda pathway activity led to similar postnatal maturation defects.

I decided to focus on the loss-of-function mutation and used RNA sequencing to compare *Eda*$^{-/-}$ and control LG transcriptomes in adults (13 wo). The analysis highlighted significant changes in *Eda*$^{-/-}$ gene expression profile when compared to control: 2% of the transcripts were downregulated, while 1% was upregulated in *Eda*$^{-/-}$ LG (see study III, figure 6). I validated the analysis by RT-qPCR and confirmed that *Wnt4*, reported in the study of different glands (Brisken et al. 2000), and *Lin28a* transcripts were less abundant in the mutant (0.26 fold and 0.01 fold respectively). Interestingly, *Lin28a* has been reported to promote tissue repair (Shyh-Chang et al. 2013) and to positively regulate SC metabolism (Zhang et al. 2016). In contrast, *Esp34* and *Dgat2* were more expressed in *Eda*$^{-/-}$ LG (over 8 fold and 84 fold respectively).

To summarize, all my results pointed towards a defective LG maturation upon modification in signalling activity. Moreover, the defects remained in *Eda*$^{-/-}$ LG at adult stage, as up to 1773 transcripts were misregulated in *Eda*$^{-/-}$ LG. Proper terminal differentiation is crucial for physiological LG secretion. Therefore, I studied LG function in *Eda* loss-of-function mutants.

4.3.3. *Other signalling pathways (study I)*

Wnt pathway is known to negatively regulate LG branching (Dean et al. 2005). Similarly as in the SMG development where Wnt and Eda pathways act in a positive feedback activation loop (Haara et al. 2011), both pathways seem to depict opposite activity patterns in LG morphogenesis (*study III* and (Dean et al. 2005)). Therefore, it is possible that the implication of Wnt pathway in LG development is complex, involving a fine tuning of its activity and a communication between mesenchyme and epithelium.

My microarray analysis revealed an enrichment of Wnt elements expression during LG formation. Notably, I noticed an upregulation of *Fat1* and *Fat4*, two components of the noncanonical PCP pathway (6.34 fold and 67.7 fold respectively) and of three Wnt pathway inhibitors (namely *Sfrp1* (71.39 fold), *Dkk2* (60.5 fold) and *Dkk3* (18.87 fold)). I performed the study on whole LGs (both epithelium and mesenchyme) and the activation/inhibition experiments described by previous authors mainly recapitulate the involvement of Wnt pathway in LG embryonic epithelium (Dean et al. 2005). Therefore, it would be interesting to assess the expression of Wnt pathway elements in mesenchymal versus epithelial compartments in embryonic LG, and to specifically investigate the role of Wnt pathway in LG mesenchyme.

4.4. LG physiological functions (study II and III)

4.4.1. *Dry eye disease*

Eda$^{-/-}$ mutant is an established dry eye model. However so far, the symptoms are categorized as evaporative, due to meibomian glands deficiency (Wang et al. 2016). I confirmed dry eye symptoms by assessing the blinking rate for three adult ages, ranging from 13 to 64 wo. I revealed a striking increase in the number of blinks per minute in the mutants compared to the controls (from 6 to 12 fold depending on the age group). At any stage, however, gain-of-function mutants did not display a different blinking rate from the control one. In the case of the loss-of-function mutation, the difference was the highest at 13 wo (12 fold). Therefore, I measured the tear production and established that *Eda*$^{-/-}$ mutants secreted less tears than the controls at 13 wo (0.38 fold) (see study III, figure 5). LG encounters for the majority of the tear fluid and together with my previous results, this pointed towards a defective LG function in *Eda*$^{-/-}$ mutants. Therefore, I hypothesized that the aetiology of *Eda*$^{-/-}$ mutants' dry eye directly involved the LG. This would establish the *Eda*$^{-/-}$ mouse model as a multifactorial, instead of evaporative, dry eye model, making it a more suitable clinical model.

In addition, the RNA sequencing results highlighted a misregulation of particular growth factors produced by the LG in the tear fluid. *Egf* was not differently expressed in *Eda*$^{-/-}$ compared to control LGs. However, RT-qPCR analysis confirmed the downregulation of *Fgf7*, *Igf1*, *Hgf* and *Tgfb1* expression levels in *Eda*$^{-/-}$ LGs (0.48 fold, 0.33 fold, 0.73 fold and 0.34 fold respectively) (see study III, figure 7C). All four genes were reported to act on corneal epithelium maturation and/or maintenance during homeostasis among other functions (for review, (Klenkler et al. 2007)). Notably, IGF-1 can be found in the tear film and IGF-1 receptor is present in the corneal epithelium (Rocha et al. 2002). A recent study on human subjects revealed the high concentration of IGF-1 in the tear film of young adults, and its decrease in elderly. This was associated with dry eye symptoms in older adults (Patel et al. 2018).

In contrast, *Gdf5* and *Cxcl10* were more expressed in *Eda*$^{-/-}$ LG (14 fold and 1.2 fold respectively) (see study III, figure 6C and 7C). *Gdf5* was previously involved in the inhibition of corneal epithelial cells proliferation (You et al. 1999), and decreased cell proliferation was reported in *Eda*$^{-/-}$ corneas (Li et al. 2017). GDF5 has also been reported to induce angiogenesis on the cornea (Yamashita et al. 1997), known to alter visual acuity by affecting corneal transparency (for review, (Maddula et al. 2011)). Moreover, increased concentration of CXCL10 in the tear film has been associated with DEDs (Yoon et al. 2010).

Nonetheless, impaired cornea wound healing was observed in *Eda*$^{-/-}$ animals. These defects were so far attributed to severely affected MGs (Wang et al. 2016).

4.4.2. Cornea wound healing

In normal conditions, the tear film is responsible for the maintenance of the CE homeostatic state. Upon eye surface injury, the protein composition can tremendously vary both qualitatively and quantitatively to support the recovery of the corneal integrity (for review, (Klenkler et al. 2007)). Several techniques are available to study wound closure in mouse models. Chemical burns usually affect both CE, stroma and the surrounding conjunctiva (Bai et al. 2016), and often lead to severe outcomes (Bai et al. 2016). Other techniques rely on mechanical disruptions of the eye surface. Those include the use of blades or sharp objects and commonly penetrate through the stroma (Blanco-Mezquita et al. 2011; Blanco-Mezquita et al. 2013).

In the study II, we described a reliable method to *in vivo* abrade a delimited region of the CE without disrupting the basal membrane and the underlying stromal compartment. This technique of CE debridement was firstly elaborated using blades on *ex vivo* corneas (Gipson and Kiorpes 1982). In our protocol, the use of an ocular burr permitted to strictly delimit the injury area to the CE in a reproductible manner (see study II, figure 1). The resulting wound resembled the most common corneal abrasion found clinically in human (Jackson 1960). We followed the corneal wound healing process with fluorescein staining and described the timeline of full recovery. At 18 hrs post wound, the wound was remarkedly diminished in size and we found that already after 72 hrs, the CE was fully re-epithelialized (see study II, figure 3).

I hypothesized that the defective response of *Eda*$^{-/-}$ LG described in the study III participates to the impaired cornea wound healing process and further investigated LG response to corneal injury, using the established CE abrasion protocol.

4.4.3. Cornea repair in dry eye context

I confirmed the delayed healing process by using our corneal abrasion model (*study II*) and followed CE closure with fluorescein staining (see study III, figure S2). Since we recently reported an active healing state at 18 hrs post wound in the cornea (Kalha et al. 2018b), we used this time point to study the impact of the injury on Eda pathway activity. As recombinant EDA supplementation was reported to be beneficial for CE regeneration (Li et al. 2017), I first studied Eda pathway activity in the CE. Although I observed little expression of *Eda* and *Edar* in the embryonic CE, and high *Edar* expression in the adult cornea, no Eda pathway activity was detected in the control cornea at any stage (see study III, figure S3). In addition, I did not detect any activity before nor after the abrasion. However, NF-κB-gal staining showed a complete inhibition of the pathway in the LG after the abrasion (**figure 14**). This was confirmed by RT-qPCR, revealing a striking downregulation of *Eda* and *Edar* expression 18 hrs after the abrasion in comparison to unwounded LGs (0.36 fold and 0.15 fold respectively) (see study III, figure 7A and B).

Eda pathway inhibition was extended to the contralateral LG, on the unwounded eye side. This last result confirmed a cross-talk occurring between LG and cornea, but most importantly, tended to indicate a communication between the two LGs.

I followed *Egf*, *Hgf*, *Tgfb1, Igf1*, *Fgf7*, *Cxcl10*, *Mmp2* and *Bmp1* expression 18 hrs after epithelial abrasion (see study III, figure 7C). LG factors secretion are known to change upon corneal insult and the modulation of the tear fluid composition supports the wound healing process (Klenkler et al. 2007). Particularly, EGF tear concentration increases immediately at the time of wound but rapidly returns to basal levels one day after the injury (Sheardown and Cheng 1996). My results showed that although *Egf* expression was similar in pre and 18 hrs post wound in the control LG, *Egf* expression was upregulated in post wounded *Eda*$^{-/-}$ samples compared to unwounded *Eda*$^{-/-}$ samples (1.14 fold). This could mean that *Eda*$^{-/-}$ LG defective function results in a delayed return to *Egf* basal levels.

HGF concentration has been reported to decrease one day post injury (Tervo et al. 1997). My results depicted a reduced *Hgf* expression already after 18 hrs post abrasion in *Eda*$^{-/-}$ LGs only (0.75 fold). Similarly, it was shown that *Tgfb1* concentration is drastically reduced in human tears two days post cornea operation but is back to basal levels three months after (Tuominen et al. 2001). In contrast, I noticed a striking increase in *Tgfb1* expression after cornea injury, both in control and *Eda*$^{-/-}$ LGs (2.77 fold and 5.1 fold respectively).

After cornea wounding, the IGF-1 present in the tear film was linked to limbal SC differentiation, needed to support the healing process (Trosan et al. 2012). Contrastingly, I found that *Igf1* expression was reduced 18 hrs after corneal abrasion in control LGs (0.31 fold) but remained unaffected in *Eda*$^{-/-}$ samples.

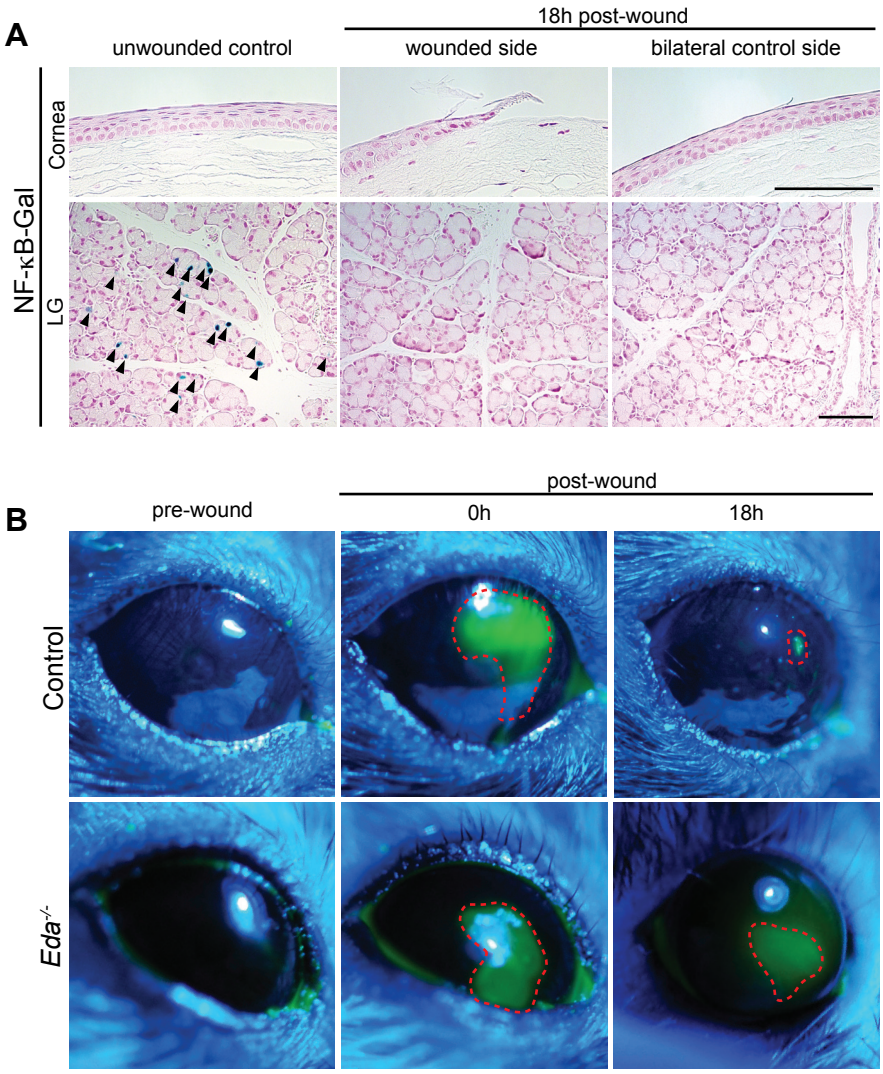

Figure 14: Eda pathway is involved in corneal epithelium regeneration after abrasion. (**A**) NF-κB-gal reporter is used to detect Eda activity in both corneal epithelium (upper row) and lacrimal gland (LG, lower row) samples at 13 wo during a cornea wound healing experiment. In unwounded controls, Eda pathway is active in the LG (black arrowheads). At 18 hrs post wound, Eda activity is not detected in either LGs, demonstrating a transmission of the injury signal to the bilateral LG, side of the untouched eye. Eda pathway is not active in the cornea, whether prior or after corneal abrasion. **Scale bars:** 100 µm. (**B**) Fluorescein staining is used to visualize the wounded region at the time of the wound (0 hrs post wound) and after 18 hrs, in control and *Eda*$^{-/-}$ animals. Following cornea wound healing reveals that at 18 hrs post wound, the impaired corneal area appears almost healed in control animals, while a consequent wounded area is still visible in *Eda*$^{-/-}$ mutants. Cornea wound healing is delayed in *Eda*$^{-/-}$ mutant compared to control. The red dotted line delimits the wounded area.

Fgf7 expression has been reported to increase upon cornea injury (Wilson et al. 1999). Disparagingly, I showed that *Fgf7* was downregulated both in control and *Eda*$^{-/-}$ LGs after injury (0.36 fold and 0.21 fold respectively).

I reported a decrease in *Cxcl10* expression after corneal abrasion in *Eda*$^{-/-}$ samples (0.05 fold). It was reported that *Cxcl10* expression is induced upon wounding in mice. However, endogenous *Cxcl10* expression increase is impaired in diabetic mice, which happen to also suffer from delayed cornea wound healing. Exogenous CXCL10 supplements can overcome this defect and support cornea restoration in diabetic mice (Yan et al. 2016). The downregulation of *Cxcl10* expression in my model could participate to the delayed healing process observed in *Eda*$^{-/-}$ animals.

MMP2 concentration highly increases in the tear film following feline cornea injury, as early as 8 hrs after the wound (Petznick et al. 2013). The presence of this protease in the tear film seems to improve the healing process (Ollivier et al. 2007). I did not find similar results, as *Mmp2* expression was reduced both in control and *Eda*$^{-/-}$ LGs after the abrasion in our analysis (0.47 fold and 0.64 fold respectively).

Finally, *Bmp1*, a protease previously reported as support for the corneal wound healing, was shown to be upregulated in mouse corneal epithelium 7 days after wounding (Malecaze et al. 2014). In contrast, I noticed a drastic inhibition of *Bmp1* expression both in control and *Eda*$^{-/-}$ LGs 18 hrs after wounding (0.06 fold and 0.1 fold respectively). This inhibition could be transient and preceding the augmentation in the later stages of corneal healing.

Importantly, it needs to be pointed out that the gene expression differences observed in my study compared to previously published results could be due to the 18 hrs time point chosen in my study.

As a conclusion, although *Eda*$^{-/-}$ LG is able to modulate its secretion upon corneal injury, the regulation is abnormal and different to the control. Together, this could lead to the observed delay in CE wound healing. Previous reports demonstrated that epithelial wound healing follows numerous steps (Petznick et al. 2013). To go further, it would be crucial to measure the above-mentioned gene expression dynamics across the wound healing process, from the wounding time to three days post wound, when the CE is fully restored (Kalha et al. 2018a).

5. CONCLUDING REMARKS AND FUTURE PERSPECTIVES

Instrumental to corneal health and therefore to clear vision, the LG has extensively been studied in its pathological conditions, looking through the prism of proper eyesight maintenance. Considering the increasing prevalence of DEDs, solid basic knowledge is required to successfully apply regenerative medicine in future therapies. The fundamental directives followed by embryonic tissues, in order to form the fully functional LG biological system from the conjunctival epithelium remain rich in mysteries.

In my work, I participated in enhancing the general knowledge on LG morphogenesis and maturation processes, together leading to the proper function of the organ and production of potent tears.

Notably, my work contributed to delineate the crucial role of Notch pathway in acinar territory boundaries formation and maintenance. The Notch aspect of my work was mainly focused on embryonic development and showed that transient inhibition of Notch signalling leads to suprabasal cell loss, rapidly regenerated after inhibition removal. Notch pathway was reported to play a role in kidney regeneration (Ma et al. 2018). It would be interesting to study further the involvement of Notch in adult LG maintenance and repair.

Previous studies suggested a role for Eda pathway in LG biology (Grüneberg 1971; Kowalczyk-Quintas et al. 2015), but the striking MGs atrophy in *Eda* loss-of-function mutants (Grüneberg 1971; Wang et al. 2016) had so far led to ignore and side-line the LG phenotype. In my studies, I investigated Eda signalling implication in LG formation, maturation and function. In light of my results demonstrating acinar and ductal compartments maturation defects in $Eda^{-/-}$ LG, I suggested a new paradigm on $Eda^{-/-}$ dry eye, alternative to the current evaporative theory. I hypothesize that $Eda^{-/-}$ dry eye results in the combination of multiscale defective lacrimal apparatus components. Together, this further highlights the need for a finely integrated regulatory network.

To test my hypothesis, I could inject EDA recombinant proteins in adult LG. Together with LG high regenerative potential (Zoukhri et al. 2008), it would be interesting to see if it is possible to compensate $Eda^{-/-}$ defective maturation and restore an adequate LG secretion. XLHED was previously rescued by postnatal injection of EDA in dog (Casal et al. 2007), and recombinant EDA supplementation have been reported to ameliorate $Eda^{-/-}$ dry eye symptoms (Li et al. 2017).

Lot of efforts have been put into the development of topical eye drops. In this thesis, I highlighted the fluctuation of previously reported growth factors involved in cornea wound healing (Klenkler et al. 2007). In this perspective, following the dynamics of these growth factors during corneal wound healing, from the time of the wound until the complete recovery will most certainly spotlight new factors in play. Subsequently, specific growth factors could be used for the development of customizable artificial tear substitutes containing all the essential tear components for a faster and most efficient CE regeneration. However, the techniques used in my thesis rely on transcriptomic dynamic

changes, implying that the changes observed in gene expression are mirroring the protein concentrations in the tear film. More efforts on proteomic assessments should be carried out in the future, to potentialize the tear substitute and address the required factors to each recipient organ.

One problem is the low retention of the drugs delivered on the eye surface. Commonly, any delivered component on the eye is cleared away within three hours. To overcome the low retention time, engineered nanoparticles and microparticles are developed (for review, (Ravi Kumar 2000)). Among them, mucoadhesive nanoparticles were reported to increase the ocular retention (Liu et al. 2016), and other microsphere were formulated to create a gel on the ocular surface (Albertsson et al. 1996) It would be interesting to combine bioengineered molecules with artificial tear substitutes. These artificial tears could be tested on the extra-orbital lobe removal model (Shinomiya et al. 2018), together with our ocular wounding protocol.

Lastly, the use of our well-established CE abrasion method, together with the Eda pathway reporter mouse line led to the confirmation that both LG and cornea function together to transmit distress signals from one eye to the other and permit a faster healing process of both eyes (**figure 15**).

To conclude, the outcome of my research could help to the development of new therapeutic strategies aiming at improving the ocular surface condition, both in physiological, aging and wounded situations.

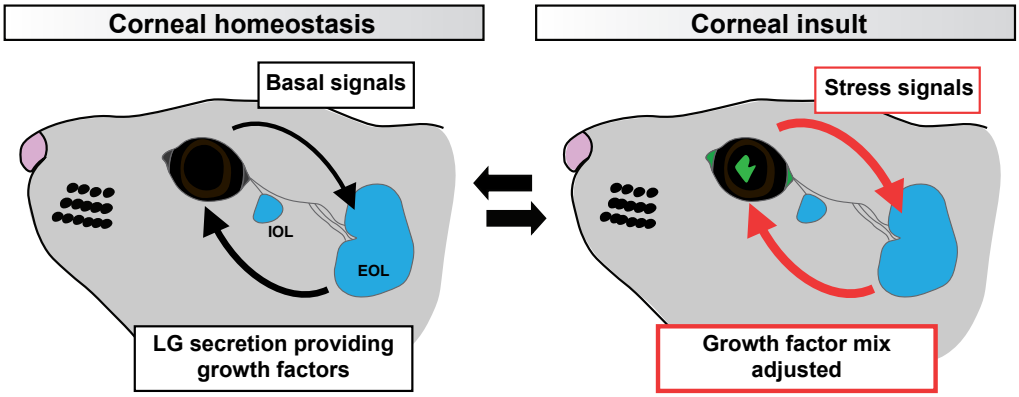

Figure 15: The cornea-LG feedback loop. The communication occurring between the lacrimal apparatus and the cornea leads to the adjustment of the tear film composition after CE injury or stress signal from the ocular surface.

6. ACKNOWLEDGEMENTS

J'aimerais dédier cette thèse à Mamie Bus, qui me sourirait avec bienveillance et prétendrait comprendre mon charabia.

I am dedicating this dissertation to my grand-mother who would smile with kindness and nod at me pretending she understands my gibberish.

As a child, I did not dream of becoming a Scientist.

In early school, I was surrounded by an environment promoting other kind of greatness. My friends wanted to become teachers, veterinarians or nurses. As for me, I was fascinated by the shape and function of teeth, and wanted to become a dentist. Medicine was probably the highest educational path in my mind and curing people the highest reward.

I encountered my greatest deception after I failed medicine school and went to Biology. At that time, Biology sounded to me like the looser discipline that failing students would take after being kicked out of medicine for not being smart enough.

My dear biologist friends, don't get offended. I realized that medicine studies were highly relying on memory and that biologists and medical staff are complementary forces.

I now believe that, for me, Biology has opened a world of incredible possibilities and of increasingly promising innovations aiming at helping mankind. Deep understanding on how the body works is definitely the key to sustainable health improvement. I am grateful to Life for leading me to follow a path I would never have expected, because of my ignorance.

"Science has taught me that everything is more complicated than we first assume, and that being able to derive happiness from discovery is a recipe for a beautiful life."
— **Hope Jahren**, Lab Girl (2016)

Fixing symptoms is one way to bury causes, but isn't it better to understand the origins of problems and prevent them from happening? Using a different metaphor, would you try to fix a television without knowing what makes it function in the first place?

I have great expectations on the evolution of children's awareness concerning the multitude of possibilities that the world offers. Let them know that failure is part of the process, and that failure brings new opportunities for discovering one's true self. Let them know that veterinarian is not the only path to contribute to animal care, and that failing in one domain does not close doors but rather opens more. Let them know how great their mind is, how smart and imaginative they can be and how these are the most valuable characteristics that will help them build their future and adapt, in order to use different path towards a same goal.

The only barriers limiting yourself are the ones you set up alone.

I had the incredible chance to be raised by encouraging parents, that always taught me to give the best of myself in whatever I would undertake. They both allowed me to be the weird child who enjoys going to the dentist to look into her parent's mouth. They taught me open-mindedness and respect.

I am grateful to my mum, who is the most loving and the strongest person I know. She taught me tolerance, along with preciseness and perseverance.

Ma dad definitely taught me patience and independency, and I thank him a lot for that. I am thankful to my whole family, from close and further away, including Trevor and Danielle.

You all took care of me in your own way, particularly during my physical distress period when I must have been a pain to cope with!

I am grateful to Gerard who did not always know how to communicate with me, but was always there for me when I needed it. Coming from a recomposed household, I know that family is not only blood-established relations, but rather the people on whom you can rely in time of need.

In this matter, I learnt that family also includes people that you choose for yourself. These are the few friends that you know accept you the way you are, and reciprocally, and for whom time and distance does not change the invisible connection that is reactivated once you see each other again. I am especially thinking about Anna, Blanca, Ewe, Isabel and Marie, without whom I definitely could not have gone through the whole PhD process here in Finland.

I would like to thank Doc. Satu Kuure and Prof. Jukka Jernvall, from my very supportive, good advising thesis committee, my two reviewers Prof. Heli Skottman and Prof. Kai Kaarniranta for their fair, incredibly fast and nice comments on my dissertation. I would like to thank Prof. Juha Partanen for taking the time to endorse the Custodian duty during the defence itself, and Prof. Susanna Fagerholm for accepting to grade my public defence. Lastly, I would like to acknowledge my opponent Prof. Igor Adameyko for taking the time to assess my scientific abilities and for challenging me on my defence day. I feel grateful and honoured to count all of you in the graduation process.

This research could not have been conducted without the generous support of the CIMO (centre for international mobility) and the FCF (Finnish cultural foundation), which partly funded my PhD. In addition, I would like to acknowledge the different funding agencies supporting the Michon's team, including the Jane and Aatos Erkko foundation and the Academy of Finland, endowing our research.

To all my past supervisors, DR Cécile Gauthier-Rouvière (CRBM Montpellier), Dr. Gisella Puga-Yung (HUG Geneve), Prof. Keith Martin (BRC Cambridge), Prof. Michalis Averof and Dr. Frederike Alwes (IGFL Lyon), I am grateful to all of you for giving me a chance to learn by your side, develop my skills, knowledge and to become humble about my own weaknesses. Particularly, I am very grateful to Doc. Andreia Bernardo (Francis Crick Institute London) who helped me discovering my passion for Developmental Biology. Differentiating hESCs into beating cardiomyocytes remains one of my most memorable joy of being a scientist.

I am grateful to the numerous scientists, friends and colleagues as much in the professional as well as in the personal environment who encouraged my path towards academia, taught me life lessons, team spirit and experimental skills. These include, obviously in a non-exhaustive manner, Kevin, Qiang, Aida, Arvydas and Giulio, Doc. Marja Mikkola and her team, Doc. Laura Ahtiainen and her team, Prof. Laurent Viriot and his team (IGFL Lyon), Prof. Irma Thesleff and her team, Agnes, Camille, Ibrahim, Kate, Lisandro, Carla, Aki, Pawel, Julien, Fabien…

You all participated in a way to whom I am and will become, and to the person I constantly try to adapt. Even in the most difficult times and the negative encounters, I find positive rewards and feel grateful for all the experiences I went through with all of you. On a more practical note, I would like to thank FuGu for their valuable participation in my transcriptomic analysis. I am very grateful to Marko Crivaro (LMU) and Miko Kivento (FuGU), who patiently helped me work out my data, make beautiful pictures and get fascinated by my own results. I could not have reached my aims without you two.

I am grateful for every little thing each one of you brought into my life, which allowed me to feel part of a bigger whole and overtake the negative loneliness feelings. My PhD period particularly contributed to my self-awareness and growth (which I will actively continue to pursue my whole life), and to my understanding of self-compassion, self-happiness. Thanks to all of you, I understood the positive aspects of being alone without feeling lonely.

Because we don't do it enough, I would like to thank the cleaning personnel and the personnel from the animal facilities in Viikki. All these people contribute to our everyday life in order to make it more comfortable. Having a good working environment is needed for the development of fruitful work. In addition, some of them were particularly kind and joyful and it contributed to making my days from times to times.

Obviously, I would like to thank all the members from the Michon team, that contributed over the years to the Science made in the team. Kaisa, Solja, Maria, Vassilis, Nicky and Yasemin, our lovely summer interns, Annina and Ana Cathia. I thank you all for your patience towards me, and for the help you all gave me whenever I was in need. I feel the necessity to acknowledge a second time Kaisa, who is entirely part of my success as a PhD

student. Kaisa, you helped me so much through these years, not only on a professional level but as well on a personal level. I owe you a lot. Your kindness, dedication, your patience and expertise are only a short non-exhaustive list of your qualities that makes you an invaluable piece of my puzzle and a wonderful person.

Finally, because there would not be any good science without a determined, exigent and motivating mentor, I thank you Fred, for all these years of patience and relentlessness. You became an important person in my life, and you helped me build up what I am now, and who I'll become in the future. I am grateful for what you brought me, and for the Science we shaped together. I truly discovered myself as a Scientist by your side. I am leaving home, but home isn't a place, it's where the mind belongs. And I hope to create the continuity of this home in my further quest for greatness.

— Alison

7. REFERENCES

Abelson MB, Ousler GW, 3rd, Maffei C. 2009. Dry eye in 2008. *Curr Opin Ophthalmol* **20**: 282-286.

Acan D, Kurtgoz P. 2017. Influence of selective serotonin reuptake inhibitors on ocular surface. *Clin Exp Optom* **100**: 83-86.

Albertsson AC, Carlfors J, Sturesson C. 1996. Preparation and characterisation of poly(adipic anhydride) microspheres for ocular drug delivery. *J Appl Polym Sci* **62**: 695-705.

Alves M, Novaes P, Morraye Mde A, Reinach PS, Rocha EM. 2014. Is dry eye an environmental disease? *Arq Bras Oftalmol* **77**: 193-200.

Andersson ER, Sandberg R, Lendahl U. 2011. Notch signalling: simplicity in design, versatility in function. *Development* **138**: 3593-3612.

Andl T, Ahn K, Kairo A, Chu EY, Wine-Lee L, Reddy ST, Croft NJ, Cebra-Thomas JA, Metzger D, Chambon P et al. 2004. Epithelial Bmpr1a regulates differentiation and proliferation in postnatal hair follicles and is essential for tooth development. *Development* **131**: 2257-2268.

Andl T, Reddy ST, Gaddapara T, Millar SE. 2002. WNT signals are required for the initiation of hair follicle development. *Dev Cell* **2**: 643-653.

Babloyantz A, Hiernaux J. 1975. Models for cell differentiation and generation of polarity in diffusion-governed morphogenetic fields. *Bull Math Biol* **37**: 637-657.

Bai JQ, Qin HF, Zhao SH. 2016. Research on mouse model of grade II corneal alkali burn. *Int J Ophthalmol* **9**: 487-490.

Barabino S, Shen L, Chen L, Rashid S, Rolando M, Dana MR. 2005. The controlled-environment chamber: a new mouse model of dry eye. *Invest Ophthalmol Vis Sci* **46**: 2766-2771.

Bayes M, Hartung AJ, Ezer S, Pispa J, Thesleff I, Srivastava AK, Kere J. 1998a. The anhidrotic ectodermal dysplasia gene (EDA) undergoes alternative splicing and encodes ectodysplasin-A with deletion mutations in collagenous repeats. *Hum Mol Genet* **7**: 1661-1669.

Bayes R, Campoy C, Molina-Font JA. 1998b. Some current controversies on nutritional requirements of full-term and pre-term newborn infants. *Early Hum Dev* **53 Suppl**: S3-13.

Berczeli O, Vizvari E, Katona M, Torok D, Szalay L, Rarosi F, Nemeth I, Rakonczay Z, Hegyi P, Ding C et al. 2018. Novel Insight Into the Role of CFTR in Lacrimal Gland Duct Function in Mice. *Invest Ophthalmol Vis Sci* **59**: 54-62.

Bhakar AL, Tannis LL, Zeindler C, Russo MP, Jobin C, Park DS, MacPherson S, Barker PA. 2002. Constitutive nuclear factor-kappa B activity is required for central neuron survival. *J Neurosci* **22**: 8466-8475.

Bhanot P, Brink M, Samos CH, Hsieh JC, Wang Y, Macke JP, Andrew D, Nathans J, Nusse R. 1996. A new member of the frizzled family from Drosophila functions as a Wingless receptor. *Nature* **382**: 225-230.

Blanco-Mezquita JT, Hutcheon AE, Stepp MA, Zieske JD. 2011. alphaVbeta6 integrin promotes corneal wound healing. *Invest Ophthalmol Vis Sci* **52**: 8505-8513.

Blanco-Mezquita JT, Hutcheon AE, Zieske JD. 2013. Role of thrombospondin-1 in repair of penetrating corneal wounds. *Invest Ophthalmol Vis Sci* **54**: 6262-6268.

Blomberg Jensen M, Jorgensen A, Nielsen JE, Steinmeyer A, Leffers H, Juul A, Rajpert-De Meyts E. 2012. Vitamin D metabolism and effects on pluripotency genes and cell differentiation in testicular germ cell tumors in vitro and in vivo. *Neoplasia* **14**: 952-963.

Botchkarev VA, Sharov AA. 2004. BMP signalling in the control of skin development and hair follicle growth. *Differentiation* **72**: 512-526.

Brewitt H, Sistani F. 2001. Dry eye disease: the scale of the problem. *Surv Ophthalmol* **45 Suppl 2**: S199-202.

Brisken C, Heineman A, Chavarria T, Elenbaas B, Tan J, Dey SK, McMahon JA, McMahon AP, Weinberg RA. 2000. Essential function of Wnt-4 in mammary gland development downstream of progesterone signalling. *Genes Dev* **14**: 650-654.

Bron AJ. 1997. The Doyne Lecture. Reflections on the tears. *Eye (Lond)* **11 (Pt 5)**: 583-602.

Butovich IA. 2017. Meibomian glands, meibum, and meibogenesis. *Exp Eye Res* **163**: 2-16.

Campbell K, Casanova J, Skaer H. 2010. Mesenchymal-to-epithelial transition of intercalating cells in Drosophila renal tubules depends on polarity cues from epithelial neighbours. *Mech Dev* **127**: 345-357.

Carroll TJ, Das A. 2013. Defining the signals that constitute the nephron progenitor niche. *J Am Soc Nephrol* **24**: 873-876.

Casal ML, Lewis JR, Mauldin EA, Tardivel A, Ingold K, Favre M, Paradies F, Demotz S, Gaide O, Schneider P. 2007. Significant correction of disease after postnatal administration of recombinant ectodysplasin A in canine X-linked ectodermal dysplasia. *Am J Hum Genet* **81**: 1050-1056.

Chaloin-Dufau C, Pavitt I, Delorme P, Dhouailly D. 1993. Identification of keratins 3 and 12 in corneal epithelium of vertebrates. *Epithelial Cell Biol* **2**: 120-125.

Chastain JB, Sindwani R. 2006. Anatomy of the orbit, lacrimal apparatus, and lateral nasal wall. *Otolaryngol Clin North Am* **39**: 855-864, v-vi.

Chen Z, Huang J, Liu Y, Dattilo LK, Huh SH, Ornitz D, Beebe DC. 2014. FGF signalling activates a Sox9-Sox10 pathway for the formation and branching morphogenesis of mouse ocular glands. *Development* **141**: 2691-2701.

Cho SJ, Valles Y, Giani VC, Jr., Seaver EC, Weisblat DA. 2010. Evolutionary dynamics of the wnt gene family: a lophotrochozoan perspective. *Mol Biol Evol* **27**: 1645-1658.

Chu EY, Hens J, Andl T, Kairo A, Yamaguchi TP, Brisken C, Glick A, Wysolmerski JJ, Millar SE. 2004. Canonical WNT signalling promotes mammary placode development and is essential for initiation of mammary gland morphogenesis. *Development* **131**: 4819-4829.

Craig JP, Nichols KK, Akpek EK, Caffery B, Dua HS, Joo CK, Liu Z, Nelson JD, Nichols JJ, Tsubota K et al. 2017. TFOS DEWS II Definition and Classification Report. *Ocul Surf* **15**: 276-283.

Cui CY, Smith JA, Schlessinger D, Chan CC. 2005. X-linked anhidrotic ectodermal dysplasia disruption yields a mouse model for ocular surface disease and resultant blindness. *Am J Pathol* **167**: 89-95.

Dartt DA. 2009. Neural regulation of lacrimal gland secretory processes: relevance in dry eye diseases. *Prog Retin Eye Res* **28**: 155-177.

de Aquino SN, Paranaiba LM, Swerts MS, Martelli DR, de Barros LM, Martelli Junior H. 2012. Orofacial features of hypohidrotic ectodermal dysplasia. *Head Neck Pathol* **6**: 460-466.

de la Cuadra-Blanco C, Peces-Pena MD, Merida-Velasco JR. 2003. Morphogenesis of the human lacrimal gland. *J Anat* **203**: 531-536.

Dean C, Ito M, Makarenkova HP, Faber SC, Lang RA. 2004. Bmp7 regulates branching morphogenesis of the lacrimal gland by promoting mesenchymal proliferation and condensation. *Development* **131**: 4155-4165.

Dean CH, Miller LA, Smith AN, Dufort D, Lang RA, Niswander LA. 2005. Canonical Wnt signalling negatively regulates branching morphogenesis of the lung and lacrimal gland. *Dev Biol* **286**: 270-286.

Dhouailly D, Pearton DJ, Michon F. 2014. The vertebrate corneal epithelium: from early specification to constant renewal. *Dev Dyn* **243**: 1226-1241.

Dickson KM, Bhakar AL, Barker PA. 2004. TRAF6-dependent NF-kB transcriptional activity during mouse development. *Dev Dyn* **231**: 122-127.

Dietz J, Kaercher T, Schneider AT, Zimmermann T, Huttner K, Johnson R, Schneider H. 2013. Early respiratory and ocular involvement in X-linked hypohidrotic ectodermal dysplasia. *Eur J Pediatr* **172**: 1023-1031.

Ding C, Lu M, Huang J. 2011. Changes of the ocular surface and aquaporins in the lacrimal glands of rabbits during pregnancy. *Mol Vis* **17**: 2847-2855.

Ding XW, Wu JH, Jiang CP. 2010. ABCG2: a potential marker of stem cells and novel target in stem cell and cancer therapy. *Life Sci* **86**: 631-637.

Dorey K, Amaya E. 2010. FGF signalling: diverse roles during early vertebrate embryogenesis. *Development* **137**: 3731-3742.

Draper CE, Adeghate EA, Singh J, Pallot DJ. 1999. Evidence to suggest morphological and physiological alterations of lacrimal gland acini with ageing. *Exp Eye Res* **68**: 265-276.

Dvoriantchikova G, Tao W, Pappas S, Gaidosh G, Tse DT, Ivanov D, Pelaez D. 2017. Molecular Profiling of the Developing Lacrimal Gland Reveals Putative Role of Notch Signalling in Branching Morphogenesis. *Invest Ophthalmol Vis Sci* **58**: 1098-1109.

Eiraku N, Hingorani R, Ijichi S, Machigashira K, Gregersen PK, Monteiro J, Usuku K, Yashiki S, Sonoda S, Osame M et al. 1998. Clonal expansion within CD4+ and CD8+ T cell subsets in human T lymphotropic virus type I-infected individuals. *J Immunol* **161**: 6674-6680.

Elo T, Lindfors PH, Lan Q, Voutilainen M, Trela E, Ohlsson C, Huh SH, Ornitz DM, Poutanen M, Howard BA et al. 2017. Ectodysplasin target gene Fgf20 regulates mammary bud growth and ductal invasion and branching during puberty. *Sci Rep* **7**: 5049.

Ervin AM, Law A, Pucker AD. 2017. Punctal occlusion for dry eye syndrome. *Cochrane Database Syst Rev* **6**: CD006775.

Farmer DT, Nathan S, Finley JK, Shengyang Yu K, Emmerson E, Byrnes LE, Sneddon JB, McManus MT, Tward AD, Knox SM. 2017. Defining epithelial cell dynamics and lineage relationships in the developing lacrimal gland. *Development* **144**: 2517-2528.

Fischer AJ, Reh TA. 2000. Identification of a proliferating marginal zone of retinal progenitors in postnatal chickens. *Dev Biol* **220**: 197-210.

Foulks GN, Bron AJ. 2003. Meibomian gland dysfunction: a clinical scheme for description, diagnosis, classification, and grading. *Ocul Surf* **1**: 107-126.

Garcia-Gallastegui P, Ibarretxe G, Garcia-Ramirez JJ, Baladron V, Aurrekoetxea M, Nueda ML, Naranjo AI, Santaolalla F, Sanchez-del Rey A, Laborda J et al. 2014. DLK1 regulates branching morphogenesis and parasympathetic innervation of salivary glands through inhibition of NOTCH signalling. *Biol Cell* **106**: 237-253.

Gasser RF, Cork RJ, Stillwell BJ, McWilliams DT. 2014. Rebirth of human embryology. *Dev Dyn* **243**: 621-628.

Gayton JL. 2009. Etiology, prevalence, and treatment of dry eye disease. *Clin Ophthalmol* **3**: 405-412.

Gierer A, Meinhardt H. 1972. A theory of biological pattern formation. *Kybernetik* **12**: 30-39.

Gipson IK. 2004. Distribution of mucins at the ocular surface. *Exp Eye Res* **78**: 379-388.

-. 2016. Goblet cells of the conjunctiva: A review of recent findings. *Prog Retin Eye Res* **54**: 49-63.

Gipson IK, Kiorpes TC. 1982. Epithelial sheet movement: protein and glycoprotein synthesis. *Dev Biol* **92**: 259-262.

Grahn BH, Storey ES. 2004. Lacrimostimulants and lacrimomimetics. *Vet Clin North Am Small Anim Pract* **34**: 739-753.

Granata A, Bernard WG, Zhao N, McCafferty J, Lilly B, Sinha S. 2015. Temporal and embryonic lineage-dependent regulation of human vascular SMC development by NOTCH3. *Stem Cells Dev* **24**: 846-856.

Gromova A, Voronov DA, Yoshida M, Thotakura S, Meech R, Dartt DA, Makarenkova HP. 2017. Lacrimal Gland Repair Using Progenitor Cells. *Stem Cells Transl Med* **6**: 88-98.

Grüneberg H. 1971. The glandular aspects of the tabby syndrome in the mouse. *Journal of embryology and experimental morphology* **25**: 1-19.

Haara O, Fujimori S, Schmidt-Ullrich R, Hartmann C, Thesleff I, Mikkola ML. 2011. Ectodysplasin and Wnt pathways are required for salivary gland branching morphogenesis. *Development* **138**: 2681-2691.

Hamann S, Zeuthen T, La Cour M, Nagelhus EA, Ottersen OP, Agre P, Nielsen S. 1998. Aquaporins in complex tissues: distribution of aquaporins 1-5 in human and rat eye. *Am J Physiol* **274**: C1332-1345.

Hawley D, Ding J, Thotakura S, Haskett S, Aluri H, Kublin C, Michel A, Clapisson L, Mingueneau M, Zoukhri D. 2017. RNA-Seq and CyTOF immuno-profiling of regenerating lacrimal glands identifies a novel subset of cells expressing muscle-related proteins. *PLoS One* **12**: e0179385.

Headon DJ, Emmal SA, Ferguson BM, Tucker AS, Justice MJ, Sharpe PT, Zonana J, Overbeek PA. 2001. Gene defect in ectodermal dysplasia implicates a death domain adapter in development. *Nature* **414**: 913-916.

Heitzler P. 2010. Biodiversity and noncanonical Notch signalling. *Curr Top Dev Biol* **92**: 457-481.

Hernandez Galindo EE, Theiss C, Steuhl KP, Meller D. 2003. Expression of Delta Np63 in response to phorbol ester in human limbal epithelial cells expanded on intact human amniotic membrane. *Invest Ophthalmol Vis Sci* **44**: 2959-2965.

Hirayama M, Ogawa M, Oshima M, Sekine Y, Ishida K, Yamashita K, Ikeda K, Shimmura S, Kawakita T, Tsubota K et al. 2013a. Functional lacrimal gland regeneration by transplantation of a bioengineered organ germ. *Nat Commun* **4**: 2497.

Hirayama M, Oshima M, Tsuji T. 2013b. Development and prospects of organ replacement regenerative therapy. *Cornea* **32 Suppl 1**: S13-21.

Hirayama M, Tsubota K, Tsuji T. 2015. Bioengineered Lacrimal Gland Organ Regeneration in Vivo. *J Funct Biomater* **6**: 634-649.

-. 2017. Generation of a Bioengineered Lacrimal Gland by Using the Organ Germ Method. *Methods Mol Biol* **1597**: 153-165.

Hodges RR, Dartt DA. 2003. Regulatory pathways in lacrimal gland epithelium. *Int Rev Cytol* **231**: 129-196.

Holly FJ, Lemp MA. 1977. Tear physiology and dry eyes. *Surv Ophthalmol* **22**: 69-87.

Hori K, Sen A, Artavanis-Tsakonas S. 2013. Notch signalling at a glance. *J Cell Sci* **126**: 2135-2140.

Imam S, Elagin RB, Jaume JC. 2013. Diabetes-associated dry eye syndrome in a new humanized transgenic model of type 1 diabetes. *Mol Vis* **19**: 1259-1267.

Ishida N, Hirai SI, Mita S. 1997. Immunolocalization of aquaporin homologs in mouse lacrimal glands. *Biochem Bioph Res Co* **238**: 891-895.

Jabs DA, Prendergast RA. 1994. Murine models of Sjogren's syndrome. *Adv Exp Med Biol* **350**: 623-630.

Jackson H. 1960. Effect of eye-pads on healing of simple corneal abrasions. *Br Med J* **2**: 713.

Jaskoll T, Zhou YM, Trump G, Melnick M. 2003. Ectodysplasin receptor-mediated signalling is essential for embryonic submandibular salivary gland development. *Anat Rec A Discov Mol Cell Evol Biol* **271**: 322-331.

Javadi MA, Feizi S. 2011. Dry eye syndrome. *J Ophthalmic Vis Res* **6**: 192-198.

Jiang LY, Zhang XL, Du P, Zheng JH. 2011. gamma-Secretase Inhibitor, DAPT Inhibits Self-renewal and Stemness Maintenance of Ovarian Cancer Stem-like Cells In Vitro. *Chin J Cancer Res* **23**: 140-146.

Jing J, Jiang X, Chen J, Yao X, Zhao M, Li P, Pan Y, Ren Y, Liu W, Lyu L. 2017. Notch signalling pathway promotes the development of ovine ovarian follicular granulosa cells. *Anim Reprod Sci* **181**: 69-78.

Johnson ME, Murphy PJ. 2004. Changes in the tear film and ocular surface from dry eye syndrome. *Prog Retin Eye Res* **23**: 449-474.

Jones KB, Goodwin AF, Landan M, Seidel K, Tran DK, Hogue J, Chavez M, Fete M, Yu W, Hussein T et al. 2013. Characterization of X-linked hypohidrotic ectodermal dysplasia (XL-HED) hair and sweat gland phenotypes using phototrichogram analysis and live confocal imaging. *Am J Med Genet A* **161A**: 1585-1593.

Kalha S, Kuony A, Michon F. 2018a. Corneal Epithelial Abrasion with Ocular Burr As a Model for Cornea Wound Healing. *J Vis Exp*.

Kalha S, Shrestha B, Sanz Navarro M, Jones KB, Klein OD, Michon F. 2018b. Bmi1+ Progenitor Cell Dynamics in Murine Cornea During Homeostasis and Wound Healing. *Stem Cells* **36**: 562-573.

Kangas AT, Evans AR, Thesleff I, Jernvall J. 2004. Nonindependence of mammalian dental characters. *Nature* **432**: 211-214.

Katona M, Vizvari E, Nemeth L, Facsko A, Venglovecz V, Rakonczay Z, Jr., Hegyi P, Toth-Molnar E. 2014. Experimental evidence of fluid secretion of rabbit lacrimal gland duct epithelium. *Invest Ophthalmol Vis Sci* **55**: 4360-4367.

Kels BD, Grzybowski A, Grant-Kels JM. 2015. Human ocular anatomy. *Clin Dermatol* **33**: 140-146.

Kim W, Barron DA, San Martin R, Chan KS, Tran LL, Yang F, Ressler SJ, Rowley DR. 2014. RUNX1 is essential for mesenchymal stem cell proliferation and myofibroblast differentiation. *Proc Natl Acad Sci U S A* **111**: 16389-16394.

King-Smith PE, Fink BA, Fogt N, Nichols KK, Hill RM, Wilson GS. 2000. The thickness of the human precorneal tear film: evidence from reflection spectra. *Invest Ophthalmol Vis Sci* **41**: 3348-3359.

Kinney PL. 2008. Climate change, air quality, and human health. *Am J Prev Med* **35**: 459-467.

Klenkler B, Sheardown H, Jones L. 2007. Growth factors in the tear film: role in tissue maintenance, wound healing, and ocular pathology. *Ocul Surf* **5**: 228-239.

Kojima T, Higuchi A, Goto E, Matsumoto Y, Dogru M, Tsubota K. 2008. Autologous serum eye drops for the treatment of dry eye diseases. *Cornea* **27 Suppl 1**: S25-30.

Koledova Z, Zhang X, Streuli C, Clarke RB, Klein OD, Werb Z, Lu P. 2016. SPRY1 regulates mammary epithelial morphogenesis by modulating EGFR-dependent stromal paracrine signalling and ECM remodeling. *Proc Natl Acad Sci U S A* **113**: E5731-5740.

Kopan R, Ilagan MX. 2009. The canonical Notch signalling pathway: unfolding the activation mechanism. *Cell* **137**: 216-233.

Kowalczyk-Quintas C, Schuepbach-Mallepell S, Willen L, Smith TK, Huttner K, Kirby N, Headon DJ, Schneider P. 2015. Pharmacological stimulation of Edar signalling in the adult enhances sebaceous gland size and function. *J Invest Dermatol* **135**: 359-368.

Kowalczyk C, Dunkel N, Willen L, Casal ML, Mauldin EA, Gaide O, Tardivel A, Badic G, Etter AL, Favre M et al. 2011. Molecular and therapeutic characterization of anti-ectodysplasin A receptor (EDAR) agonist monoclonal antibodies. *J Biol Chem* **286**: 30769-30779.

Kucerova R, Dora N, Mort RL, Wallace K, Leiper LJ, Lowes C, Neves C, Walczysko P, Bruce F, Fowler PA et al. 2012. Interaction between hedgehog signalling and PAX6 dosage mediates maintenance and regeneration of the corneal epithelium. *Mol Vis* **18**: 139-150.

Kumar A, Eby MT, Sinha S, Jasmin A, Chaudhary PM. 2001. The ectodermal dysplasia receptor activates the nuclear factor-kappaB, JNK, and cell death pathways and binds to ectodysplasin A. *J Biol Chem* **276**: 2668-2677.

Kuony A, Michon F. 2017. Epithelial Markers aSMA, Krt14, and Krt19 Unveil Elements of Murine Lacrimal Gland Morphogenesis and Maturation. *Front Physiol* **8**: 739.

Ladoux B, Mege RM. 2017. Mechanobiology of collective cell behaviours. *Nat Rev Mol Cell Biol* **18**: 743-757.

LeBleu VS, Taduri G, O'Connell J, Teng Y, Cooke VG, Woda C, Sugimoto H, Kalluri R. 2013. Origin and function of myofibroblasts in kidney fibrosis. *Nat Med* **19**: 1047-1053.

Lee BH, Tudares MA, Nguyen CQ. 2009. Sjogren's syndrome: an old tale with a new twist. *Arch Immunol Ther Exp (Warsz)* **57**: 57-66.

Lee GA, Chen SX. 2008. Autologous serum in the management of recalcitrant dry eye syndrome. *Clin Exp Ophthalmol* **36**: 119-122.

Lehtosalo J, Uusitalo H, Mahrberg T, Panula P, Palkama A. 1989. Nerve fibers showing immunoreactivities for proenkephalin A-derived peptides in the lacrimal glands of the guinea pig. *Graefes Arch Clin Exp Ophthalmol* **227**: 455-458.

Levine M, Tjian R. 2003. Transcription regulation and animal diversity. *Nature* **424**: 147-151.

Levitt AE, Galor A, Weiss JS, Felix ER, Martin ER, Patin DJ, Sarantopoulos KD, Levitt RC. 2015. Chronic dry eye symptoms after LASIK: parallels and lessons to be learned from other persistent post-operative pain disorders. *Mol Pain* **11**: 21.

Li S, Zhou J, Bu J, Ning K, Zhang L, Li J, Guo Y, He X, He H, Cai X et al. 2017. Ectodysplasin A protein promotes corneal epithelial cell proliferation. *J Biol Chem* **292**: 13391-13401.

Liu F, Chu EY, Watt B, Zhang Y, Gallant NM, Andl T, Yang SH, Lu MM, Piccolo S, Schmidt-Ullrich R et al. 2008. Wnt/beta-catenin signalling directs multiple stages of tooth morphogenesis. *Dev Biol* **313**: 210-224.

Liu F, Millar SE. 2010. Wnt/beta-catenin signalling in oral tissue development and disease. *J Dent Res* **89**: 318-330.

Liu S, Dozois MD, Chang CN, Ahmad A, Ng DL, Hileeto D, Liang H, Reyad MM, Boyd S, Jones LW et al. 2016. Prolonged Ocular Retention of Mucoadhesive Nanoparticle Eye Drop Formulation Enables Treatment of Eye Diseases Using Significantly Reduced Dosage. *Mol Pharm* **13**: 2897-2905.

Lorber M. 2007. Gross characteristics of normal human lacrimal glands. *Ocul Surf* **5**: 13-22.

Lu X, Wang X, Nian H, Yang D, Wei R. 2017. Mesenchymal stem cells for treating autoimmune dacryoadenitis. *Stem Cell Res Ther* **8**: 126.

Lubis RR, Gultom MTH. 2018. The Correlation between Daily Lens Wear Duration and Dry Eye Syndrome. *Open Access Maced J Med Sci* **6**: 829-834.

Lwigale PY. 2015. Corneal Development: Different Cells from a Common Progenitor. *Prog Mol Biol Transl Sci* **134**: 43-59.

Lwigale PY, Bronner-Fraser M. 2007. Lens-derived Semaphorin3A regulates sensory innervation of the cornea. *Dev Biol* **306**: 750-759.

Ma Q, Wang Y, Zhang T, Zuo W. 2018. Notch-mediated Sox9(+) cell activation contributes to kidney repair after partial nephrectomy. *Life Sci* **193**: 104-109.

Mac Sweeney A, Gil-Parrado S, Vinzenz D, Bernardi A, Hein A, Bodendorf U, Erbel P, Logel C, Gerhartz B. 2008. Structural basis for the substrate specificity of bone morphogenetic protein 1/tolloid-like metalloproteases. *J Mol Biol* **384**: 228-239.

Macleod A, Kumar PA, Hertess I, Newing R. 1990. Microvascular submandibular gland transfer; an alternative approach for total xerophthalmia. *Br J Plast Surg* **43**: 437-439.

Maddula S, Davis DK, Maddula S, Burrow MK, Ambati BK. 2011. Horizons in therapy for corneal angiogenesis. *Ophthalmology* **118**: 591-599.

Madisen L, Zwingman TA, Sunkin SM, Oh SW, Zariwala HA, Gu H, Ng LL, Palmiter RD, Hawrylycz MJ, Jones AR et al. 2010. A robust and high-throughput Cre reporting and characterization system for the whole mouse brain. *Nat Neurosci* **13**: 133-140.

Makarenkova HP, Dartt DA. 2015. Myoepithelial Cells: Their Origin and Function in Lacrimal Gland Morphogenesis, Homeostasis, and Repair. *Curr Mol Biol Rep* **1**: 115-123.

Makarenkova HP, Ito M, Govindarajan V, Faber SC, Sun L, McMahon G, Overbeek PA, Lang RA. 2000. FGF10 is an inducer and Pax6 a competence factor for lacrimal gland development. *Development* **127**: 2563-2572.

Malecaze F, Massoudi D, Fournie P, Tricoire C, Cassagne M, Malbouyres M, Hulmes DJ, Moali C, Galiacy SD. 2014. Upregulation of bone morphogenetic protein-1/mammalian tolloid and procollagen C-proteinase enhancer-1 in corneal scarring. *Invest Ophthalmol Vis Sci* **55**: 6712-6721.

Marfurt CF, Cox J, Deek S, Dvorscak L. 2010. Anatomy of the human corneal innervation. *Exp Eye Res* **90**: 478-492.

Matsumoto Y, Tanabe T, Ueda S, Kawata M. 1992. Immunohistochemical and enzymehistochemical studies of peptidergic, aminergic and cholinergic innervation of the lacrimal gland of the monkey (Macaca fuscata). *J Auton Nerv Syst* **37**: 207-214.

McCulley JP, Shine WE. 2003. Meibomian gland function and the tear lipid layer. *Ocul Surf* **1**: 97-106.

McKenna CC, Lwigale PY. 2011. Innervation of the mouse cornea during development. *Invest Ophthalmol Vis Sci* **52**: 30-35.

Messmer EM. 2015. The pathophysiology, diagnosis, and treatment of dry eye disease. *Dtsch Arztebl Int* **112**: 71-81; quiz 82.

Michon F, Forest L, Collomb E, Demongeot J, Dhouailly D. 2008. BMP2 and BMP7 play antagonistic roles in feather induction. *Development* **135**: 2797-2805.

Mikkola ML. 2009. Molecular aspects of hypohidrotic ectodermal dysplasia. *Am J Med Genet A* **149A**: 2031-2036.

Mikkola ML, Pispa J, Pekkanen M, Paulin L, Nieminen P, Kere J, Thesleff I. 1999. Ectodysplasin, a protein required for epithelial morphogenesis, is a novel TNF homologue and promotes cell-matrix adhesion. *Mech Dev* **88**: 133-146.

Muller LJ, Marfurt CF, Kruse F, Tervo TM. 2003. Corneal nerves: structure, contents and function. *Exp Eye Res* **76**: 521-542.

Munne PM, Narhi K, Michon F. 2013. Analysis of tissue interactions in ectodermal organ culture. *Methods Mol Biol* **945**: 401-416.

Murube J. 2009. Basal, reflex, and psycho-emotional tears. *Ocul Surf* **7**: 60-66.

Mustonen T, Pispa J, Mikkola ML, Pummila M, Kangas AT, Pakkasjarvi L, Jaatinen R, Thesleff I. 2003. Stimulation of ectodermal organ development by Ectodysplasin-A1. *Dev Biol* **259**: 123-136.

Muzumdar MD, Tasic B, Miyamichi K, Li L, Luo L. 2007. A global double-fluorescent Cre reporter mouse. *Genesis* **45**: 593-605.

Nakamachi T, Ohtaki H, Seki T, Yofu S, Kagami N, Hashimoto H, Shintani N, Baba A, Mark L, Lanekoff I et al. 2016. PACAP suppresses dry eye signs by stimulating tear secretion. *Nat Commun* **7**: 12034.

Nasser W, Amitai-Lange A, Soteriou D, Hanna R, Tiosano B, Fuchs Y, Shalom-Feuerstein R. 2018. Corneal-Committed Cells Restore the Stem Cell Pool and Tissue Boundary following Injury. *Cell Rep* **22**: 323-331.

Neben CL, Lo M, Jura N, Klein OD. 2017. Feedback regulation of RTK signalling in development. *Dev Biol*.

Nedvetsky PI, Emmerson E, Finley JK, Ettinger A, Cruz-Pacheco N, Prochazka J, Haddox CL, Northrup E, Hodges C, Mostov KE et al. 2014. Parasympathetic innervation regulates tubulogenesis in the developing salivary gland. *Dev Cell* **30**: 449-462.

Nguyen MB, Cohen I, Kumar V, Xu Z, Bar C, Dauber-Decker KL, Tsai PC, Marangoni P, Klein OD, Hsu YC et al. 2018. FGF signalling controls the specification of hair placode-derived SOX9 positive progenitors to Merkel cells. *Nat Commun* **9**: 2333.

O'Brien PD, Collum LM. 2004. Dry eye: diagnosis and current treatment strategies. *Curr Allergy Asthma Rep* **4**: 314-319.

Obata H. 2002. Anatomy and histopathology of human meibomian gland. *Cornea* **21**: S70-74.

-. 2006. Anatomy and histopathology of the human lacrimal gland. *Cornea* **25**: S82-89.

Obata H, Horiuchi H, Miyata K, Tsuru T, Machinami R. 1994. [Histopathological study of the meibomian glands in 72 autopsy cases]. *Nippon Ganka Gakkai Zasshi* **98**: 765-771.

Obata H, Yamamoto S, Horiuchi H, Machinami R. 1995. Histopathologic study of human lacrimal gland. Statistical analysis with special reference to aging. *Ophthalmology* **102**: 678-686.

Ollivier FJ. 2004. The precorneal tear film in horses: its importance and disorders. *Vet Clin North Am Equine Pract* **20**: 301-318.

Ollivier FJ, Gilger BC, Barrie KP, Kallberg ME, Plummer CE, O'Reilly S, Gelatt KN, Brooks DE. 2007. Proteinases of the cornea and preocular tear film. *Vet Ophthalmol* **10**: 199-206.

Orge FH, Boente CS. 2014. The lacrimal system. *Pediatr Clin North Am* **61**: 529-539.

Ornitz DM, Itoh N. 2015. The Fibroblast Growth Factor signalling pathway. *Wiley Interdiscip Rev Dev Biol* **4**: 215-266.

Osumi N, Shinohara H, Numayama-Tsuruta K, Maekawa M. 2008. Concise review: Pax6 transcription factor contributes to both embryonic and adult neurogenesis as a multifunctional regulator. *Stem Cells* **26**: 1663-1672.

Ouyang H, Xue Y, Lin Y, Zhang X, Xi L, Patel S, Cai H, Luo J, Zhang M, Zhang M et al. 2014. WNT7A and PAX6 define corneal epithelium homeostasis and pathogenesis. *Nature* **511**: 358-361.

Pan Q, Angelina A, Zambrano A, Marrone M, Stark WJ, Heflin T, Tang L, Akpek EK. 2013. Autologous serum eye drops for dry eye. *Cochrane Database Syst Rev*: CD009327.

Patel DV, McGhee CN. 2005. Mapping of the normal human corneal sub-Basal nerve plexus by in vivo laser scanning confocal microscopy. *Invest Ophthalmol Vis Sci* **46**: 4485-4488.

Patel N, Sharpe PT, Miletich I. 2011. Coordination of epithelial branching and salivary gland lumen formation by Wnt and FGF signals. *Dev Biol* **358**: 156-67.

Patel R, Zhu M, Robertson DM. 2018. Shifting the IGF-axis: An age-related decline in human tear IGF-1 correlates with clinical signs of dry eye. *Growth Horm IGF Res* **40**: 69-73.

Paulsen FP, Berry MS. 2006. Mucins and TFF peptides of the tear film and lacrimal apparatus. *Prog Histochem Cytochem* **41**: 1-53.

Paulsen FP, Schaudig U, Thale AB. 2003. Drainage of tears: impact on the ocular surface and lacrimal system. *Ocul Surf* **1**: 180-191.

Pearson AA. 1980. The development of the eyelids. Part I. External features. *J Anat* **130**: 33-42.

Pearton DJ, Ferraris C, Dhouailly D. 2004. Transdifferentiation of corneal epithelium: evidence for a linkage between the segregation of epidermal stem cells and the induction of hair follicles during embryogenesis. *Int J Dev Biol* **48**: 197-201.

Petznick A, Madigan MC, Garrett Q, Sweeney DF, Evans MD. 2013. Contributions of ocular surface components to matrix-metalloproteinases (MMP)-2 and MMP-9 in feline tears following corneal epithelial wounding. *PLoS One* **8**: e71948.

Pispa J, Jung HS, Jernvall J, Kettunen P, Mustonen T, Tabata MJ, Kere J, Thesleff I. 1999. Cusp patterning defect in Tabby mouse teeth and its partial rescue by FGF. *Dev Biol* **216**: 521-534.

Pispa J, Mikkola ML, Mustonen T, Thesleff I. 2003. Ectodysplasin, Edar and TNFRSF19 are expressed in complementary and overlapping patterns during mouse embryogenesis. *Gene Expr Patterns* **3**: 675-679.

Pispa J, Mustonen T, Mikkola ML, Kangas AT, Koppinen P, Lukinmaa PL, Jernvall J, Thesleff I. 2004. Tooth patterning and enamel formation can be manipulated by misexpression of TNF receptor Edar. *Dev Dyn* **231**: 432-440.

Pispa J, Pummila M, Barker PA, Thesleff I, Mikkola ML. 2008. Edar and Troy signalling pathways act redundantly to regulate initiation of hair follicle development. *Hum Mol Genet* **17**: 3380-3391.

Ravi Kumar MN. 2000. Nano and microparticles as controlled drug delivery devices. *J Pharm Pharm Sci* **3**: 234-258.

Reynolds BA, Weiss S. 1992. Generation of neurons and astrocytes from isolated cells of the adult mammalian central nervous system. *Science* **255**: 1707-1710.

Rios JD, Horikawa Y, Chen LL, Kublin CL, Hodges RR, Dartt DA, Zoukhri D. 2005. Age-dependent alterations in mouse exorbital lacrimal gland structure, innervation and secretory response. *Exp Eye Res* **80**: 477-491.

Rocha EM, Alves M, Rios JD, Dartt DA. 2008. The aging lacrimal gland: changes in structure and function. *Ocul Surf* **6**: 162-174.

Rocha EM, Cunha DA, Carneiro EM, Boschero AC, Saad MJ, Velloso LA. 2002. Identification of insulin in the tear film and insulin receptor and IGF-1 receptor on the human ocular surface. *Invest Ophthalmol Vis Sci* **43**: 963-967.

Rozsa AJ, Beuerman RW. 1982. Density and organization of free nerve endings in the corneal epithelium of the rabbit. *Pain* **14**: 105-120.

Sakakibara S, Imai T, Hamaguchi K, Okabe M, Aruga J, Nakajima K, Yasutomi D, Nagata T, Kurihara Y, Uesugi S et al. 1996. Mouse-Musashi-1, a neural RNA-binding protein highly enriched in the mammalian CNS stem cell. *Dev Biol* **176**: 230-242.

Sakaue-Sawano A, Kurokawa H, Morimura T, Hanyu A, Hama H, Osawa H, Kashiwagi S, Fukami K, Miyata T, Miyoshi H et al. 2008. Visualizing spatiotemporal dynamics of multicellular cell-cycle progression. *Cell* **132**: 487-498.

Schechter JE, Warren DW, Mircheff AK. 2010. A lacrimal gland is a lacrimal gland, but rodent's and rabbit's are not human. *Ocul Surf* **8**: 111-134.

Scheitz CJ, Tumbar T. 2013. New insights into the role of Runx1 in epithelial stem cell biology and pathology. *J Cell Biochem* **114**: 985-993.

Schermer A, Galvin S, Sun TT. 1986. Differentiation-related expression of a major 64K corneal keratin in vivo and in culture suggests limbal location of corneal epithelial stem cells. *J Cell Biol* **103**: 49-62.

Schey KL, Wang Z, J LW, Qi Y. 2014. Aquaporins in the eye: expression, function, and roles in ocular disease. *Biochim Biophys Acta* **1840**: 1513-1523.

Shatos MA, Haugaard-Kedstrom L, Hodges RR, Dartt DA. 2012. Isolation and characterization of progenitor cells in uninjured, adult rat lacrimal gland. *Invest Ophthalmol Vis Sci* **53**: 2749-2759.

Sheardown H, Cheng YL. 1996. Tear EGF concentration following corneal epithelial wound creation. *J Ocul Pharmacol Ther* **12**: 239-243.

Shimmura S, Ueno R, Matsumoto Y, Goto E, Higuchi A, Shimazaki J, Tsubota K. 2003. Albumin as a tear supplement in the treatment of severe dry eye. *Br J Ophthalmol* **87**: 1279-1283.

Shinomiya K, Ueta M, Kinoshita S. 2018. A new dry eye mouse model produced by exorbital and intraorbital lacrimal gland excision. *Sci Rep* **8**: 1483.

Shyh-Chang N, Zhu H, Yvanka de Soysa T, Shinoda G, Seligson MT, Tsanov KM, Nguyen L, Asara JM, Cantley LC, Daley GQ. 2013. Lin28 enhances tissue repair by reprogramming cellular metabolism. *Cell* **155**: 778-792.

Sigurdsson V, Ingthorsson S, Hilmarsdottir B, Gustafsdottir SM, Franzdottir SR, Arason AJ, Steingrimsson E, Magnusson MK, Gudjonsson T. 2013. Expression and functional role of sprouty-2 in breast morphogenesis. *PLoS One* **8**: e60798.

Snippert HJ, van der Flier LG, Sato T, van Es JH, van den Born M, Kroon-Veenboer C, Barker N, Klein AM, van Rheenen J, Simons BD et al. 2010. Intestinal crypt homeostasis results from neutral competition between symmetrically dividing Lgr5 stem cells. *Cell* **143**: 134-144.

Srivastava AK, Pispa J, Hartung AJ, Du Y, Ezer S, Jenks T, Shimada T, Pekkanen M, Mikkola ML, Ko MS et al. 1997. The Tabby phenotype is caused by mutation in a mouse homologue of the EDA gene that reveals novel mouse and human exons and encodes a protein (ectodysplasin-A) with collagenous domains. *Proc Natl Acad Sci U S A* **94**: 13069-13074.

Swamynathan SK. 2013. Ocular surface development and gene expression. *J Ophthalmol* **2013**: 103947.

Tabbara K, Sharara N. 1999. Sjogren's syndrome: pathogenesis. *Eur J Ophthalmol* **9**: 1-7.

Takacs E, Boto P, Simo E, Csuth TI, Toth BM, Raveh-Amit H, Pap A, Kovacs EG, Kobolak J, Benko S et al. 2017. Immunogenic Dendritic Cell Generation from Pluripotent Stem Cells by Ectopic Expression of Runx3. *J Immunol* **198**: 239-248.

Takahashi Y, Watanabe A, Matsuda H, Nakamura Y, Nakano T, Asamoto K, Ikeda H, Kakizaki H. 2013. Anatomy of secretory glands in the eyelid and conjunctiva: a photographic review. *Ophthalmic Plast Reconstr Surg* **29**: 215-219.

Tervo T, Vesaluoma M, Bennett GL, Schwall R, Helena M, Liang Q, Wilson SE. 1997. Tear hepatocyte growth factor (HGF) availability increases markedly after excimer laser surface ablation. *Exp Eye Res* **64**: 501-504.

Thisse B, Thisse C. 2005. Functions and regulations of fibroblast growth factor signalling during embryonic development. *Dev Biol* **287**: 390-402.

Thomadakis G, Ramoshebi LN, Crooks J, Rueger DC, Ripamonti U. 1999. Immunolocalization of Bone Morphogenetic Protein-2 and -3 and Osteogenic Protein-1 during murine tooth root morphogenesis and in other craniofacial structures. *Eur J Oral Sci* **107**: 368-377.

Tiffany JM. 2008. The normal tear film. *Dev Ophthalmol* **41**: 1-20.

Tiwari S, Ali MJ, Balla MM, Naik MN, Honavar SG, Reddy VA, Vemuganti GK. 2012. Establishing human lacrimal gland cultures with secretory function. *PLoS One* **7**: e29458.

Tiwari S, Ali MJ, Vemuganti GK. 2014. Human lacrimal gland regeneration: Perspectives and review of literature. *Saudi J Ophthalmol* **28**: 12-18.

Toshida H, Nguyen DH, Beuerman RW, Murakami A. 2007. Evaluation of novel dry eye model: preganglionic parasympathetic denervation in rabbit. *Invest Ophthalmol Vis Sci* **48**: 4468-4475.

Tost FH, Geerling G. 2008. Plugs for occlusion of the lacrimal drainage system. *Dev Ophthalmol* **41**: 193-212.

Trosan P, Svobodova E, Chudickova M, Krulova M, Zajicova A, Holan V. 2012. The key role of insulin-like growth factor I in limbal stem cell differentiation and the corneal wound-healing process. *Stem Cells Dev* **21**: 3341-3350.

Tsao PN, Chen F, Izvolsky KI, Walker J, Kukuruzinska MA, Lu J, Cardoso WV. 2008. Gamma-secretase activation of notch signalling regulates the balance of proximal and distal fates in progenitor cells of the developing lung. *J Biol Chem* **283**: 29532-29544.

Tsubota K. 1998. Tear dynamics and dry eye. *Prog Retin Eye Res* **17**: 565-596.

Tucker AS, Headon DJ, Courtney JM, Overbeek P, Sharpe PT. 2004. The activation level of the TNF family receptor, Edar, determines cusp number and tooth number during tooth development. *Dev Biol* **268**: 185-194.

Tuominen IS, Tervo TM, Teppo AM, Valle TU, Gronhagen-Riska C, Vesaluoma MH. 2001. Human tear fluid PDGF-BB, TNF-alpha and TGF-beta1 vs corneal haze and regeneration of corneal epithelium and subbasal nerve plexus after PRK. *Exp Eye Res* **72**: 631-641.

Tyagi P, Tyagi V, Hashim AA. 2011. Ocular and non-ocular manifestations of hypohidrotic ectodermal dysplasia. *BMJ Case Rep* **2011**.

Uchino Y, Kawakita T, Ishii T, Ishii N, Tsubota K. 2012. A new mouse model of dry eye disease: oxidative stress affects functional decline in the lacrimal gland. *Cornea* **31 Suppl 1**: S63-67.

van Amerongen R, Nusse R. 2009. Towards an integrated view of Wnt signalling in development. *Development* **136**: 3205-3214.

Vanderburg CR, Hay ED. 1996. E-cadherin transforms embryonic corneal fibroblasts to stratified epithelium with desmosomes. *Acta Anat (Basel)* **157**: 87-104.

Veiga Neto ER, Tamega OJ, Zorzetto NL, Dall Pai V. 1992. Anatomical aspects of the lacrimal gland of the tufted capuchin (Cebus apella). *J Anat* **180 (Pt 1)**: 75-80.

Violini S, Gorni C, Pisani LF, Ramelli P, Caniatti M, Mariani P. 2012. Isolation and differentiation potential of an equine amnion-derived stromal cell line. *Cytotechnology* **64**: 1-7.

Vizvari E, Katona M, Orvos P, Berczeli O, Facsko A, Rarosi F, Venglovecz V, Rakonczay Z, Jr., Hegyi P, Ding C et al. 2016. Characterization of Na+-K+-2Cl- Cotransporter Activity in Rabbit Lacrimal Gland Duct Cells. *Invest Ophthalmol Vis Sci* **57**: 3828-3835.

Voronov D, Gromova A, Liu D, Zoukhri D, Medvinsky A, Meech R, Makarenkova HP. 2013. Transcription factors Runx1 to 3 are expressed in the lacrimal gland epithelium and are involved in regulation of gland morphogenesis and regeneration. *Invest Ophthalmol Vis Sci* **54**: 3115-3125.

Walcott B. 1998. The Lacrimal Gland and Its Veil of Tears. *News Physiol Sci* **13**: 97-103.

Wang F, Flanagan J, Su N, Wang LC, Bui S, Nielson A, Wu X, Vo HT, Ma XJ, Luo Y. 2012. RNAscope: a novel in situ RNA analysis platform for formalin-fixed, paraffin-embedded tissues. *J Mol Diagn* **14**: 22-29.

Wang J, Fonn D, Simpson TL, Jones L. 2003. Precorneal and pre- and postlens tear film thickness measured indirectly with optical coherence tomography. *Invest Ophthalmol Vis Sci* **44**: 2524-2528.

Wang RN, Green J, Wang Z, Deng Y, Qiao M, Peabody M, Zhang Q, Ye J, Yan Z, Denduluri S et al. 2014. Bone Morphogenetic Protein (BMP) signalling in development and human diseases. *Genes Dis* **1**: 87-105.

Wang S, Sekiguchi R, Daley WP, Yamada KM. 2017. Patterned cell and matrix dynamics in branching morphogenesis. *J Cell Biol* **216**: 559-570.

Wang YC, Li S, Chen X, Ma B, He H, Liu T, Yu J, Zhang L, Chen Y, Liu Z et al. 2016. Meibomian Gland Absence Related Dry Eye in Ectodysplasin A Mutant Mice. *Am J Pathol* **186**: 32-42.

Wang YL, Tan Y, Satoh Y, Ono K. 1995. Morphological changes of myoepithelial cells of mouse lacrimal glands during postnatal development. *Histol Histopathol* **10**: 821-827.

Warren DW. 1994. Hormonal influences on the lacrimal gland. *Int Ophthalmol Clin* **34**: 19-25.

Weaver M, Dunn NR, Hogan BL. 2000. Bmp4 and Fgf10 play opposing roles during lung bud morphogenesis. *Development* **127**: 2695-2704.

Wells KL, Patel N. 2010. Lumen formation in salivary gland development. *Front Oral Biol* **14**: 78-89.

Wilson SE, Liang Q, Kim WJ. 1999. Lacrimal gland HGF, KGF, and EGF mRNA levels increase after corneal epithelial wounding. *Invest Ophthalmol Vis Sci* **40**: 2185-2190.

Wozney JM. 1998. The bone morphogenetic protein family: multifunctional cellular regulators in the embryo and adult. *Eur J Oral Sci* **106 Suppl 1**: 160-166.

Xiao X, He H, Lin Z, Luo P, He H, Zhou T, Zhou Y, Liu Z. 2012. Therapeutic effects of epidermal growth factor on benzalkonium chloride-induced dry eye in a mouse model. *Invest Ophthalmol Vis Sci* **53**: 191-197.

Yamashita H, Shimizu A, Kato M, Nishitoh H, Ichijo H, Hanyu A, Morita I, Kimura M, Makishima F, Miyazono K. 1997. Growth/differentiation factor-5 induces angiogenesis in vivo. *Exp Cell Res* **235**: 218-226.

Yan C, Gao N, Sun H, Yin J, Lee P, Zhou L, Fan X, Yu FS. 2016. Targeting Imbalance between IL-1beta and IL-1 Receptor Antagonist Ameliorates Delayed Epithelium Wound Healing in Diabetic Mouse Corneas. *Am J Pathol* **186**: 1466-1480.

Yan Q, Quan Y, Sun H, Peng X, Zou Z, Alcorn JL, Wetsel RA, Wang D. 2014. A site-specific genetic modification for induction of pluripotency and subsequent isolation of derived lung alveolar epithelial type II cells. *Stem Cells* **32**: 402-413.

Yanagita M. 2005. BMP antagonists: their roles in development and involvement in pathophysiology. *Cytokine Growth Factor Rev* **16**: 309-317.

Yang AY, Chow J, Liu J. 2018. Corneal Innervation and Sensation: The Eye and Beyond. *Yale J Biol Med* **91**: 13-21.

Yao Y, Zhang Y. 2017. The lacrimal gland: development, wound repair and regeneration. *Biotechnol Lett* **39**: 939-949.

Yin H, Cabrera-Perez J, Lai Z, Michael D, Weller M, Swaim WD, Liu X, Catalan MA, Rocha EM, Ismail N et al. 2013. Association of bone morphogenetic protein 6 with exocrine gland dysfunction in patients with Sjogren's syndrome and in mice. *Arthritis Rheum* **65**: 3228-3238.

Yoo CB, Yun SM, Jo C, Koh YH. 2012. gamma-Secretase-dependent cleavage of E-cadherin by staurosporine in breast cancer cells. *Cell Commun Adhes* **19**: 11-16.

Yoon KC, Park CS, You IC, Choi HJ, Lee KH, Im SK, Park HY, Pflugfelder SC. 2010. Expression of CXCL9, -10, -11, and CXCR3 in the tear film and ocular surface of patients with dry eye syndrome. *Invest Ophthalmol Vis Sci* **51**: 643-650.

You L, Kruse FE, Pohl J, Volcker HE. 1999. Bone morphogenetic proteins and growth and differentiation factors in the human cornea. *Invest Ophthalmol Vis Sci* **40**: 296-311.

You S, Avidan O, Tariq A, Ahluwalia I, Stark PC, Kublin CL, Zoukhri D. 2012. Role of epithelial-mesenchymal transition in repair of the lacrimal gland after experimentally induced injury. *Invest Ophthalmol Vis Sci* **53**: 126-135.

You S, Kublin CL, Avidan O, Miyasaki D, Zoukhri D. 2011. Isolation and propagation of mesenchymal stem cells from the lacrimal gland. *Invest Ophthalmol Vis Sci* **52**: 2087-2094.

Yu GY, Zhu ZH, Mao C, Cai ZG, Zou LH, Lu L, Zhang L, Peng X, Li N, Huang Z. 2004. Microvascular autologous submandibular gland transfer in severe cases of keratoconjunctivitis sicca. *Int J Oral Maxillofac Surg* **33**: 235-239.

Zhang J, Ratanasirintrawoot S, Chandrasekaran S, Wu Z, Ficarro SB, Yu C, Ross CA, Cacchiarelli D, Xia Q, Seligson M et al. 2016. LIN28 Regulates Stem Cell Metabolism and Conversion to Primed Pluripotency. *Cell Stem Cell* **19**: 66-80.

Zhang X, M VJ, Qu Y, He X, Ou S, Bu J, Jia C, Wang J, Wu H, Liu Z et al. 2017. Dry Eye Management: Targeting the Ocular Surface Microenvironment. *Int J Mol Sci* **18**.

Zhang Y, Yeh LK, Zhang S, Call M, Yuan Y, Yasunaga M, Kao WW, Liu CY. 2015. Wnt/beta-catenin signalling modulates corneal epithelium stratification via inhibition of Bmp4 during mouse development. *Development* **142**: 3383-3393.

Zhao B, Yu M, Neitzel M, Marugg J, Jagodzinski J, Lee M, Hu K, Schenk D, Yednock T, Basi G. 2008. Identification of gamma-secretase inhibitor potency determinants on presenilin. *J Biol Chem* **283**: 2927-2938.

Zieske JD. 2004. Corneal development associated with eyelid opening. *Int J Dev Biol* **48**: 903-911.

Zoukhri D. 2006. Effect of inflammation on lacrimal gland function. *Exp Eye Res* **82**: 885-898.

Zoukhri D, Fix A, Alroy J, Kublin CL. 2008. Mechanisms of murine lacrimal gland repair after experimentally induced inflammation. *Invest Ophthalmol Vis Sci* **49**: 4399-4406.

Zoukhri D, Macari E, Kublin CL. 2007. A single injection of interleukin-1 induces reversible aqueous-tear deficiency, lacrimal gland inflammation, and acinar and ductal cell proliferation. *Exp Eye Res* **84**: 894-904.

Recent Publications in this Series

93/2018 Marit Ilves
Immunomodulatory Effects of Engineered Nanomaterials in Healthy and Diseased Lungs and Skin
94/2018 Laura Lahdentausta
Serum and Saliva Biomarkers in Cardiovascular Diseases and Periodontitis—Smoking as a Confounding Factor
95/2018 Joni Lindbohm
Unfolding Lipid Profile- and Sex-Paradoxes in Epidemiology of Subarachnoid Haemorrhage
96/2018 Anna But
Mitigating Bias and Dealing with Multiple Time Scales in Cohort Studies — Studying Medications and Complications of Diabetes
97/2018 Ashwini S. Nagaraj
Unravelling Lung Cancer Heterogeneity and Associated Therapeutic Responses Using *In Vivo* and *Ex Vivo* Model Systems
98/2018 Lotta Schepel
Strategies for Medication Safety: An Organization-Based Approach Focusing on High-Alert Medications and Clinical Pharmacy Services in Helsinki University Hospital
1/2019 Cristina Fevola
Distribution and Clinical Associations of Ljungan Virus (Parechovirus B)
2/2019 Anita Valkama
Dietary Change, Obesity, and Metabolic Markers in Pregnancy — Studies in Women at Risk for Gestational Diabetes Mellitus
3/2019 Feng Deng
Structure-Activity Relationships of Efflux Transporter Inhibitors
4/2019 Leena Yadav
Human Protein Phosphatase Interactions and Dynamics: Proteomic and Functional Perspective
5/2019 Luca Trotta
Genetics of Primary Immunodeficiency in Finland
6/2019 Laura Kolsi
Synthesis of Abietane-Type Diterpenoids with Anticancer Activity
7/2019 Christian Benner
FINEMAP — a Statistical Method for Identifying Causal Genetic Variants
8/2019 Paula Savola
Somatic Mutations in Autoimmunity
9/2019 Reinis Svarcbahs
Underlying Mechanisms of Prolyl Oligopeptidase Inhibition, Deletion, and Restoration on the α-Synuclein Aggregation Process
10/2019 Natalia Skogberg
Cardiovascular Risk Factors among Russian, Somali and Kurdish Origin Populations in Finland
11/2019 Johanna Troberg
Glucuronidation Activity of Individual UDP-Glucuronosyltransferases: Comparison of Activity and Substrate Specificity among Recombinant Human UGT Enzymes and Differences between Dog and Human Subfamily 1A UGT Enzymes
12/2019 Kari Aaltonen
Suicidal Behavior in Depressive or Bipolar Disorders
13/2019 Sakari Leino
Nicotinic Acetylcholine Receptors in Experimental Models of Parkinson's Disease and Levodopa-Induced Dyskinesia: Focus on α5 Subunit-Containing Receptors

Helsinki 2019 **ISSN 2342-3161** **ISBN 978-951-51-4913-8**